Final Technical Report
Federal Agency to which Report is submitted: DOE EERE – Water Power Program

Department of Energy Office of Energy Efficiency and Renewable Energy
DE-FOA-0002080 - Water Power Technologies Office 2019 Research Funding Opportunity
Final Technical Report
Grant
Abe Schneider, Chief Technical Officer abe@natelenergy.com 510.606.9071 Natel Energy, Inc.
Private Company
EE0008946 - Advanced Compact Generation Module with Fish Safe Runner Technology
PI: Abe Schneider, Chief Technical Officer
Prime Recipient's DUNS number: 141815709
DOE Technical Project Officer/Manager- Corey Vezina DOE Project Monitor- Sarah Kosbab DOE Contracting Officer/Manager – Laura Merrick DOE Contract Specialist - Stephanie Sites
Date of Report: January 27, 2023
Period Covered: April 28, 2020 - September 30, 2022

Signature of Submitting Official: _____
(electronic signature is acceptable)

Gregor Cadman V.P., Engineering, Natel Energy Inc. gregor@natelenergy.com

Name, Title, Contact information of Submitting Official

Authors

Gregor Cadman V.P., Engineering, Natel Energy
Kelsey Seto Staff Mechanical Engineer, Natel Energy
Sterling Watson Staff Mechanical Engineer, Natel Energy
Abraham Schneider PI; CTO, Natel Energy

Acknowledgements

The authors would like to acknowledge and express their appreciation to the following groups for their participation, review, comments, and support of this project.

The broader Natel Energy engineering and technician teams

Pacific Northwest National Laboratory's Energy & Environment Directorate

Kleinschmidt Group, Inc.

Oak Ridge National Laboratory, in particular members of the Manufacturing Demonstration Facility

DOE Water Power Technologies Office

This material is based upon work supported by the U.S. Department of Energy's Office of Energy Efficiency and Renewable Energy (EERE) under the Water Power Technologies Office, 2019 Research Funding Opportunity Award Number DE-EE0008946.

Abstract

Hydropower is an important contributor of stable, load-leveling renewable energy to our national grid. Increasingly, the development of new hydropower facilities or the retrofit of existing ones hinges not only on minimizing costs but also environmental impact. In this report, the analysis and testing of a modular and scalable low-head hydropower generation design using Natel Energy's Restoration Hydro Turbine is described. This design leverages many established industry approaches for compactness and efficiency while simultaneously allowing for safe downstream fish passage through the turbines themselves. This unique approach reduces overall hydropower facility costs and enables a simpler inclusive method of project design and operation.

To assess this design, mechanical and fluid computational analyses were used to study and optimize key parameters. Passage tests of important migratory species (salmonids, American eel) were conducted through representative turbines. The unique propeller geometry of the fish-safe Restoration Hydro Turbine was subjected to detailed design and testing using advanced manufacturing composite techniques. Comprehensive module cost models were developed and assessed alongside hydraulic efficiency. The results of this project show promising and economical applications for downstream passage of fish through Restoration Hydro Turbine modules.

Table of Contents

1. Introduction

1.1 Summary

This report documents an effort led by Natel Energy, in close collaboration with the Pacific Northwest National Laboratory, and with review support from Kleinschmidt Group and staff from Oak Ridge National Laboratory's (ORNL) Manufacturing Demonstration Facility, to advance the design of a compact, fish-safe, low head generation module formulated within the guidelines and requirements of ORNL's Exemplary Design Envelope Specification (EDES). In this module, Natel's fish-safe Restoration Hydro Turbine (RHT) design is incorporated for industry-leading fish safety. The concept studied leverages existing industry approaches and technologies across much of its design, thus minimizing performance and cost risk. The novel aspects pertain specifically to the runner hydraulic design, which delivers high fish passage survival rates without compromising efficiency. This capability allows for reduced overall installation cost by relieving the exclusion burden on fish passage module design. Further, the axially compact nature of the turbine design substantially improves modularity and ease of siting.

Module configuration, hydraulic, and component designs were assessed by the development of performance and cost models. A combination of subcomponent and full-scale testing occurred on elements of the proposed fish-safe module design, advancing industry understanding of a) turbine design for fish safety and b) the fabrication, durability, and performance of thick turbine runner blades constructed using advanced manufacturing techniques.

Outputs of the project include a preliminary design of submersible fish-safe run-of-river generation modules, including performance assessments and tradeoffs as well as cost assessments; detailed design of a scalable runner utilizing advanced manufacturing techniques to produce unique fish-safe geometry accompanied by assessments of materials, analysis, manufacturing methods, down selection, and validation tests; and peer-reviewed publications of fish passage testing of key representative species (salmonids, American eel) demonstrating safety for proportionately large fish (~1/4 runner diameter) and eel (~1 runner diameter).

Findings:

- Compact overflowed fish-safe generation modules of the configurations studied can be designed to perform efficiently and effectively, with inflow / outflow ("plant level") head losses of around 5% (typical for hydro facilities) and turbine hydraulic efficiencies greater than 90%.
- Cost-effective fish-safe plants are achievable through the novel blade geometries of the RHT turbine design, which allow for high blade strike speeds on fish (~20m/s) with excellent survival (no significant difference between control and treatment groups of tested salmonid and anguillid species) for proportionately large fish (length of up to 30%

of turbine diameter for salmonids, and up to 120% of turbine diameter for eels). (Watson et al, 2022)

- Advanced manufacturing methods may be successfully used to construct robust full-scale RHT-type runner blades that meet all the strength, fatigue, stiffness, and environmental durability criteria studied, offer the manufacturing benefit of formed net-shape parts without machining, and would be expected to last 30+ years in typical service.
- For the range of module design heads studied (3 to 10m) estimated installed module costs (turbine and generator, module civil elements, transportation, and labor) become increasingly compelling with higher heads. The installed cost for a 10m module is approximately $1600/kW (which is attractive, considering that a complete plant needs to be not more than $5000-6000/kW to be economical). For lower heads, the number of economic sites is reduced: at 5m, the module installed cost is $3-4000/kW, and at 3m, $5-6000/kW. Lower head sites will require advantages elsewhere, such as close proximity to interconnection and access, existing non-powered structure, etc. Modules can be arranged with up to 3 units in tandem and multiple in parallel, though the simplest 1x2 arrangement illustrated below is the most generally applicable.

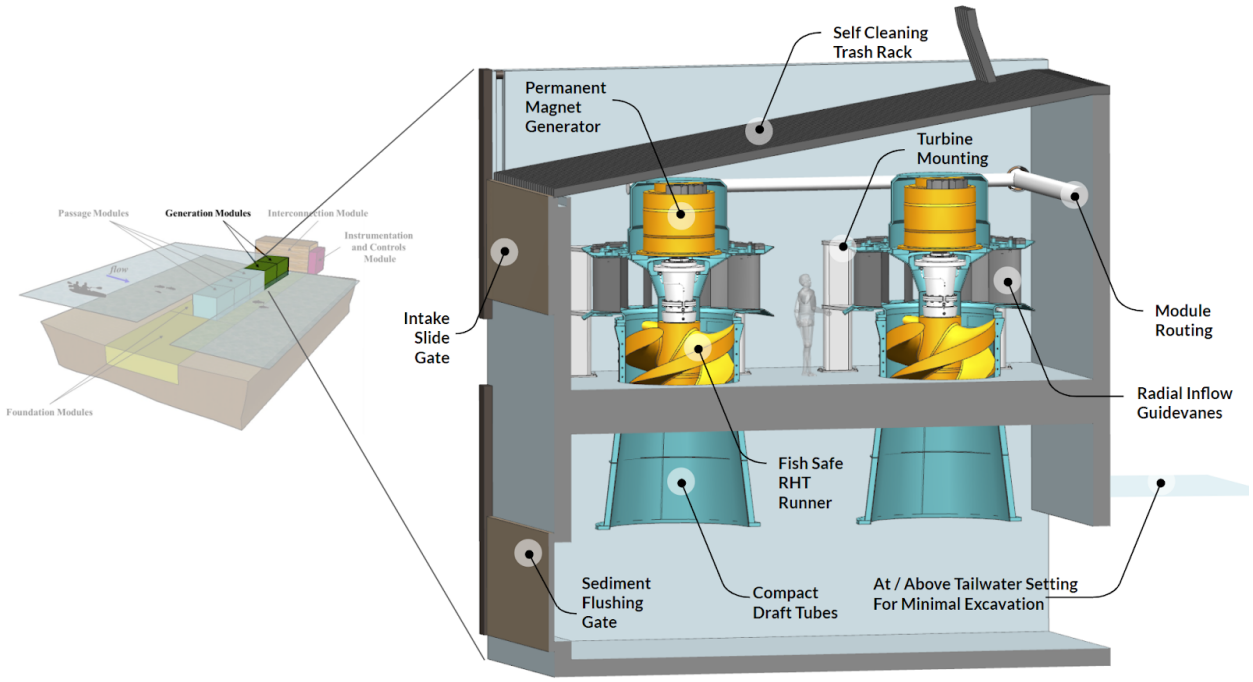

Figure 1: an illustration of the fish-safe generation module concept in the context of the Standard Modular Hydropower schematic.

Intended outcomes of this work, some of which have already been realized, are to enable usage and acceptance of advanced manufacturing in the production of next-generation, fish-safe runners; to increase awareness, quantification, and application of fish inclusion as a viable design strategy backed by peer-reviewed publications; and to provide guidance and references for

improved run-of-river plant design, methods of analyzing fish safety and plant performance, modularity tradeoffs, and future EDES updates.

Figure 2: a rainbow trout recovers after a post-turbine passage examination.

1.2 Relevance

The Water Power Technologies Office Multi-Year Program Plan presents a structured challenge-based model for the hydropower program goals over the coming several years. Of the five major challenges identified, this project targeted work germane to three areas: limited growth opportunities, the addressing of environmental impacts, and the lack of access to support decision making. Figure 3 illustrates how this project's objectives specifically nest within the relevant challenges, map to relevant approaches, and should lead to some of the desired long-term outcomes of the WPTO hydropower plan.

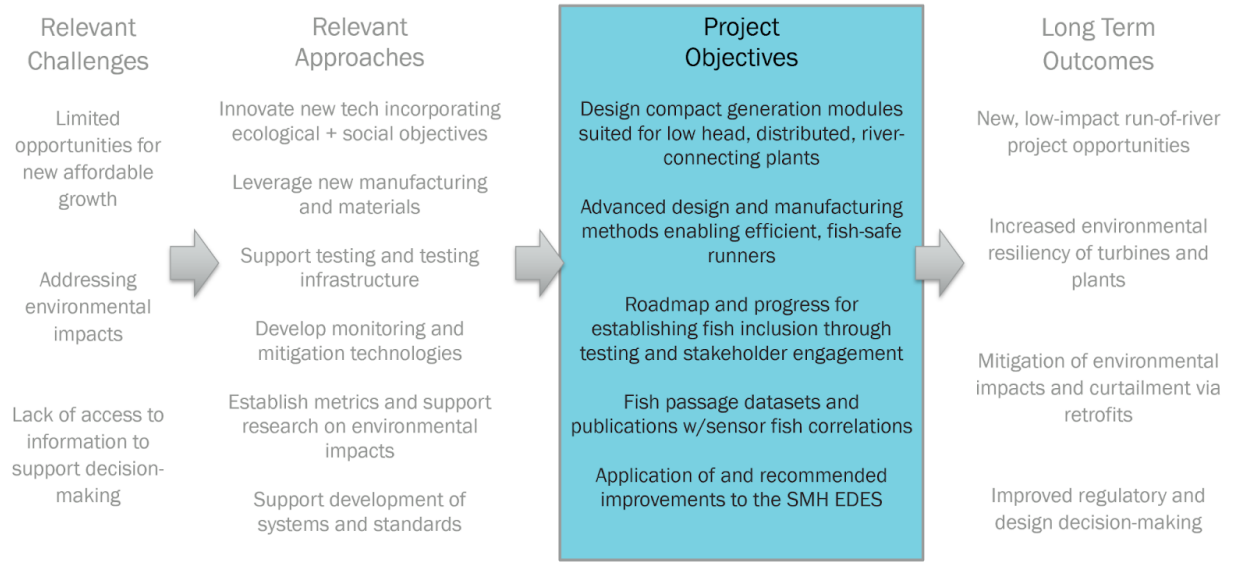

Figure 3: Project objectives in the context of WPTO's Multi-Year Program Plan.

Hydropower dams pose a significant threat to the survival of fish species that migrate between the river and the ocean to complete their life cycle, and fish typically must pass through multiple hydro plants on their downstream migrations, multiplying the risk to any single fish. The status quo for fish passage has been to exclude fish from hydro turbines using screens and to direct fish to alternate routes downstream, which can delay migrations and expose fish to predators. Additionally, fish may become impinged on the screens or pass through and enter turbines regardless of the screen, and risk traumatic injury or death from blade strikes and impingement. Some hydropower plants impose temporary plant shutdowns at night during migration season, but still operate during the day. These conventional methods for managing fish passage all increase plant operation costs and reduce power generation, and still do not do enough to help fish safely travel downstream. Hydro turbines that can safely pass downstream-migrating fish ensure that upstream habitat is viable for fish populations while allowing hydropower facilities to maximize production.

1.3 Areas of Focus

Project work was separated into two budget periods with a go/no-go decision point prior to Budget Period 2. Work and learnings from Budget Period 1 informed the assessment of opportunities and high value focus areas for Budget Period 2.

The project team started with proposed module concepts (both horizontal and vertical axis) and a hydraulic (runner) designed for fish safe passage; this runner had been evaluated by CFD and scale model testing to demonstrate >90% hydraulic efficiency, and representative blade shapes had been studied in a scale linear strike study (Amaral et al, 2020), however the broader module design had not been studied nor had passage studies through actual turbines been conducted.

Focus areas of the project largely fell into three categories: system- and turbine-level design and analysis; detailed design and testing of a fish safe runner utilizing advanced manufacturing techniques; and testing of fish passage through turbines to quantify survival rates and sublethal effects.

Budget Period 1 Scope:

- Overall system downselection, maturation, and performance assessment via detailed design, fluid mechanics and structural analysis, and cost modeling.
- Assessment and downselection to the most applicable advanced manufacturing process and material(s) for runner blade production, along with the completion of a detailed design of the runner unit within this context.
- Full-scale salmonid passage evaluation using an established field test facility of a turbine consistent with the proposed design.

Budget Period 2 Scope:

- Continued overall system design and modeling updates with a focus on module level performance (efficiency, debris handling, etc);
- Furthering downstream passage work with additional tests of larger salmonids as well as groundbreaking American eel passage testing;
- Advanced manufacturing runner testing for environmental longevity and component-level strength, stiffness, and fatigue.

1.4 Objectives and Results

Objective 1: System Design, Analysis, and Review.

The project team rapidly evaluated and downselected between two module configurations (vertical radial inflow bay, axial pit/bulb). Factors and constraints affecting the proposed module's performance against high level metrics (market, LCOE, SMH Specification Requirements) were considered. For the selected vertical axis option, derived requirements and architectural details were derived for sub-module design activities. Detailed requirements and Design Failure Mode and Effect Analysis (DFMEA) documents were developed and reviewed within the project team, with ORNL, and WPTO. Designs of modules and incorporated turbines were developed and reviewed, with installed costs estimated. Module hydraulic performance and losses under typical circumstances (head/flow duration curves, trash handling) were studied via CFD; inclusion and assessment of additional module variants (horizontal axis, alternate in/outflow configurations) were assessed for tradeoffs. Vertical axis units allow for tandem arrangements underneath overflowed, self-cleaning trash racks, increasing power density / reducing plant footprint; this configuration is preferable when site elevations (headwater,

tailwater, and streambed / excavation to foundation) permit. Horizontal arrangements are better suited for low head (2-5 or 6 meters) where it's impractical to fit the axial length of a turbine unit vertically without extensive excavation.

Objective 2: Full-scale Performance Testing; Gathering Data to Advance Downstream Fish Passage Market Adoption.

Natel's prior/parallel work to field a utility-scale turbine of a prototype fish-safe design immediately offered a unique opportunity to conduct field testing at scale early in this program and use results to inform design tasks. To this end, the project team developed and executed a testing plan to evaluate fish survival with full-scale tagged fish through a 1.9m–diameter 300kW turbine, in conjunction with PNNL. Downstream fish passage survival (immediate and delayed mortality) met the targeted 99.5% survival[1] for both sets of test groups (up to 400mm in length in Budget Period 1, and then up to 600mm in length in Budget Period 2). Further, yellow- and silver-stage American eel passage was studied at Natel's Hydraulic Test Facility to document qualitative and quantitative aspects of turbine passage and survival of this important species, also in conjunction with PNNL. One open access journal article documenting the American eel passage study has been published at the time of this report (Watson et al, 2022); a separate publication on the rainbow trout testing being authored.

Objective 3: Detailed Design, Downselection, and Manufacturing / Testing of Advanced Manufactured Runner.

Natel Energy's RHT turbine runner design has unique geometry that is well suited to take advantage of advanced manufacturing techniques to produce net shape parts with greatly reduced machining needs vs conventional cast blades. Literature review combined with industry collaboration and review with ORNL's Manufacturing Demonstration Facility (MDF) informed a downselection for combinations of substrate and coating(s) that could compete for durable, low-cost runner production. Physical testing was conducted on a subset of options to evaluate durability. The resulting selected design elements were incorporated into a full scale (1.9m diameter) runner design. Individual full scale prototype blades were manufactured and underwent laboratory static and fatigue structural testing to evaluate both the manufacturing approach as well as resulting component performance, while lab component tests of coupons assessed impact, immersion, and thermal effects on predicted runner blade life.

[1] Survival rate adjusted for control survival; the 2022 test had delayed mortalities of both treatment and control groups due to high temperatures and handling stress. Details and analysis of these tests will be forthcoming in a joint publication from PNNL and Natel Energy, Inc; submission expected in 2023.

1.5 Approach

The project team leveraged existing guidance from the Oak Ridge Standard Modular Hydropower Exemplary Design Envelope Specification as well as typical industry approaches and solutions for many elements of the turbine and civil elements. Novel work was applied selectively and focused on the core elements enabling the module to generate power efficiently while simultaneously passing fish downstream safely; and in these areas (overall module configuration, runner mechanical, and fish passage) a requirements and risk based approach was used to focus work. Stakeholder guidance and engagement was an important part of this process, not only to generate the initial concepts but to guide the details of the project as it progressed.

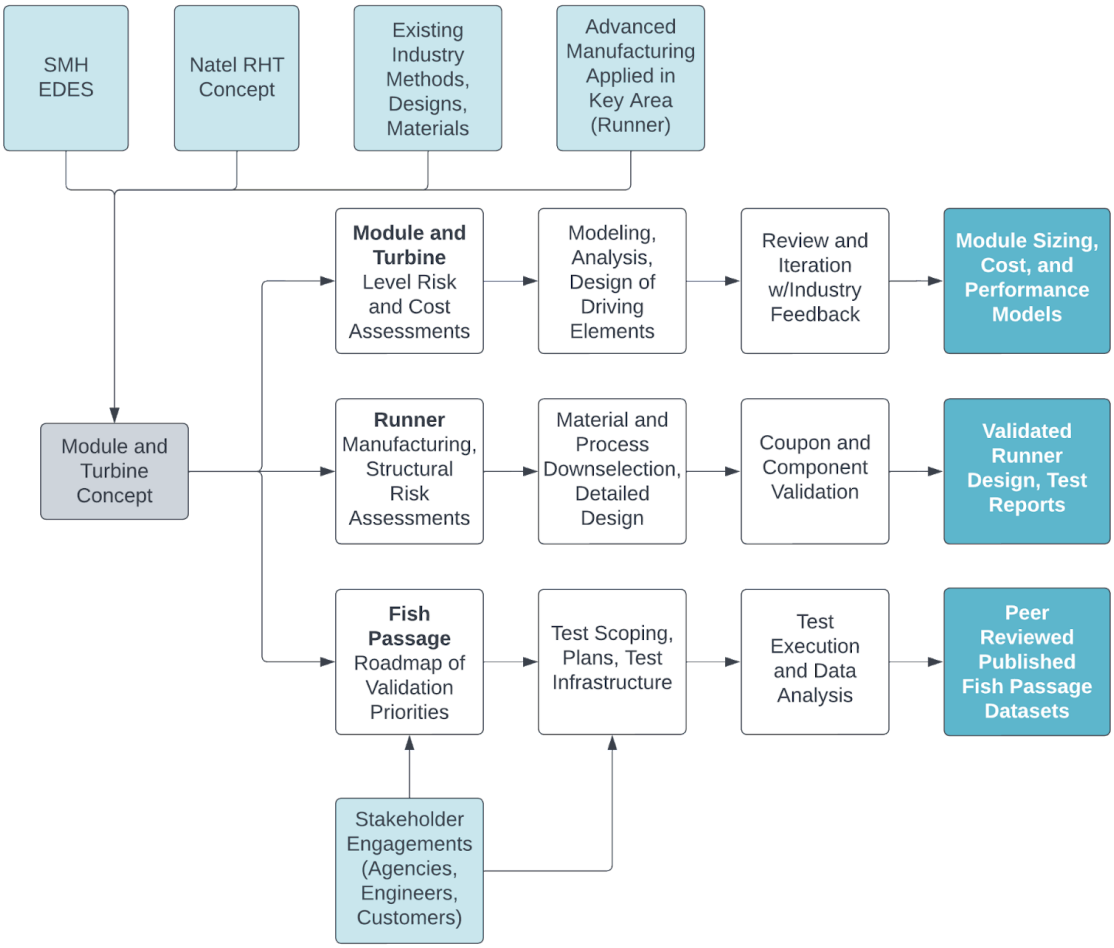

Figure 4: Project Approach and workflow.

Primary stakeholders and end users of the outputs of this work (module design and corresponding performance test data) are industry customers as well as regulatory bodies. Both seek validated plant design options for robust, efficient, economical systems that improve upon status quo (exclusion difficulties, high project civil costs, etc.) Early and frequent engagement on

multiple fronts included leveraging Natel's existing customer and industry network, along with ORNL's SMH team and other sources (conferences, publications etc) to understand viability and market needs; working with experienced engineering firms such as Kleinschmidt Group to review requirements and designs, and recommend improvements; and engagement with regulatory agencies and fish passage experts to review passage test objectives, detailed test plans, and results as they were developed.

Project results have and will continue to be disseminated or utilized through a combination of peer reviewed journal publications, industry presentations, continued outreach, turbine product offerings, greenfield and restoration project design, and EDES / DOE feedback.

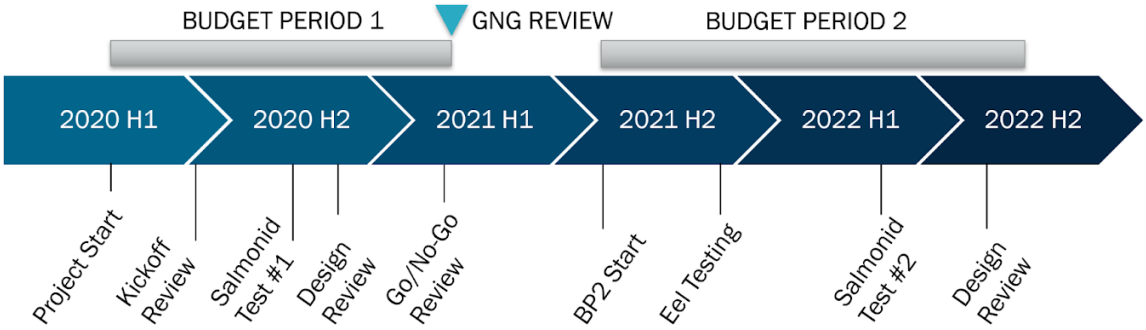

Figure 5: project timeline highlights. The major passage test events are highlighted as key discrete milestones; other design and testing work was interspersed.

In addition to the milestones highlighted in the timeline, continuous ongoing work during the project included module and turbine design, sizing, and costing; module performance analysis via CFD; runner detailed design and analysis; material and manufacturing assessments for the runner; and test planning, data analysis, and report authoring.

The following reviews were conducted during the period of performance and served as critical milestones and sources of helpful guidance.

- 2020Q2: Preliminary Module Design Review: Natel, DOE and ORNL participating.
- 2020Q2: NEPA review of proposed BP1 Fish Passage Test Plan.
- 2020Q4: Runner Manufacturing Review: Natel and ORNL participating.
- 2020Q4: System (module) Level Design Review: Natel and Kleinschmidt participating.
- 2021Q1: Go/No-Go Review: Natel, DOE, PNNL, and external reviewers participating.
- 2021Q2-Q4: Various reviews of eel test plans with industry and agency representatives.
- 2021Q2: NEPA review of proposed BP2 Fish Passage Test Plans.
- 2022Q2: WPTO Project Peer Review
- 2022Q3: System (module) Level Design Review: Natel, ORNL, Kleinschmidt participating.

2. Technical Discussions and Findings

This section of the report discusses the three major focus areas of the project (module design, fish passage, and advanced manufacturing of an RHT runner) in detail.

2.1 Module Design

2.1.1 Function

As described within the SMH design specification this module serves the following major functions:

- Generation functionality. Hydraulic energy is consumed for the generation of electrical power. Required equipment to accomplish this energy conversion and deliver it to the grid competitively is considered.
- Structural functionality. In conjunction with adjacent modules, contributes toward impoundment needs and safe watershed handling in all conditions.
- Environmental functionality. Module presence and operation does not result in undesirable impact to the surrounding environment. Significantly for this module and turbine design, this includes the ability to safely pass fish populations downstream through the turbine itself and thereby alleviate burdens on other SMH modules as well as reduce overall capital costs. The module must also interface with waterway sediment in a manner not detrimental to either module functionality or overall plant functionality.

To successfully accomplish the above tasks the module includes the following features:

- Inclusion of direct drive Natel RHT (Restoration Hydro Turbine) units, designed for safe fish passage and submersible operation.
- A widely spaced, sloped self-cleaning trash rack to minimize O&M activities and impingement injury.
- Sliding gate(s) and/or stoplog slots for dewatering. (for the purposes of emergency flow shutoff or similar, weighted self closing cylinder gates under each draft tube exit or over each intake could alternately be used).
- The ability to easily access, remove, and replace entire turbine units with either rail, overhead, or barge mounted lifting equipment for shore-side servicing (the ability to close off an open turbine port with a flat plate is considered).
- Onshore control, and as warranted, variable frequency drive equipment for efficient plant operation across a broad range of available flow.
- Potential inclusion of flushing ports to allow both the passage, and clearance, of accumulated sediment load either upstream or within the module.

2.1.2 Motivation

Here, the overall generation module is referred to as the "system" being designed. For this system, the project team evaluated concepts and downselected against overall requirements, engineering sizing and analysis of the driving elements of the system was conducted, and overall system performance (hydraulic efficiency, cost) was evaluated. The core question motivating this work is under what conditions, and with which design choices, will the proposed family of generation modules be economically viable and succeed in their higher level objective of enabling lower cost plant implementation through effective module performance, minimal excavation, and eliminating downstream screening burdens.

2.1.3 Conceptual Downselection and Requirements Development

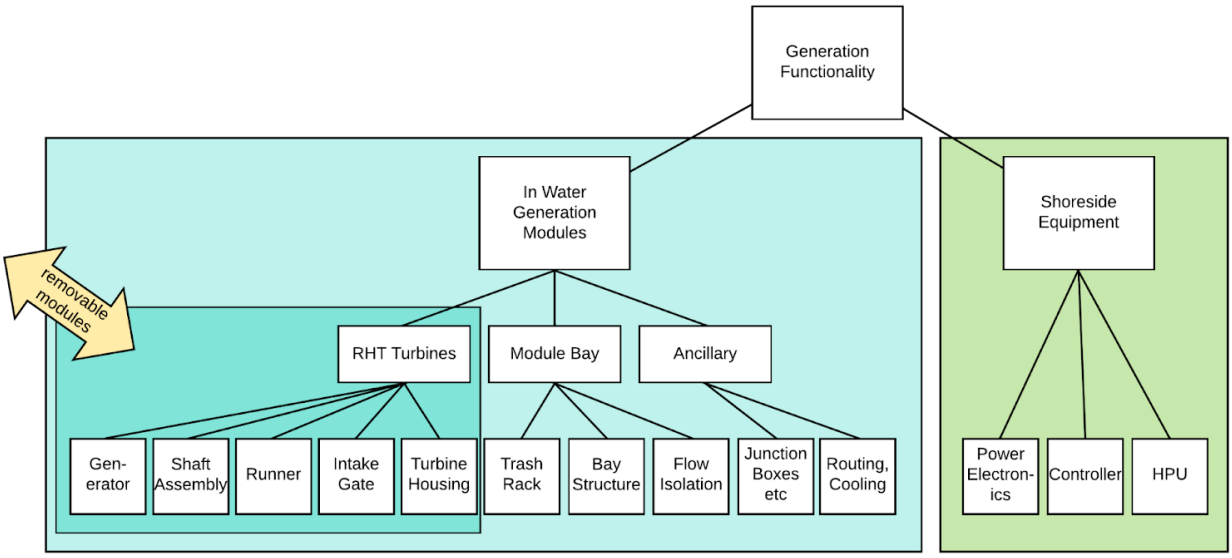

Figure 6: breakdown of the generation module functional areas.

Elements contributing to overall requirements and understanding of the module design space range from structural and mechanical, to hydraulic, to civil:

- System and mechanism requirements – Cover a wide range of best practices and functional requirements, generated from ORNL's EDES as well as Natel Energy and Kleinschmidt's design experience and a module Design Failure Modes Effects Analysis (DFMEA) documented at the onset of the project.
- Hydraulic design – Extensive work on individual RHT turbine design developed performance and loads maps (confirmed via scale testing) coming into the project work, defining the operational ranges of the generation equipment and the 'corner' cases which the structure must be capable of handling.

- Loads – Design load cases are compiled from a combination of CFD analysis as well as spreadsheet calculations, and must include the extreme cases (e.g., flood events) that potentially drive component, turbine, and/or module design. Importantly, module load cases, in conjunction with foundation module design, must consider overall hydrostatic stability.
- Fish passage design – The core of Natel's RHT design is around understanding and designing for fish survival, and this generates requirements around unit and runner geometry as well as module inflow and outflow.
- Interfaces to surrounding systems:

Load Condition	Static	Fatigue	Modal / Stiffness	Description, Examples	Rotating Equip.	Gates / Actuation	Turbine Structure	Module Structure
Power production	○	○	○	Normal hydraulic, centrifugal, thrust, actuation, structural loads across range of expected operating conditions (head, flow, shaft speed, guide vane angle, gate positions)	○	○	○	○
Transients	○	○	○	Fast grid transients leading to speed / hydraulic load changes Head/flow transients	○	○	○	○
Power production plus fault	○		○	Control system failure (loss or inadvertent GV actuation, speed control, command resulting in reverse thrust) Asymmetry (broken / jammed guidevane). Lockshaft.	○	○		
Start up	○	○	○	Hydraulic load overshoot, pressure pulsations, watering up	○	○	○	
Normal shutdown	○	○	○	Hydraulic load overshoot, pressure pulsations Dewater / vacuum loads	○	○	○	
Emergency shutdown	○		○	Full load rejection, high vibe/other fault, safety, part failure. Hydraulic load overshoot, pressure pulsations / water hammer	○	○	○	○
Parked, maintenance	○			Gravity loads, hydrostatic / buoyant forces (watered, dewatered) Module component removal / replacement			○	○
Transport and assembly	○		○	Lifting, tie-down, road loads			○	○
Seismic	○		○	Lateral loads / frequencies				○
Flood, extreme flow	○			Maximum hydrodynamic pressure / drag on module Maximum hydrostatic pressure on sealed components Debris strike				○
Thermal	○	○		Thermal expansion/contraction with resulting internal stresses	○		○	○

Logical combinations of load cases shall be considered together (eg thermal plus dynamic loads)

Figure 7: design loads table noting examples of cases, type(s) of analysis required, and the scope where a given load may drive design.

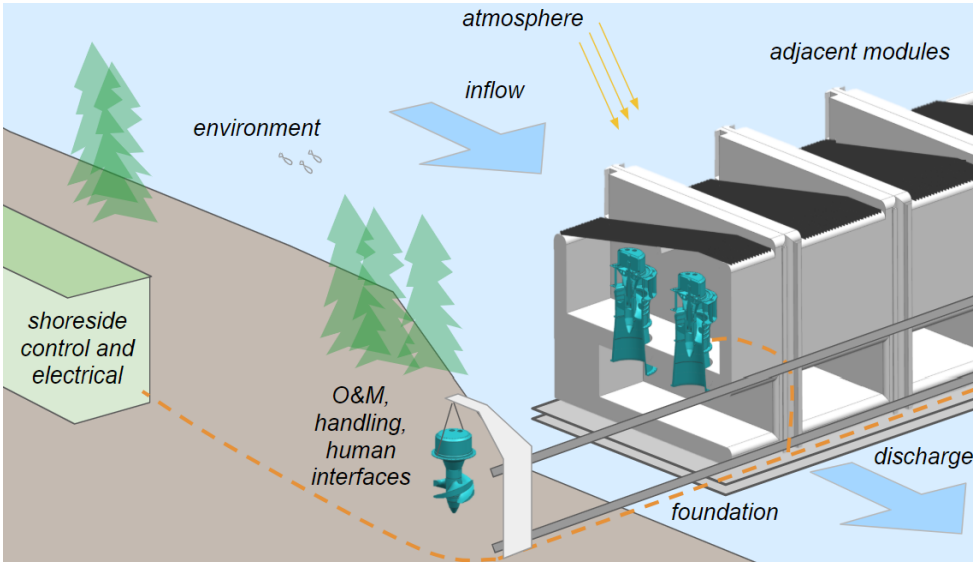

Figure 8: Illustration of high-level module interfaces

At the highest level, the generation module has the following primary interfaces:

- Hydraulic (inflow, outflow, thermal, loads, debris, sediment)
- Environmental (fish, physical pollution, noise pollution)
- Atmospheric (UV, corrosion, etc)
- Foundation module
- Adjacent module(s) (generation or otherwise)
- Shoreside electrical
- Controls and data
- Human, O&M
- Handling (lifting, tie-downs, transportation)

All of these drive requirements and some aspects of design. Within these high-level categories some of the most interesting are:

- Inflow interactions with the bay entrance, trash rack, and turbine intakes
- Hydraulic loading in driving cases (dewatered, flood / max flow)
- Sediment interactions with the modules – are flushing ports in the lower portion of the module a necessary design aspect to allow transfer and clearance of accumulated bed load, etc.
- O&M interactions – what is the most universal approach that is compatible with other SMH modules and the most site designs
- Adjacent module design, both structurally to the foundation module, as well as sealing and routing across adjacent modules

Within a single generation module, some of the most important interfaces are the structural, electrical, and possibly even hydraulic (for the sake of actuator power) connections between a single turbine unit and the surrounding bay. For a turbine to be easily removed and replaced, these connections need to be simple and robust. Given that it is possible to dewater at least the upper bay, if not the entire module, fairly easily, these interfaces do not need to be de/re-attachable without any local human intervention; but they should be designed to be nearly, if not entirely, so to minimize the potential for human error. (For turbine bay dewatering, the intake must be closed via a built-in slide gate or the placement of stoplogs; the bay must be pumped out or drained, depending on tailwater elevation relative to the upper bay floor; and then either sections of the trash rack over the units can be hinged open, or the entire rack may be lifted off by the same lifting system that will be removing the turbine unit - a mobile or permanent shoreside crane, or for larger plants, a gantry crane designed to run along the modules.)

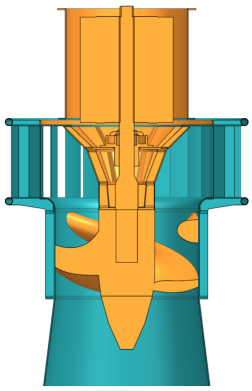

Figure 9: highlighted rotating equipment sub-module which may be easily extracted / re-inserted for servicing.

Natel considered two basic generation module configurations within which a fish-safe RHT turbine (or multiple turbines) may be fielded: one utilizing a horizontal (or near-horizontal) turbine arrangement, and the other with vertical axis units. Both configurations have significant merit when weighed against the design criteria and requirements of the SMH design specification, as well as the more general yardstick of product viability. It is important to note that both arrangements, when installed in their applicable head ranges, offer equivalent fish passage safety. Horizontal axis units are suited for very low head sites (head from 2 to 5-6m), but for higher heads up to 10m or beyond, vertical axis arrangements will be more compact, power dense, and thus economical.

As discussed further in the report section on cost, decreasing head presents increasing economic challenges. Higher head pressure allows for compact power dense designs, whereas low head units must consume more flow for equivalent power, requiring more steel and concrete. Additionally, vertical bay modules with removable turbine units are better suited to handling extreme events as well as regular service activities with lower cost and higher reliability. Trash

handling, as well as fish impingement, are better addressed by the long sloping overhead rack than they are with the horizontal module's intake rack. The latter would likely require some form of cleaning mechanism. For these reasons, much of the work in this grant project focused on the vertical axis turbine arrangements best suited for heads above 5m; however, horizontal axis types were also evaluated for hydraulic performance and installed cost.

2.1.4 Sizing, Turbine Design

RHT turbine diameters ranging from 1.3m to 1.9m in diameter were considered within this work. While modules utilizing both larger and smaller sizes could be conceived, these turbine sizes provide the most logical physical size to address the target head range of 3-10m; larger machines would require substantial excavation for sufficient submersion, and smaller turbines would not be as economically competitive.

In addition to turbine size selection, scaling can be achieved by both extending the number of tandem units (units arranged up/downstream) within a module; widening a single module to accommodate more than one row of units; and of course, arraying multiple modules together. The approach of an open forebay allows for flexible design with the only limitations on individual module bay size (number of units) being the ability to provide sufficient flow to the furthest downstream units, and footprint / handling limitations for width. Given typical constraints around these, Natel considers 1x2 (width by up/downstream number), 1x3, 2x2 and 2x3 arrangements to be the most practical. A 1x2 arrangement is illustrated in this document as it is likely the best aligned with SMH modularity (the formwork and design of this module would have the most potential site applicability, whereas larger modules are not always warranted) and handling intent (reusable formwork, and then the module itself, can be moved and installed at lower mobilization costs).

Turbine size and count is dictated by head, flow, and site elevations; fewer turbines of larger size will cost less for a fixed plant design flow, however larger units dictate deeper excavation. Once turbine size and arrangement are decided upon, a module may be sized based on inflow and outflow criteria. Module height is driven by turbine stack height as well as inflow submersion for vortex formation / air ingestion prevention, clearance under the sloped trash rack, and discharge clearance. Width and length are driven by upper bay flow clearances around the turbine radial inlets for effective performance as well as inflow Froude number across the entrance and outflow velocity. The rack is sized for a 6:1 sweeping vs normal velocity to aid with self-cleaning, and normal velocities across the rack are at or below 0.5m/s to keep both head loss and impingement low. Some examples of the resulting dimensions are noted in Figure 10.

	per tandem set	2xD130	2xD190	3x D190	
	Dia, runner	1.3	1.9	1.9	m
	Hnet reference	7	7	7	m
A	Dia, radial inlet	2.0	2.9	2.9	m
B	Height, radial inlet	0.7	1.0	1.0	m
C	Height, gen hsg	0.7	1.0	1.0	m
D	Dia, dt outlet	1.7	2.5	2.5	m
	Bay section width	3.5	5.4	6.4	m
	Min bay internal lengt	6.3	9.3	13.9	m
E	Min shaft spacing, u/d	3.2	4.6	4.6	m
	Min inlet submersion	1.6	2.3	2.3	m
M	Outlet vertical clearan	1.7	2.1	2.1	m
F	Unit height, inlet base	2.4	3.5	3.5	m
	Bay min internal heigh	6.3	8.9	8.9	m
	flow driven dimensions				
	Q11	1.35	1.35	1.35	
	Unit flow	6.0	12.9	12.9	cms
	Total flow	12.1	25.8	38.7	cms
	Design rack velocity, n	0.5	0.5	0.5	m/s
	Min bay internal lengt	6.9	9.5	12.1	m
	Min outlet height	1.3	1.8	2.2	m
G	Min inlet height	1.7	2.1	2.5	m
	Min bay internal lengt	9.6	11.9	13.9	m
	Total height req'd	3.9	4.8	5.6	m
	power				
	P11	11.7	11.7	11.7	
	Unit power, hyd	366	782	782	kW
	Total power, hyd	732	1564	2347	kW
	Summary dimensions				
	Under rack clearance	2.7	0.5	0.1	m
H	add'nl length req'd	0.0	3.3	5.3	m
I	Bay internal length	9.6	15.2	19.3	m
J	Per-set width	3.5	5.4	6.4	m
K	Bay total height	6.3	8.9	8.9	m
L	Bay outlet height	1.7	2.1	2.2	m

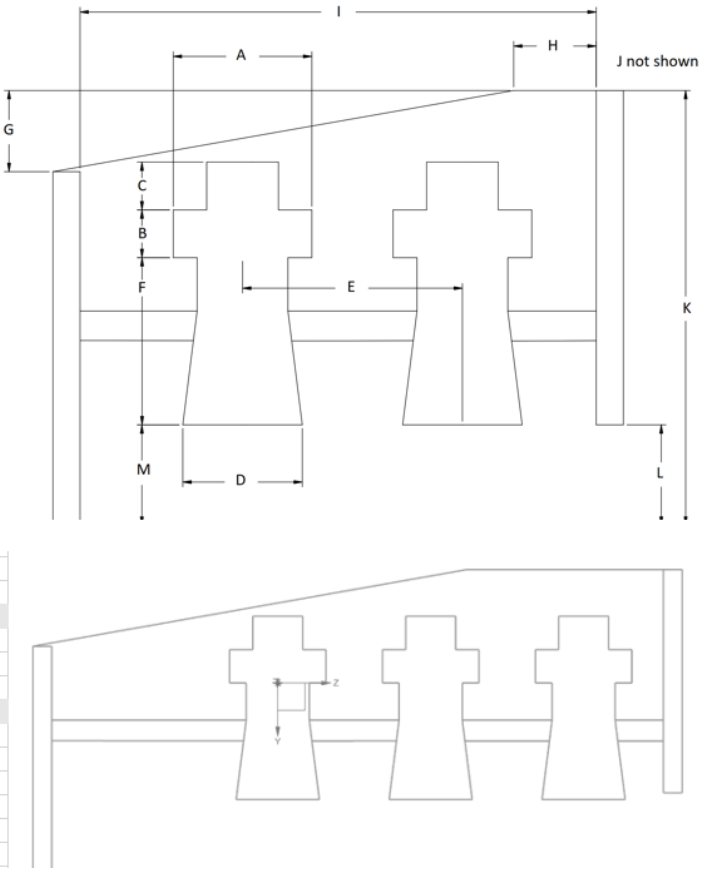

Figure 10: Module sizing - 3 examples for a 7m net head design using variants of turbine diameter and module unit count.

Turbine and Generator COGS (cost of goods sold) were targeted to be competitive with T&G points for 'conventional' low head turbine options, with overall competitiveness for plants coming from the elimination of civil costs related to submersion, fish exclusion, and powerhouse / tailrace. To help ensure tracking toward this goal, a detailed cost model was developed that considers subsystem materials and fabrication costs combined with overall machine assembly and transportation costs (see section 2.1.5). O&M costs were also modeled. The costs for each component and fabrication were based on actual vendor quotes or as built costs, and scale as appropriate for their design drivers (typically by surface area or volume or by hydraulic load). Key discontinuities in process / material options, e.g. the physical scale at which it is more practical or economical to fabricate composite runners instead of solid castings, are included.

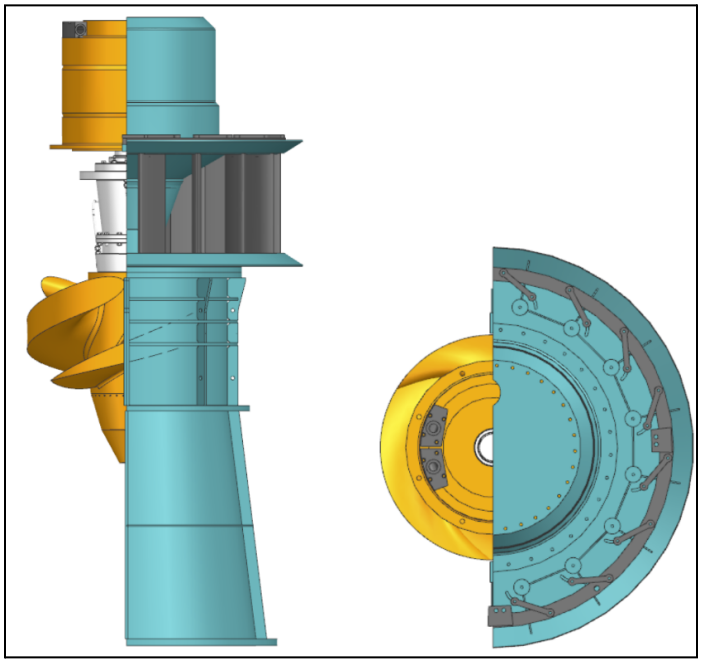

Figure 11: housing and guidevane module elements in the context of the completed RHT turbine assembly.

From initial requirements, preferred load paths were selected for sub-module loads. For the guidevanes, the operating range, solidity and airfoil geometry were selected along with proper pivot location for actuation loads. CFD results were used to inform spreadsheet models assessing the forces and moments applied to each individual guidevane, and thus the overall mechanism and actuation system; options for mechanism and mounting design were assessed including a review of the substantial amount of existing industry approaches; linkage and bearing elements, as well as actuation system options, were sized out. These results fed into aggregate module cost modeling.

Loads are borne to ground (the surrounding module structure) in the following manner: generator and guidevane torsional loads are reacted out via torque arm structures (A), while thrust is carried through the guidevane pivot shafts and down and out through the embedded joint at the runner housing to draft tube interface.

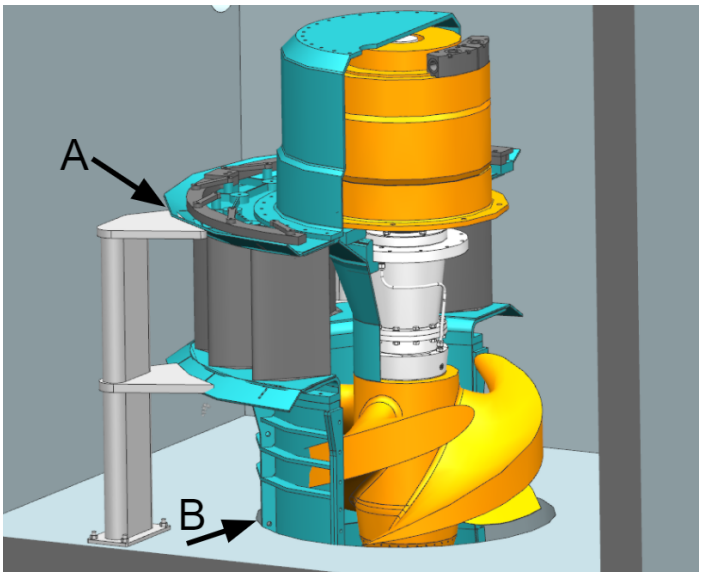

Figure 12: turbine to module load paths

Guidevane jamming is an issue which is expected to occur with some frequency during the unit lifetime; when shutting down, a piece of debris may become trapped between two adjacent vanes and could result in component overload and damage if not accounted for. Typical solutions for this are to use a friction bushing that will slip, or some type of linkage 'give' (springs, shear pin, etc). In the case of this radial inflow arrangement with an offset pivot arm, a linkage type mechanism is preferred.

Bearings, seals, shaft length and diameters, generators and couplings were identified for the potential range of turbine unit size(s) that may be applicable for use within the proposed generation module. One important architectural decision made early on was the type of primary turbine shaft 'guide' bearing, which in various examples of hydraulic turbines might be sealed roller bearings, open water-lubricated and cooled hydrodynamic bearings, or hydrostatic bearings. Of these, the former two are more commonly used for smaller machines that match the project's design space. The choice between roller and hydrodynamic bearing is a good example of the need to consider lifetime costs and O&M activities: in this case, while a hydrodynamic bearing offers some design benefits it also requires a system to deliver filtered water to the bearing area for reliable operation. High head plants can simply use head pressure to feed this flow, but low head designs such as those within the SMH EDES scope would require an active (pumped) system, creating a new combination of components subject to maintenance and failure modes. Additionally, the submersed generator housing bell would be subject to increased risk of flooding, a major issue with previously fielded submersible generator systems in the industry. For these reasons, Natel selected roller bearings with mechanical seals.

Another early decision was to use a direct drive permanent magnet generator (PMG) design rather than using a system which requires a speed increaser to drive a higher shaft speed generator. While higher speed generators are certainly less expensive, the cost of a reliable speed increaser which can tolerate all expected design conditions (including overspeed) is substantial; further, the compact and submerged nature of the generation module design demands a system that is simple and highly reliable. By minimizing the number of components that are submerged within the run of river module, O&M costs will be substantially lower than if a gearbox system (requiring alignment, lubrication, and other regular maintenance) were incorporated. Additionally, PMG units offer high efficiency across a broad range of operating conditions (whereas an induction machine will see efficiency fall off below nominal speed).

Figure 13: installing a direct drive PMG into Natel's prototype axial flow D190 turbine.

A Variable Frequency Drive (VFD) may be paired with the generator to convert generator output frequency to the required grid frequency and quality. While not necessary for certain PMG configurations of appropriate pole count and intended fixed speed, the VFD allows for speed control and thus greater efficiency across a range of head and at partial flows. Furthermore, the drive system enables grid support and protection functions such as reactive power injection, LVRT, HVRT, and frequency stabilization, and can even enable off grid and microgrid usage. VFD costs of appropriate capacity for this module design range from $100-$200/kW; Natel has incorporated numerous price point information from suppliers such as Danfoss/Vacon, Schneider, Nidec, and Yaskawa into the turbine cost model driving summary cost analysis later in this section. The inclusion of a VFD system will hinge on site head and flow characteristics: the project team has found that often the added cost is not worth the increased production, and that significant variations (or uncertainty) in head and/or flow are needed to warrant the option.

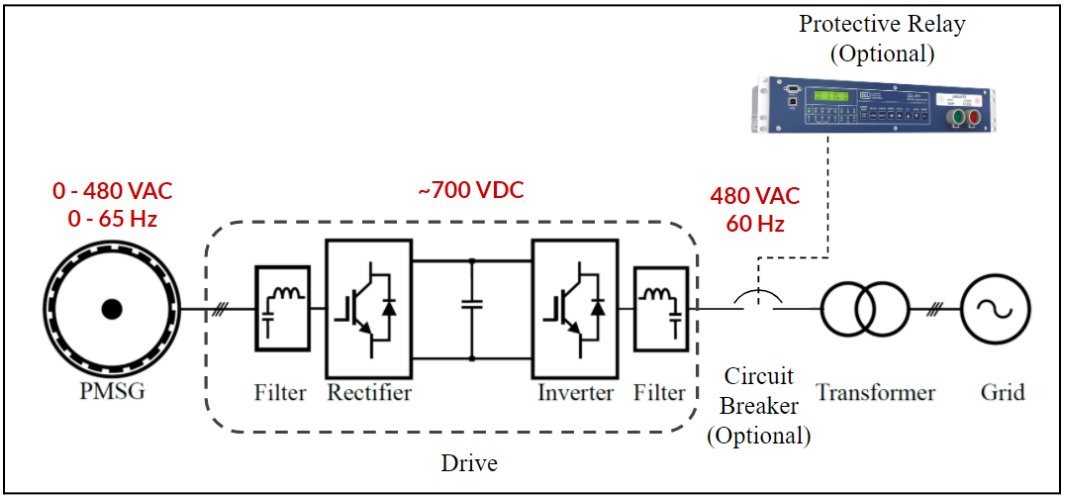

Figure 14: example one line diagram of VFD system arrangement

Surrounding the generator is a dry housing area which must be sealed. Different turbine designs approach this with different strategies, but one typical one that may be employed in this case is a pair of mechanical seals with a higher pressure buffer fluid in between (the fluid possibly being grease, oil, water, or even air). Mechanical seal options of appropriate sizes exist off the shelf from manufacturers such as John Crane (for sizes up to 4" shaft diameter) and Thordon (for larger sizes).

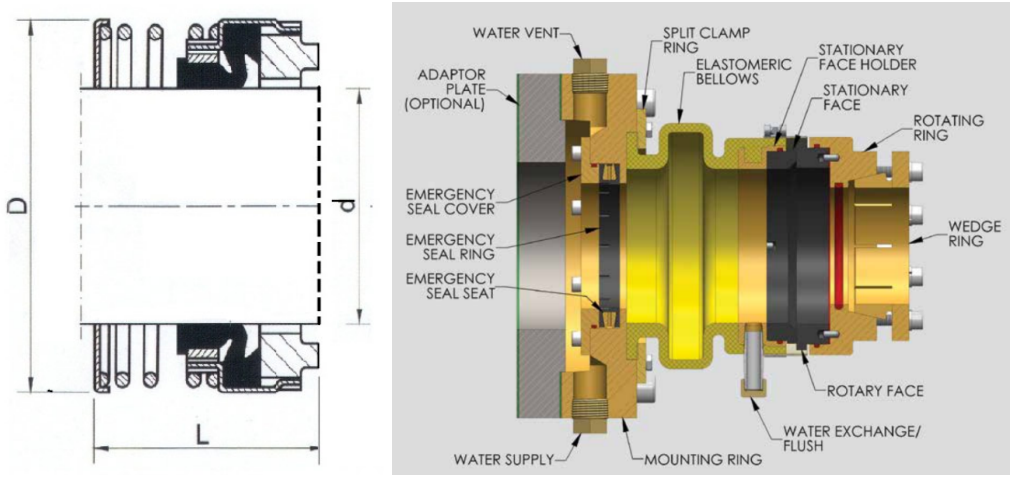

Figure 15: the type 21 mechanical seal (left, courtesy of John Crane) is commonly used in many industrial applications. For larger shafts, options exist such as this example from Thordon (right).

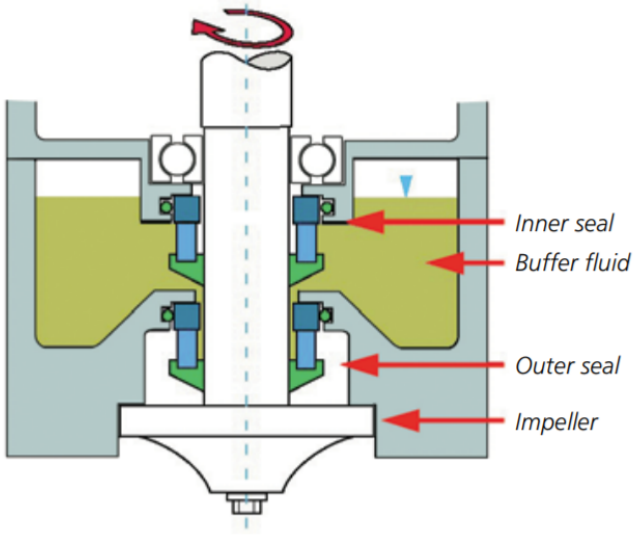

Figure 16: Flygt is one manufacturer of vertical axis submersible turbines and pumps, and their seal user guide is an informative example document for how this sealing challenge is typically addressed. (image from Flygt / Xylem)

In addition to the use of paired mechanical seals, the use of a dry gas supply (simply dry air, or some other inert gas such as nitrogen if preferred) mitigates two risks; One, dry gas in the housing will prevent the development of condensing humidity, a condition that would otherwise be challenging to avoid from any small leak over time; and two, by supplying a gas at a pressure slightly higher than the surrounding water, any potential leak that exists (from a degrading seal, or an imperfectly reassembled access hatch, etc) simply results in air leaking out rather than water leaking in. If the flow of the dry air supply increases beyond the normal very low levels, the control system can detect this as a developing leak and shut down + dewater the unit before the potential for damaging flooding occurs.

2.1.5 Module Sizing and Costing

A parametric approach was taken to develop estimations of module size, wall thicknesses, and thus costs via per unit volume or area metrics. 1x2, 2x2, 1x3, and 2x3 units were explored as well as horizontal axis types. Configurations were compared using $/kW, foundation considerations, and excavation requirements.

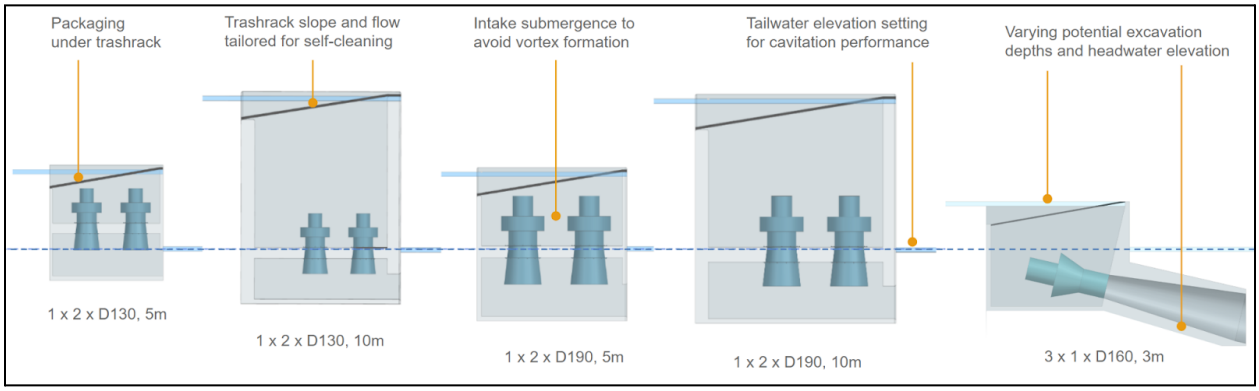

Figure 17: Elevation views of multiple configurations sharing the same tailwater elevation. Note the varying volume of the module submergence below tailwater.

Module geometry varies significantly for different head settings and turbine sizes. At higher heads, and larger runner sizes, the RHT passes more flow, and so inlet and outlet areas grow to pass sufficient flow. The tailwater elevation setting and intake submergence setting are also dependent on flow. The trash rack is set to a 10 degree slope for self-cleaning via sweeping flows. Intake submergence maintains a Froude Number (Fr) less than 0.5 to avoid vortex formation per USBR recommendations (USBR, 2016). The turbine must package underneath the trash rack. Finally, wall heights must be adjusted to meet the desired head and tailwater setting requirements.

With the plant hydraulic dimensions determined, structural sizing of the concrete panels were computed next. Simplified approaches using methods described in the American Concrete Institute's ACI-318 avoided detailed steel reinforcement design for preliminary work. The module is subdivided into a set of panels with generalized load inputs (water or concrete weight, hydrostatic pressure, turbine thrust, etc). Load Resistance Factored Design (LRFD) is used to combine dead (D) and live loads (L) into a design load input. Dead loads are treated as permanent loads, like concrete weight. Live loads are treated as a temporary input, like turbine thrust.

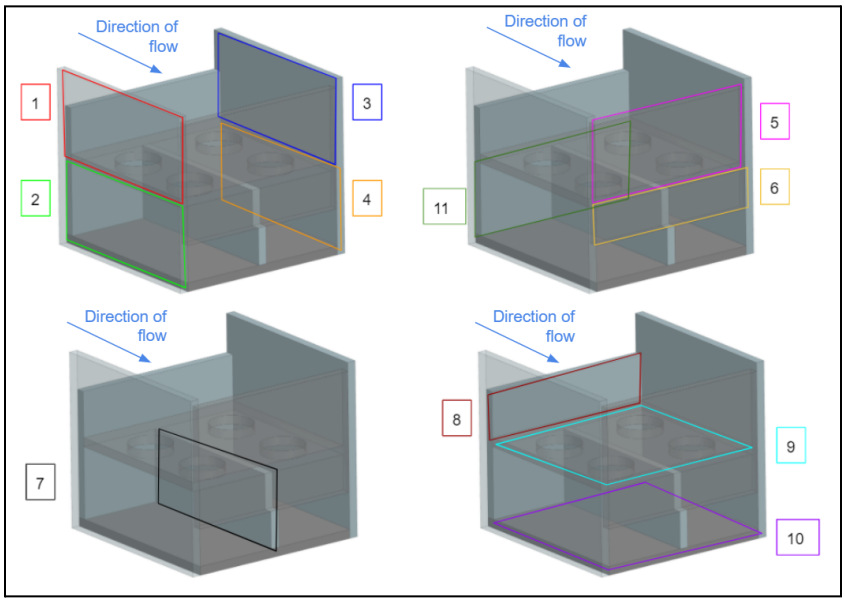

Figure 18: The bay structure is divided into 11 panels for individual analysis.

Simplified beam bending was used to compute maximum beam moment and shear in each panel for simplified scenarios. The moment is first used to calculate the required panel thickness. The spreadsheet specifically assumes a maximum reinforcement ratio required for tension control using 4 ksi concrete and 60 ksi rebar. Next, the shear capacity of the concrete and required steel reinforcement capacity are calculated using the flexure-derived thickness. A rule-of-thumb sanity check is used to ensure the panel section dimensions are sufficient for packaging the rebar stirrups needed to carry shear.

The accuracy of the moment and shear inputs to each panel vary with panel aspect ratio and the load distribution assumed. Rebar for the flexure analysis is assumed to be single-side, and flexure and shear omit packaging considerations of a given rebar bar size. Realistically a final design of concrete slab would consider the cost per strength of the rebar size chosen as well as the manufacturing complexity of assembling the rebar form.

It is important to note that the structural analyses did not assume any load sharing between modules. Walls perpendicular to the flow are designed to fully withstand the single-sided hydraulic load without any support from an adjacent bay. This maximizes compatibility with other adjacent modules, like recreation, that would not provide any support to the bay structure.

For cost modeling, volumetric costs inclusive of reinforcement and formwork were used ranging from $500 (slab), $700-800 (wall, pier) to $1000 (elevated slab). per cubic yard. These typical industry costs were derived from market data in 2020 and prior; it should be noted that 2021 and 2022 saw substantial swings in supply chain and labor costs (for steel as well as concrete) and

these numbers are low for today's market. Some rebound is expected, but the reader is encouraged to conduct additional research before utilizing these figures.

In addition to concrete, other non-turbine module cost contributors were estimated: trash rack (~$700/m^2 for 3 inch spacing), sliding gates for dewatering (actuated, $5500/m^2) or inflatable for headwater control ($11,000/m^2).

Electrical and fluid lines need to route from the turbines in the generation module to the interconnection module on shore. Figure 19 shows a simple approach for routing between adjacent generation modules. Steel pipe can be inserted in a hole on the sidewalls. Internal and external clearance to the pipe that are sealed with caulking or grout will permit some misalignment between modules. To prevent flow from seeping between modules, some or all of the perimeter between modules can be grouted. Again, this allows for misalignment between modules since exactly placing large concrete structures is not feasible. Routing should be placed on the inside of the upstream (head) wall, to maximize protection from debris. Conduits would likely need to be outfitted with dedicated junctions or bulkheads to permit easy addition or removal of adjacent generation modules.

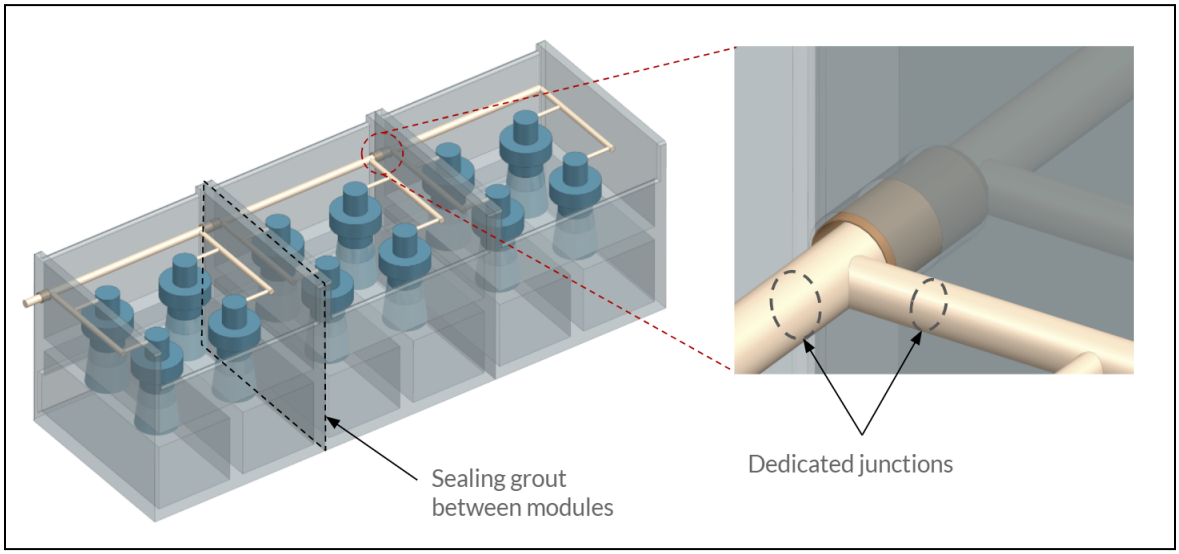

Figure 19: illustration of routing inside and between modules

The project team considered it important to develop a foundation module concept while designing the bay structure; despite not being directly in scope, a generation module placing undue requirements on a modular foundation would be baseless. For this assessment, module to foundation loads were evaluated and foundation concepts considered. Varying states of watered- and de-watered module bays were assessed for buoyant uplift conditions.

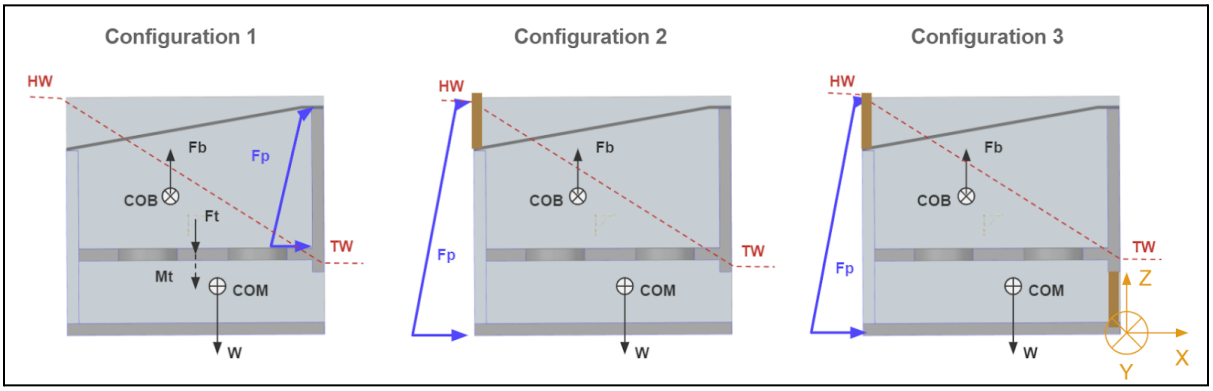

Figure 20: three static loading configurations for foundation load derivation: 1 (fully flooded and operating), 2 (non-operating, upper bay dewatered), 3 (fully dewatered).

This analysis showed that the foundation interface was always in compression in cases 1 and 2, but when the discharge bay is dewatered, net tension at some areas is seen. This could be addressed with additional ballasting, should the foundation interface benefit from consistent compression-only load.

Piles are a typical foundation approach where they may be driven into the bed at a given site. These can be connected to other concrete structures, but also frequently interface with wood or steel. The pile foundation module concept utilizes vertical and angled piers for reacting the net compression and shear that the module imposes on the foundation. The angled piles help efficiently react shear between the generation module and foundation module. Piles would be grouted into the bay structure's vertical walls. The exact length, diameter, number, and depth would ultimately be influenced by the soil type and capacity at the site, as well as compatibility with other module foundation loads.

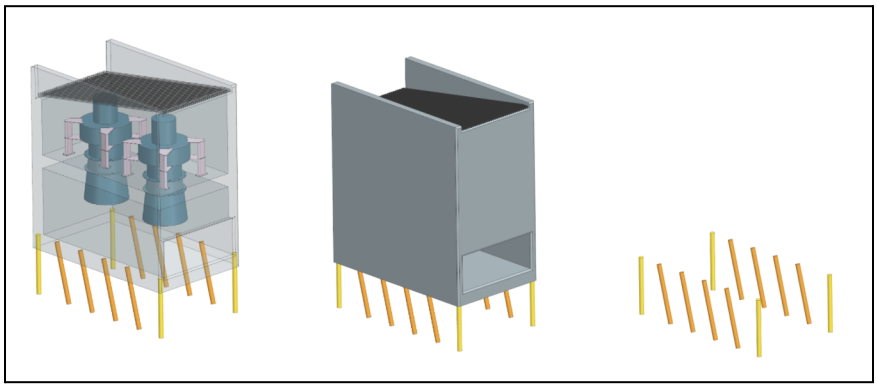

Figure 21: pile foundation approach

A pile foundation works best when the foundation module does not need to be a large slab of concrete. However, there is a similar foundation interface approach using long threaded rods that would let the generation module sit on a concrete foundation slab. Steel threaded rod can be

grouted into the slab, and similarly extended up into the generation modules. The rod would be grouted in place, and the interface pre-tensioned via a nut.

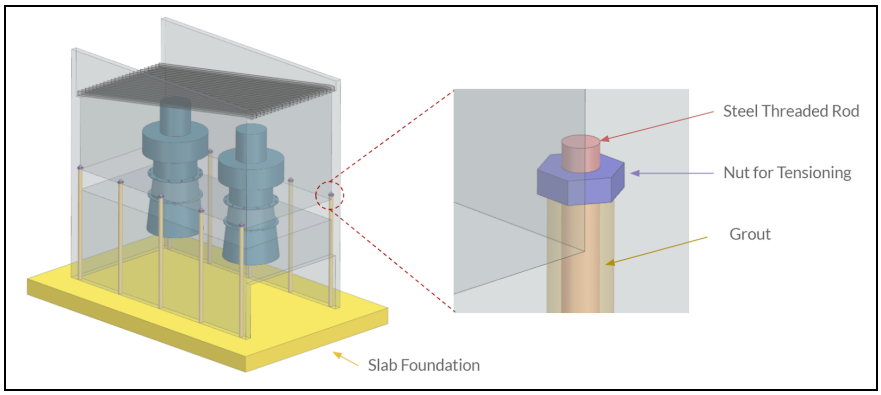

Figure 22: slab and threaded rod approach

The bay structure should be cast onsite using modular formwork to avoid the excessive cost of shipping concrete preforms. Depending on the site, the bay structure could be fully constructed on shore and then either floated and sunk into place, or lifted into place via a crane. A fully dewatered module tends to float. If the tailwater elevation is shorter than the depth to which the module will sink for neutral buoyancy, inflatable buoyancy ballast would be needed to float the module.

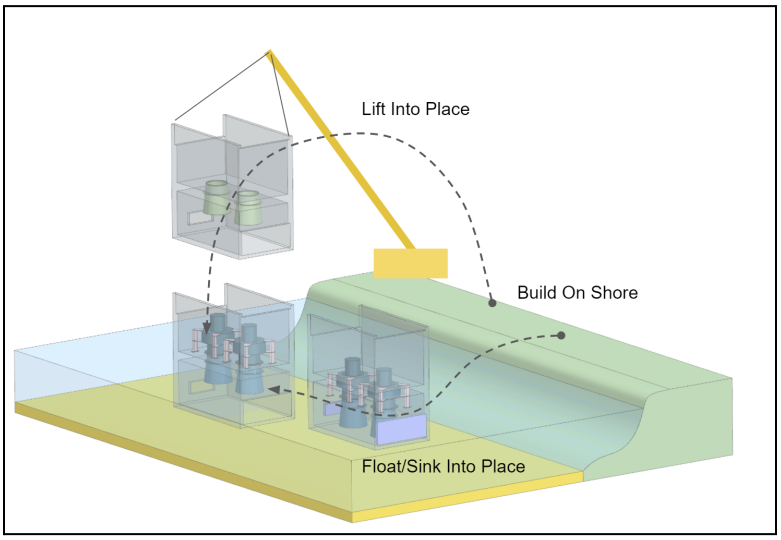

Figure 23: module assembly onshore, followed by placement

Alternatively, forms and rebar can be placed in the waterway (locally dewatered) and the structure cast in-place. This approach would avoid incurring the cost associated with lifting or floating the module and provide easier access to the foundation. One potential challenge of large concrete castings is shrinkage-induced cracking - this risk can be mitigated by pre-placing large aggregate in the forms before pumping in the cement.

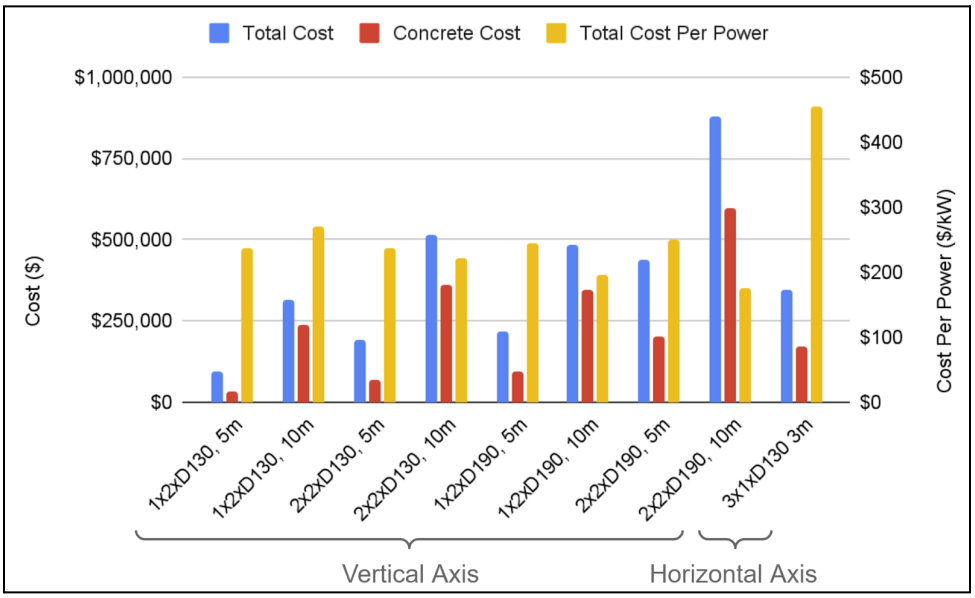

Figure 24: cost estimates for module structures (turbine and generator equipment excluded). The most economic are of course the higher head options; of more interest is that the wider modules (2x in width) are only slightly more economical than their single tandem counterparts.

Installation costs were estimated based on equipment mobilization and demob costs, onsite labor and supervision for the structural and routing work, and turbine installation and commissioning time. For the following estimate of installation costs, mobile shoreside crane(s) lift and set module formwork with integrated formwork and reinforcements into place on the prepared foundation; concrete is pumped in situ; turbines are placed followed by intermodule routing work and then commissioning. Coffering is not included - the modular approach targets reusable formwork that would be sunk into position and displace the working area.

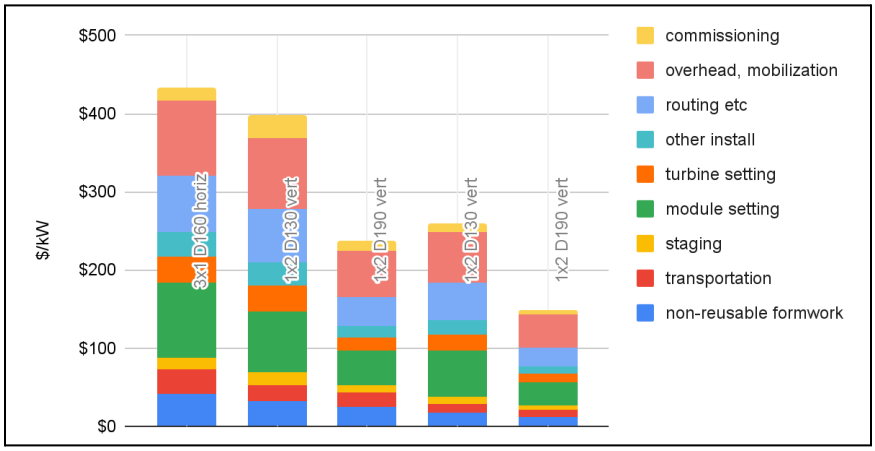

Figure 25: per-module installation and commissioning estimate, $/kW

With installation and civil work estimations, the remaining elements contributing to cost (turbine and generator, auxiliary systems and shoreside equipment with housing) can be estimated.

module type	3x1 D160 horiz	1x2 D130 vert	1x2 D190 vert	1x2 D130 vert	1x2 D190 vert
net head [m]	**3**	**5**	**5**	**10**	**10**
install and commissioning	$255,000	$138,000	$167,000	$258,000	$306,000
non-reusable formwork	$29,160	$13,200	$22,080	$20,520	$30,600
transportation to site	$21,690	$8,100	$15,720	$11,130	$20,250
Price (T&G, module)	$3,686,250	$1,492,500	$2,553,750	$2,045,000	$3,461,250
Total installed	$3,992,100	$1,651,800	$2,758,550	$2,334,650	$3,818,100
Total $/kW installed	**$5,663**	**$4,130**	**$3,208**	**$2,085**	**$1,591**

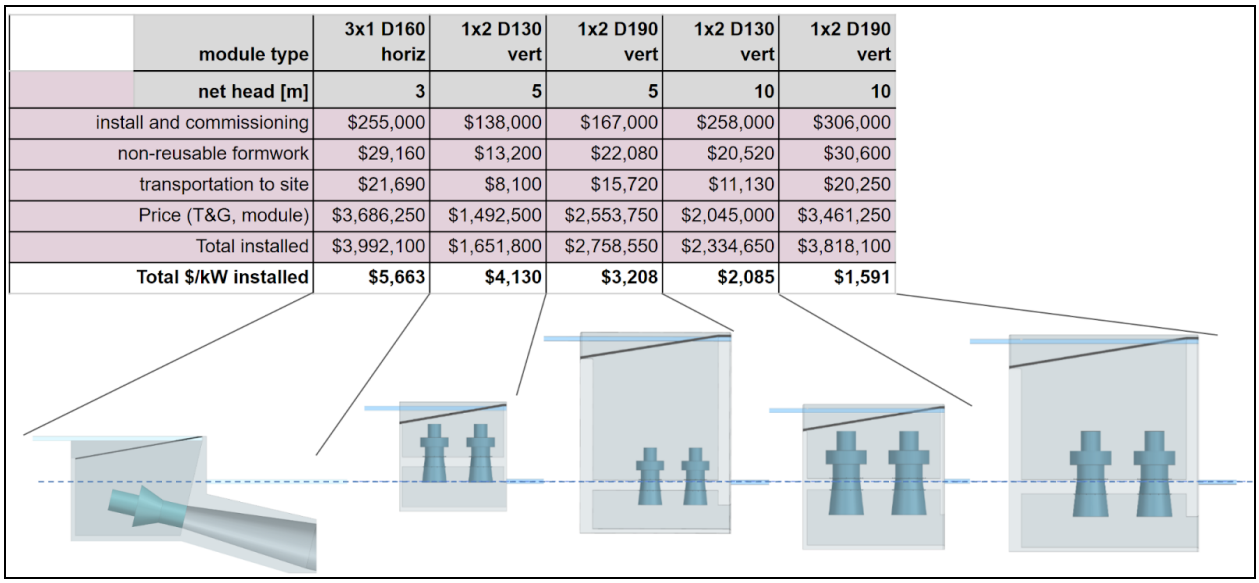

Figure 26: total installed cost for a range of module designs. Here, "non reusable formwork" refers to the subset of formwork which cannot be reused for additional modules (thus, only a subset of the required formwork).

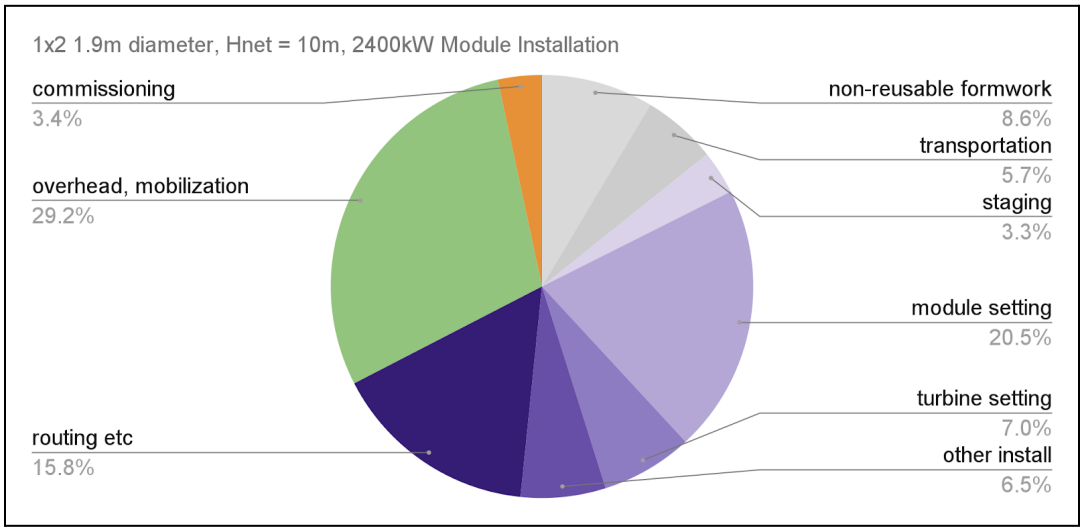

Figure 27: breakdown of module installation cost for a 2.4MW module example

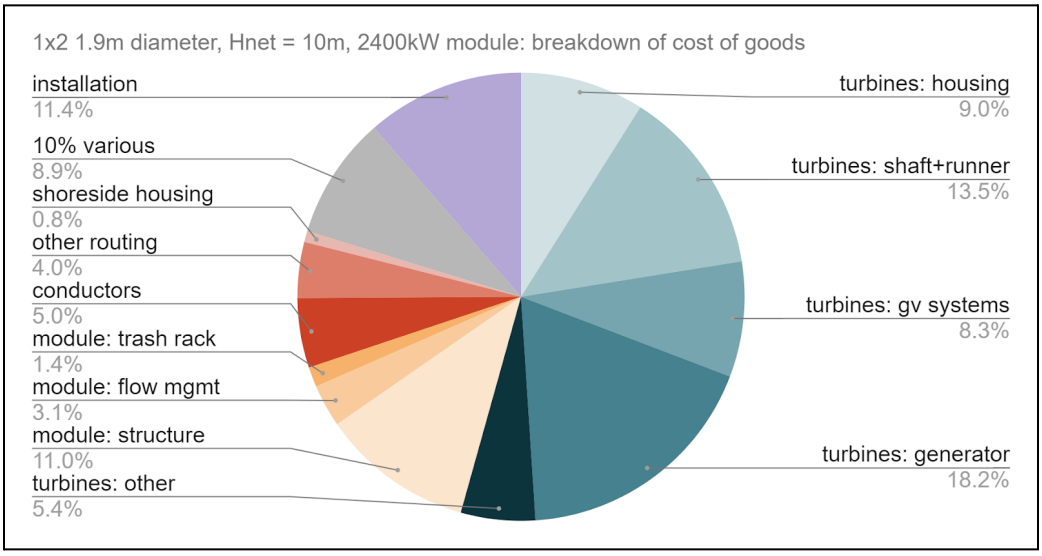

Figure 28: breakdown of module cost of goods sold for a 2.4MW module example

Operations and maintenance (O&M) costs were also estimated for the modules once installed. Here it is very important to compare to industry typical values as it can be quite risky to attempt to thoroughly estimate annual service costs in isolation. Some data is available in the US Hydropower Market Reports published by WPTO and these data suggest that overall plant O&M for plant capacity ~1MW could range from $30-$700/kW-yr with most data clustering around $70-300/kW-yr (2015$). It should be noted that a majority of these costs are plant service costs not directly related to the generation module that is the scope of this work: supervision, water fees, utility costs, rents, and overall plant maintenance is included. This dataset is also not comprehensively representative of the industry - only those plants reporting O&M expenditures on FERC Form 1 are included. The proportion of this annual cost that is directly servicing a generation module might be 30%, though this will vary as much as the top level numbers vary.

ORNL's recent study of industry O&M data resulted in a recommended estimation model of annual cost = $225,500 * $P^{0.547}$, in 2014$, with P in MW (O'Connor et al, 2015). Again, this includes all plant service and operations costs, not only that for the scope of a generating module. For the 1MW example plant this of course becomes $225,500 annually or $225/kW-yr. For a 10MW plant (four parallel 1x2 1.9m-diameter modules of the design discussed above) then annual cost is $800,000 or $80/kW-yr. R^2 for this fit to the studied data was 0.56 - scatter is significant, though the trend certainly is for proportionately decreasing costs at higher capacity. If we estimate a generation module alone as having 1/3rd of the O&M cost of a typical entire plant, then we arrive at $27-75/kW-yr ($32-90/kW-yr in 2022$).

Another typical way for estimating O&M is referred to as the "ICC Model" and is simply 2.5% annually of the upfront Installed Cost of Capital, resulting in similar ranges.

In addition to looking at O&M from a top-down, industry baseline perspective, the project team also estimated service costs for a generation model in a bottom-up manner. For this an activity based model was developed, tracking activities both planned (known service actions at specified intervals) and unplanned (issues arising in some fraction of the units over time, requiring repair or component replacement). Replacement parts cost was estimated as either fixed value or proportional to the cost of the subsystem needing service; additionally, the cost of shipping repair components was included, as was onsite labor time. Mobilization and demobilization, as well as any work required to either access the equipment or move it to a service location, was not included meaning these model estimates will be low. This study yielded annual estimates on the order of $10-15/kW-yr for a 10MW example - 2-3x lower than industry data suggests. It is quite reasonable to expect that mob+demob+access costs would bring these numbers closer to typical values.

It is likely that many projects would benefit from the inclusion of a gantry crane system. Though this adds to upfront cost as well as the complexity of inter-module alignment and rail mounting, this is recommended for consideration where plant designs locate modules in positions where a relatively small and easily mobilized truck mounted crane cannot reach the service areas. Gantry crane costs are a function of crane capacity, span, height, and location of manufacture (with domestic equipment ~3x the cost of overseas options). Cost estimation scaling from equipment quotes indicates that the threshold at which the addition of a crane would not increase cost more than $100/kW (and significantly reduce O&M mobilization costs) is for plant designs that have 2 to 5 generation modules. Thus, plants with one or two generation modules can situate these adjacent to the shore and not require a permanent crane; for modular designs larger than this where the plant extends further, a gantry crane is easily justified.

2.1.6 Performance Analysis and Optimization

At the onset of this project, Natel Energy had developed the hydraulic shape of the RHT runner utilized within this module design. The hydraulic efficiency of this design had been tested within Computational Fluid Dynamics (CFD) tools as well as in scale model testing (in conformance with PTC-18 and IEC 60193 standards) to show >90% peak hydraulic efficiency. However, the runner itself had not been studied within the context of an open flume module and intake, with multiple units in series; nor had the fish safety of the design been assessed outside of scaled down laboratory strike studies (Amaral et al, 2020; see also the passage testing section of this report).

STAR-CCM+ was utilized for all CFD work in this report. A module modeling process was developed to capture important multiphase and water surface behavior, while simplifying the overall mesh size sufficiently to allow for iterative design and testing. Multiple units are arranged in tandem and use the ‘porous baffle’ method to apply a known headloss across the runner,

enabling the study of 3D behavior of flow into and out of the units and thereby enable the optimization of geometry and the avoidance of key risks such as vortex ingestion.

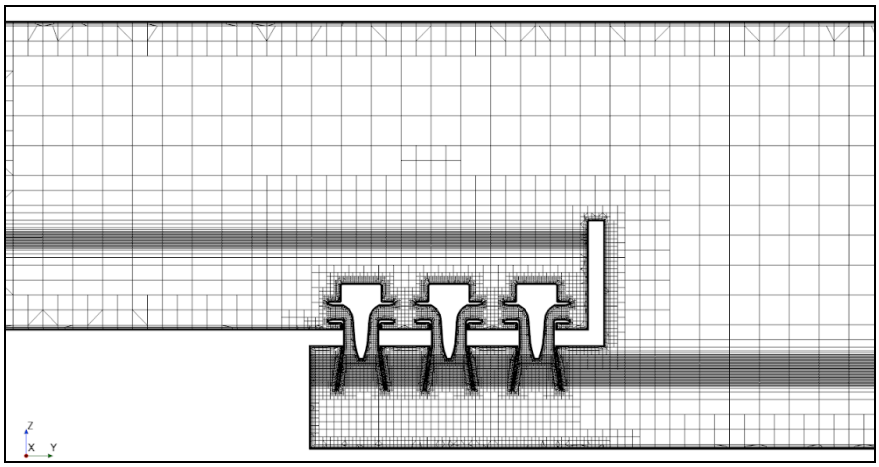

Figure 29: example of a module mesh for CFD study and optimization. Note the refined mesh areas to capture behavior of interest within the turbine areas as well as at the interfaces between water and air.

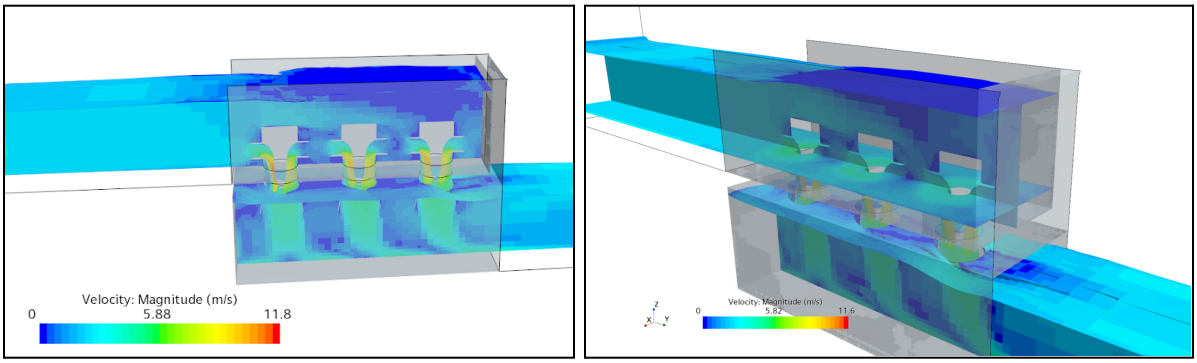

Figure 30: using this analysis setup, inflow and discharge velocity profiles may be quantified along with total pressure (head) losses.

With the methodology developed and tested, baseline turbine geometries (developed and tested outside of the context of the open flume overflowed bay) could be situated together and tested. One major area to evaluate were the overall module proportions, which had been estimated via spreadsheet to match reasonable inflow and outflow velocities but had not been shown to be suitable for sufficiently uniform unit inflow and reasonable intake + discharge headloss (overall module efficiency). Additionally, geometry of the turbine intake and draft tube was studied to achieve optimal proportions and performance, keeping required concrete volume and excavation to a minimum.

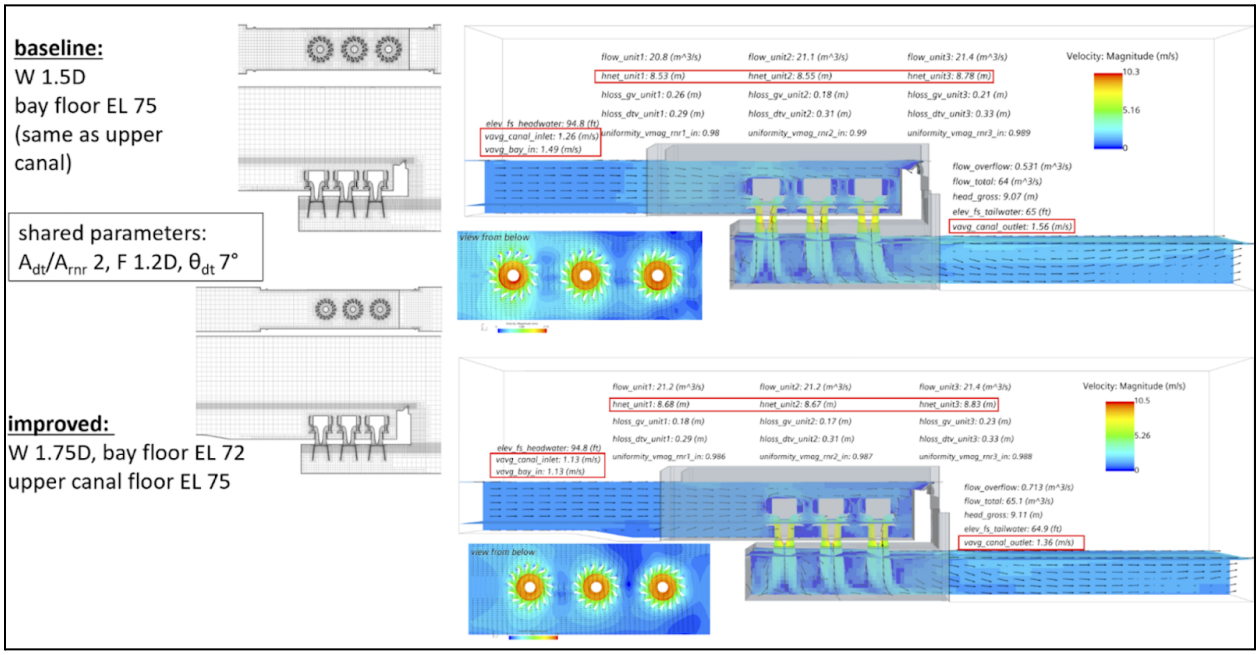

Figure 31: optimization of bay proportions to achieve acceptable trash rack and outlet velocity headloss.

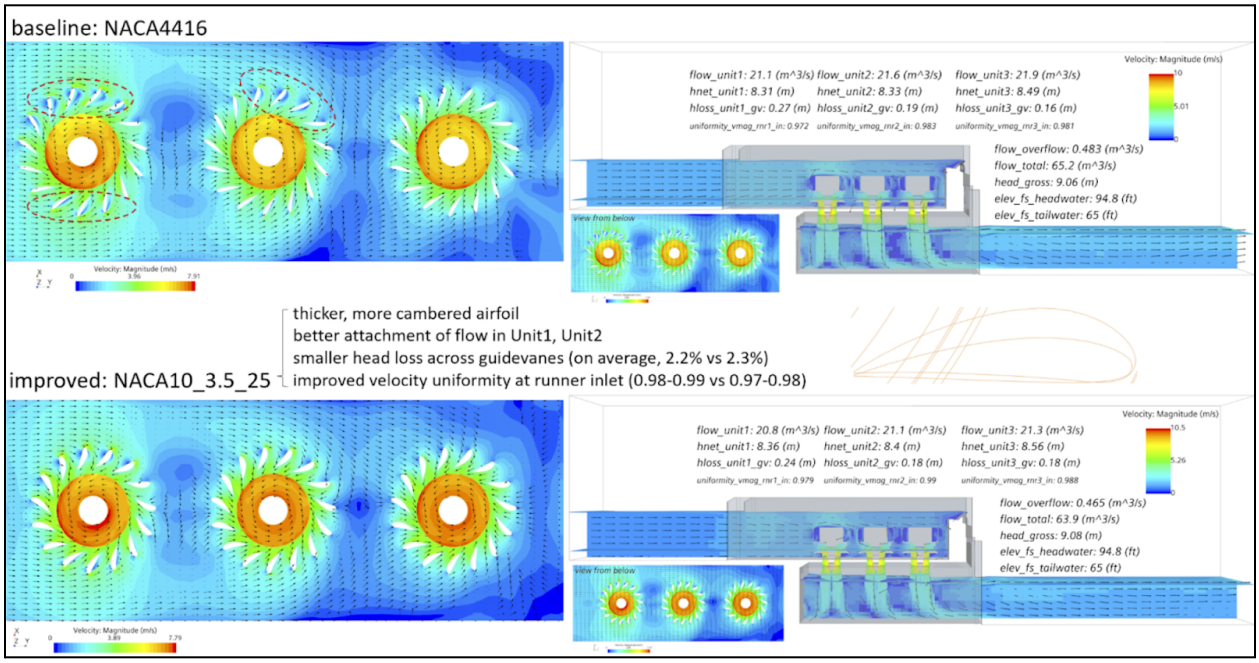

Figure 32: studying the effect of radial inflow guidevane geometry in a tandem open flume intake where flow conditions vary significantly between the most upstream and most downstream units.. Here, thicker airfoils with greater camber resulted in improved flow attachment across each condition and improved runner inflow uniformity.

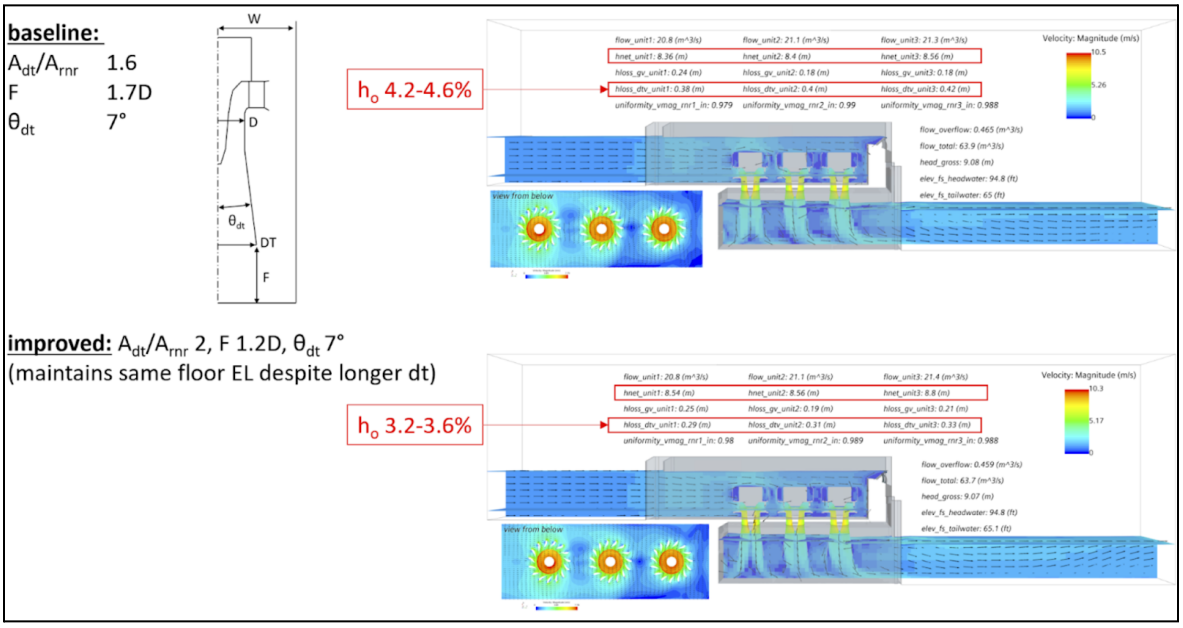

Figure 33: optimization of draft tube size and outlet channel clearance for the same level of excavation, decreasing overall module headloss from a baseline design.

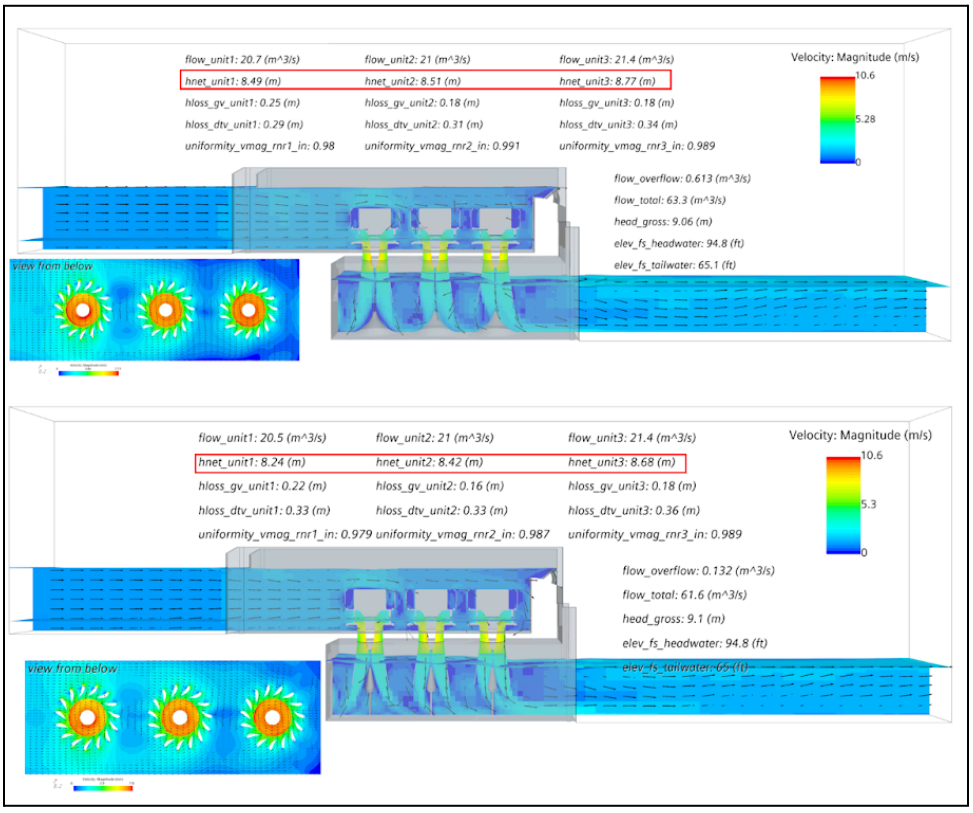

Figure 34: draft tube "insert" variants were tested to see if they would reduce headloss under close exit clearance to the outlet channel floor. These geometries were shown to increase overall headloss (baseline 8.6m of net head, reduced to an average 8.5m when tested).

Axial inflow variants were also tested in comparison with radial inflow units. Radial inflow intakes are structurally simpler and lower cost, have more space for reasonably sized submerged generators, and additionally have less of an intake vortex formation concern from the above water surface compared to vertically oriented axial intakes. However, the axial designs allow for more compact module sizes (20% reduction) and so may be worth considering in some cases.

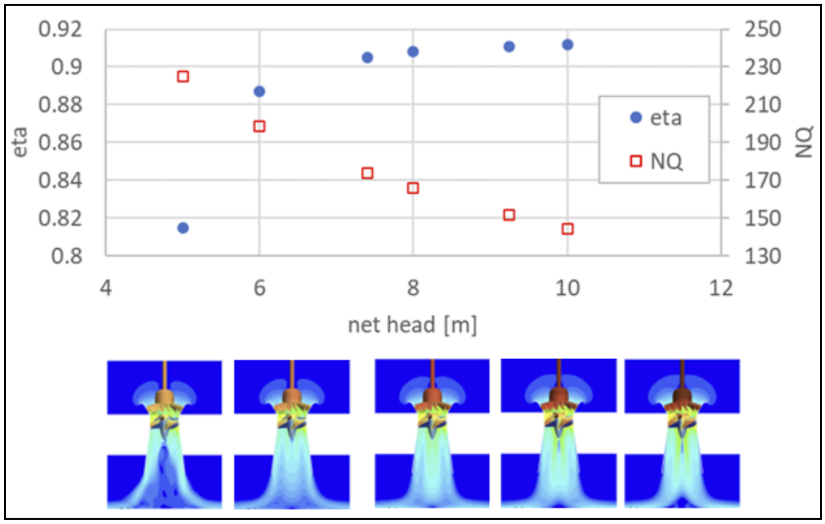

Figure 35: a sweep of module operating head for a vertical axial-inflow arrangement with fixed speed and blade pitch. A small 3% efficiency variation for a significant (40%) variation in net head is seen, demonstrating the suitability for module application under typical run of river conditions where head and tailwater level may be highly variable.

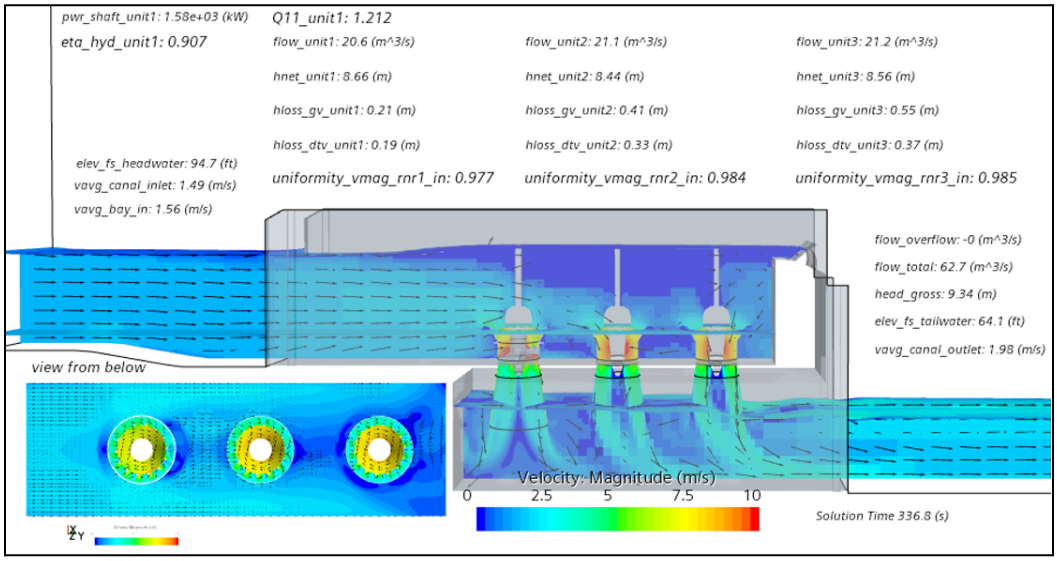

Figure 36: study of a 3-unit tandem arrangement demonstrating acceptable inflow and discharge behavior (overall head loss <4%). Axial-flow intakes allow significant reduction in bay width (2.75D vs 3.5D; 20% reduction) and are also less affected by the inherent cross-flow conditions, vs radial-inflow intakes. Risk of intake vortex formation is increased, however.

Trash accumulation and cleaning behavior was also simulated using CFD through the application of different types of Discrete Element Model (DEM) particles. Compact spherical debris, elongated "log" shapes, and stringy neutrally buoyant particles were simulated. Some challenges were encountered in the simulation of such debris behavior, including the accumulation of an excessive number of degrees of freedom within the simulation domain (slowing and at times halting the simulation) as well as limitations in trash element complexity (branching, bending) that would affect how they might accumulate and interlock against a trash rack. Nonetheless these simulations provided some valuable insight into the behavior of floating and neutrally buoyant debris, and allowed for the initial demonstration of some cleaning behaviors that temporarily direct more flow over rather than through the module. With a flushing cycle taking 30-60 seconds, 5-10 cycles a day could be easily accommodated with a minimal impact (less than 0.5%) on production. For an example 1.5MW module at 70% capacity factor with $50/MWh offtake, lost generation would be <$2000 annually; when compared with an automated trash rake at ~$60,000 for this example size ($3500 per foot of width, approximately, per reference quotes obtained by Natel Energy) this cost compares quite favorably, especially when considering service of the rake, as well as its exposure to damage during flood events, is eliminated.

This project did not allow for an in depth study of these debris modeling techniques and processes; further work in this area may be warranted to enable more effective module and plant design.

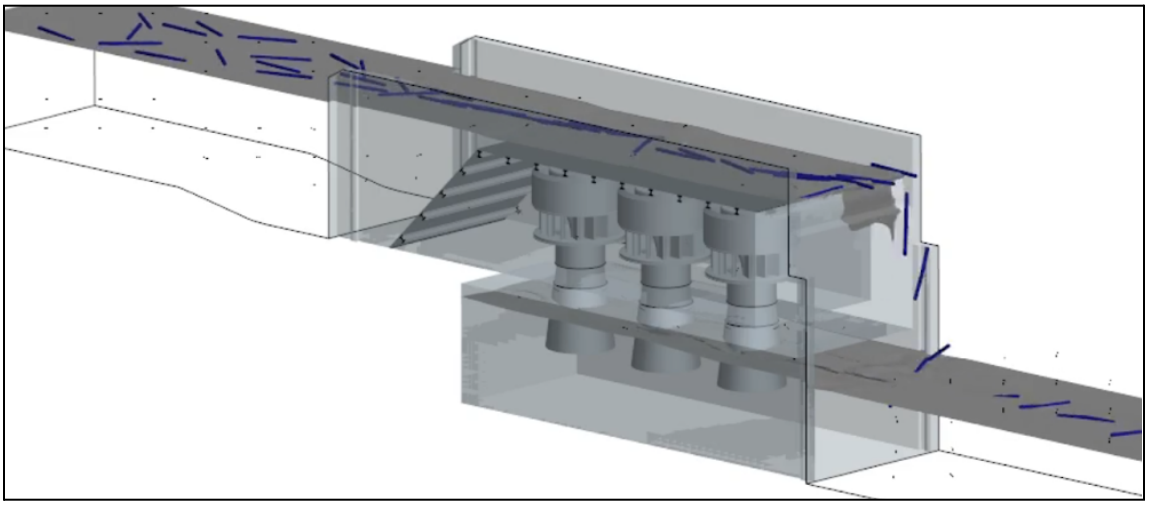

Figure 37: floating "log" particles are simulated to pass across the overflowed trash rack. Bay inflow conditions tend to align the debris with the bay as they enter; however, more complex debris (with branches or other snagging features) was not simulated. Neutrally buoyant weedy debris were simulated, however this became computationally prohibitive as excessive degrees of freedom were accumulated. Improving upon this type of debris analysis could be the subject of future research.

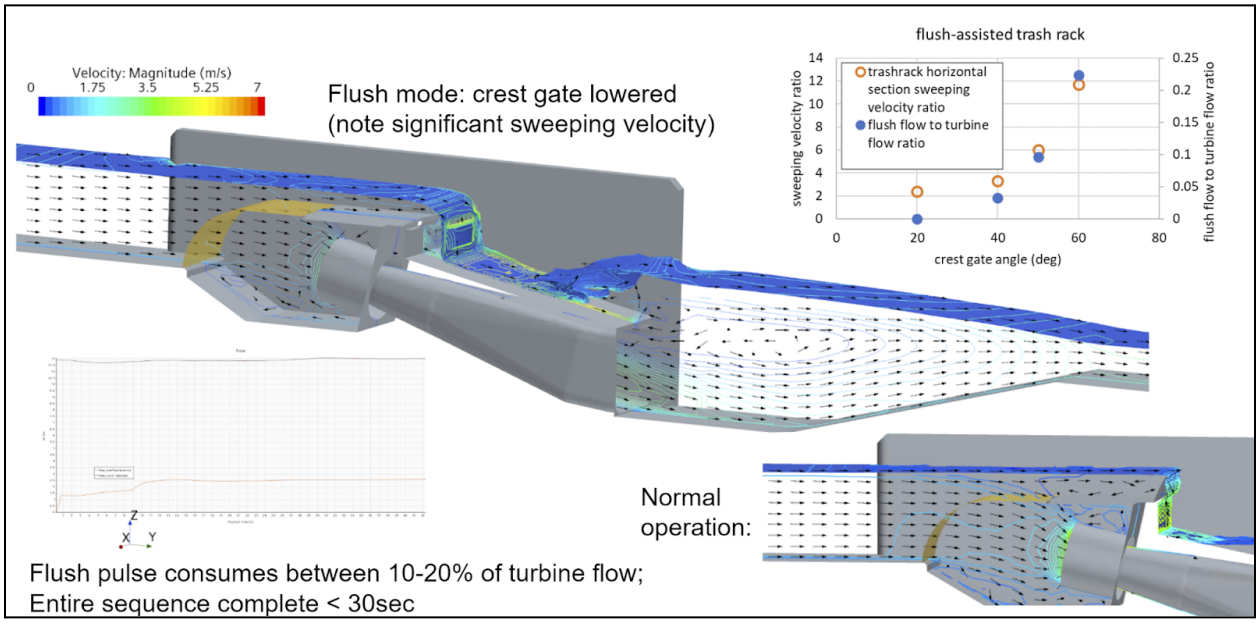

Figure 38: studying flush-assisted debris passage to achieve sweeping velocities across an overflow design.

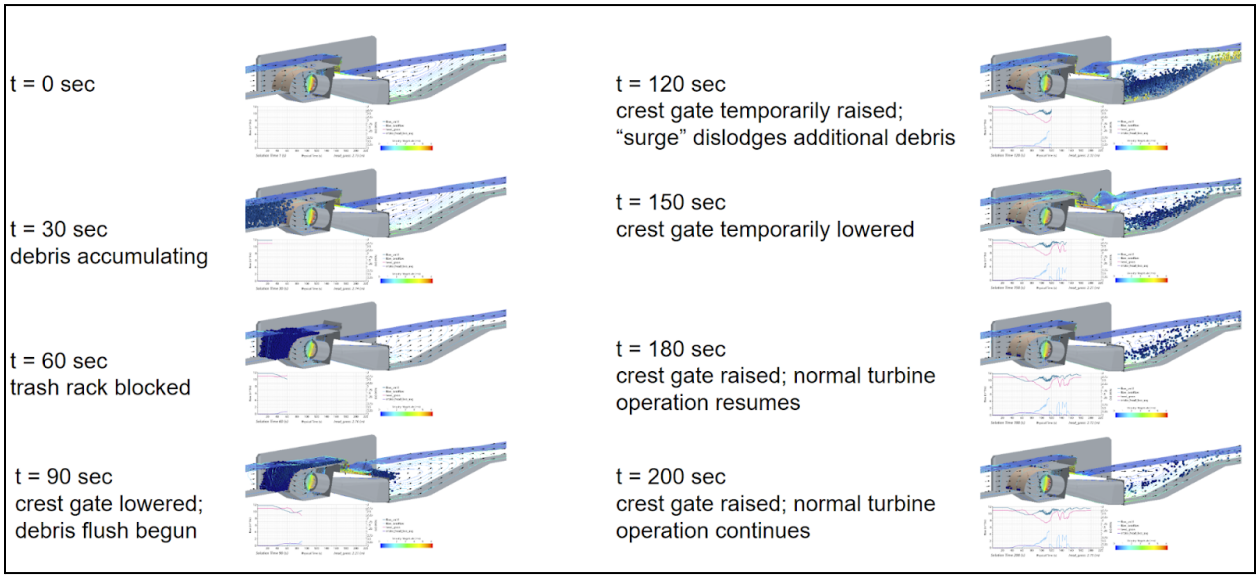

Figure 39: stages in a debris flushing simulation using discrete element modeled particles within a CFD solution.

2.1.7 System Design Reviews

Two module system level design review sessions were conducted within the project team, leveraging participants with extensive experience in both the civil and electromechanical (turbine + generator) aspects of low head hydro design. Discussion of critical features and options covered topics such as sealed and submerged unit design; guidevane system actuation

mechanisms and failure modes; civil structural design and stability; interfaces to foundation elements and appropriate foundation design; site flow management and trash rack design; and sediment management / flushing gates. Overall the design approaches described herein were found to be satisfactory.

Some of the summarize some of the notable takeaways here:

- Direct drive PMG approach is a good one for simplicity and reliability.
- Pressure housing for dry bulb area with dry gas (air or other) is commonly done and often uses monitoring of both pressure and flow of the gas, the latter being an indication of a developing leak.
- Sloped self cleaning rack designs work well (maintain a cross flow ratio of 1:4 or better); the flat rack presented is better than some other designs seen by the team which used a cylindrical shaped rack and an arc-following rack. The self cleaning approach works well for clearing most debris. Could easily have hinged section(s) for access and turbine component removal. A method to manage vacuum pressure should be considered should the racks become totally clogged, as well as considering this a design load case for the rack support system. Air blast systems might be incorporated but will likely be less efficient with a wider spaced bar rack than with tighter screen spacing.
- Installing units or other features at an incline (some angle other than horizontal or vertical) adds challenges and thus cost for contract work. Formwork, alignment etc are more easily done when plumb or horizontal.
- Hydraulic, electric, and pneumatic guidevane actuation options were discussed (with the latter noted as being quite difficult to manage, as a force rather than displacement applicator). Sometimes a pneumatic fail-closed (deadman) is envisioned as being paired with a electromechanical actuator. Hydraulics are certainly the most common.
- Civil module design: approach looks robust for preliminary level; detailed design would need to look more closely at reinforcement design and corner loads.
- Stability of the module was emphasized, considering dewatering conditions; it would be preferable to not need to transmit net upward buoyant load to foundation elements.
- Gate design: vertical or rotating gate types are preferable. A butterfly type flush gate would encounter issues. It’s not worth coupling an intake gate with a flushing gate; it is necessary to be able to work on the module without necessarily needing to waste flow through a lower bay flush.
- Conduit is recommended to be mounted on the upstream wall to be the most out of the way, with robust connections. If it prefers to be on the outside of the module on the downstream face, a steel flow shape on the overflow will help prevent water and debris from hitting components.
- On installation: it’s likely a dry foundation area will want to be created to construct the foundation; this depends on the size of the waterway the work is being done on and how

it can be reached (from shore, by barge, etc). Could then possibly place the forms in the water and float them into place, then pump the concrete in situ. Pumping concrete is relatively easy compared to the difficulty of moving heavy components. Sacrificial stay-in-place forms may be necessary (not all formwork will be reusable) to allow for light weight formed modules to be placed followed by concrete filling.

- A bulkhead system for module dewatering can be utilized for projects that have crane access.
- Applicable to the adjacent Foundation Module: Need to design this module against seepage underneath the structure. Can the base of the module and the foundation floor be the same thing? No reason to double up, if there is going to be a slab. Piles or slab, either could be a good solution, and it will depend on the makeup of the streambed where the site is located.
- A few different ways to connect the module to foundation components: could essentially grout the entirety in place, and post tension with anchor rods. Those anchor rods need to be in chases that can then be grouted full to prevent corrosion. Or with piles, these could simply be captured within an in-situ concrete pour; or there could be mating dowel-type interfaces.

2.1.8 Summary of Findings

- Overflowed generation modules of the designs presented can be reasonably sized to achieve acceptable head losses (<4%) and high turbine inflow uniformity and efficiency (>90%).
- Direct drive permanent magnet generators should be utilized for their high torque density (compact nature) in overflowed designs. These units can be combined with variable frequency drive equipment in cases where variable speed is beneficial to energy production (sites with highly variable flow and/or head). Pressurized dry gas should be used to ensure flood risk of the generator bell is minimized.
- Modular formwork should be combined with in-place concrete pouring to construct the module walls; each turbine+generator within the multiunit module should be treated as a service unit and can be conveniently extracted for shoreside service, leaving the module in place to continue to serve its structural and impoundment functions.
- Choices of generation module to foundation module interface will depend in part on site specific conditions; the module presented is compatible with multiple practical foundation approaches.
- Total installed cost for module designs presented range from $1600/kW to over $5000/kW, with site head being the largest factor affecting project economics. 6-7m sites and above will be suitable for the designs studied, and projects with head less than this will need other economic advantages that will decrease the cost of surrounding plant equipment (close proximity to interconnection, existing non powered structure, etc).

2.2 Safe Fish Passage

2.2.1 Discussion and Motivation

Natel Energy's vision for fish-safe hydropower, enabled by the Restoration Hydro Turbine (RHT), is one in which the generating turbine units additionally serve as viable downstream passage routes for fish. This is in contrast to the current standard for protection at hydropower facilities, which as defined by the 2019 release of the USFWS R5 Fish Passage Engineering Design Criteria document "does not recognize passage through the turbine intakes as an acceptable downstream route for fish" (USFWS 2019). The reason for this is expressly stated as an "absence of better information" and is based on the historical lack of comprehensive, peer-reviewed scientific study of fish passage through the turbine units.

Exclusion measures, such as fine screening in combination with guidance to one or more dedicated bypasses, are generally accepted as the mechanism for enabling hydropower operation while managing downstream passage of fish. In the best case, exclusion screens divert fish to a fraction of the downstream flow that is not being used for generation, and the fish incur no delays or injuries along the way. However, generation losses still occur due to the diversion of available flow and the head loss of the screening infrastructure. Worse outcomes for both hydropower generation and fish health can occur if exclusion systems are improperly designed.

Bypasses, by definition, divert flow from the turbines and as such are typically constructed to meet minimum flow requirements mandated by regulators (for example, 5% of station hydraulic capacity) so they can be difficult for fish to utilize (Oividio 2016, Jansen 2007, USFWS 2019). Additionally, extreme care must be taken to ensure that exclusion screens at turbine intakes are free from localized hydraulic effects that can cause impingement injury and mortality for weaker swimmers (Hanson 1977, Calles 2010). While extensive engineering guidelines exist to inform the design of exclusion systems that keep fish from entering turbines, effectively guide fish to small bypasses, and avoid causing injuries to the fish themselves (i.e. impingement), the custom nature of plant design leaves the actual effectiveness of exclusion systems far from guaranteed (Oividio 2016). If site-specific studies show that these measures fail to perform as expected, costly shutdowns may be required to protect fish populations at the site. Even managed spill, intended as a fish protection measure, can cause migration delays and sublethal injuries (Coutant 2006). This difficult reality leaves the hydropower industry and fish protection community with a real appetite for fish protection solutions that simultaneously provide effective downstream fish passage and economical hydropower plant operations.

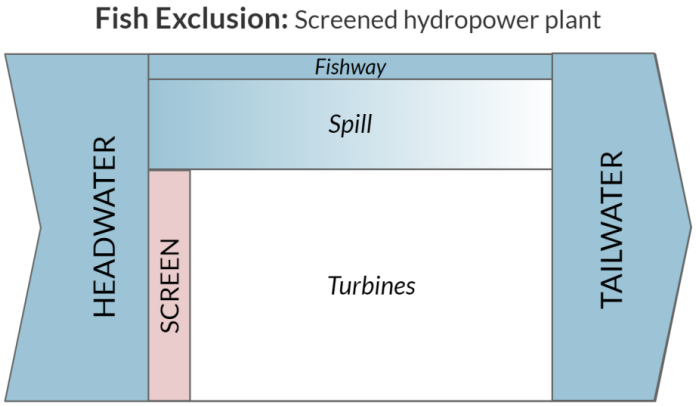

Figure 40: Schematic of a conventional screened hydropower plant, where viable downstream pathways (fishway and occasional spill) are colored in blue, and screen impingement injury and turbine passage are colored in red to indicate injury and mortality risk.

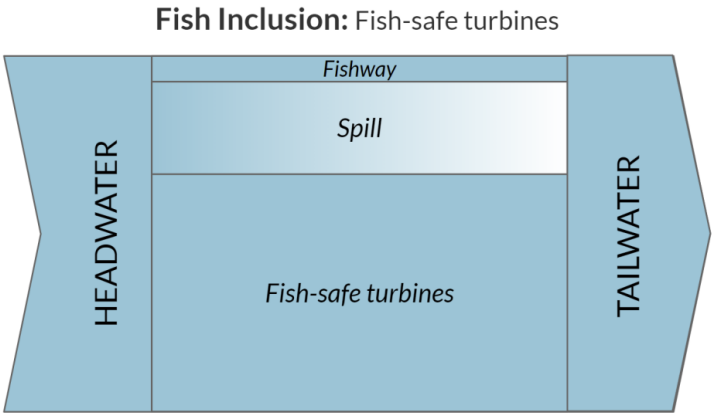

Figure 41: Schematic of an ideal hydropower plant equipped with fish-safe turbines, where all downstream passage routes are viable for fish.

A better way to achieve hydropower development and fishery management targets is through the use of fish-safe turbines. These turbines would benefit fish by opening up all or nearly all of the downstream flow to the vast majority of passing fish which are small enough to fit through a conventional trash rack (approximately 2" spacing) and eliminate impingement risks. They would simplify plant operations by minimizing site-specific engineering, monitoring, and maintenance, and would avoid generation losses associated with screening and shutdowns (Figure 41). True fish safety must be addressed at the plant level. It necessitates safe, timely, and effective upstream and downstream passage—no less of an impediment than natural features of the waterway. In the context of this project, which is focused on downstream passage, it requires safe through-turbine passage for fish that can pass through standard trash racks, and effective bypasses for large fish that cannot fit through trash racks, like large adult sturgeon. Target

survival rates for fish must consider species sensitivity and life cycle, such as the number of dams that fish must pass to reach spawning grounds.

Just as other elements of turbine performance (i.e. efficiency, power, cavitation) are characterized for laboratory-scale turbine models and applied to their performance in the field, rigorous studies of fish passage performance through turbine units can and should be conducted for turbines that serve a downstream fish passage function in a hydropower plant. These studies should engage experts within organizations such as the USFWS, NOAA NMFS, USGS, and academic communities at the design stage to maximize their relevance and acceptance. They should also apply to the most extreme conditions that fish would experience encountering these turbines in the field: smallest turbine size relative to fish size, highest operating speeds, and consideration of barotrauma for species with sensitivity to rapid pressure changes. They should produce high-quality extended duration survival and malady rate data, and also allow for direct observation of passage events to increase confidence in any actual injury mechanisms at play. Characterization studies should also evaluate sublethal effects and behavioral abnormalities (such as reduced swimming performance) that result from turbine passage.

Because turbines are hydraulically similar (i.e., flow characteristics are constant), their performance with respect to fish passage can be characterized in the laboratory with small-scale test units and applied anywhere with confidence. This is in contrast to site-specific infrastructure like custom fine screens, which may be challenging to model in the laboratory or computer simulation, and must be validated for effectiveness in the field. Laboratory characterization is much less expensive and time-consuming than field characterization, and may also allow for easier observation and more comprehensive data collection. To understand the variety of injury mechanisms that may result from turbine passage, morphologically diverse fish should be tested according to this approach. Table 1 lists species affected by hydropower in the United States, clustered by family or subfamily, which may be used as surrogates for one another in turbine passage testing.

Family/ subfamily	Species	Region	Size @ DS passage	Other considerations
Salmonidae	Rainbow trout, steelhead	Pacific	120-200 mm; 600-1200 mm	Susceptible to barotrauma
	Coho, sockeye, Chinook, chum, pink	Pacific	120-200 mm	Susceptible to barotrauma
	Brown trout, Atlantic salmon	Atlantic	120-200 mm; 600-1200 mm	Susceptible to barotrauma
Alosa	Alewife, blueback herring	Atlantic	85-135 mm; 250-400 mm	Susceptible to barotrauma
	American shad	Atlantic	40-115 mm; 300-620 mm	Susceptible to barotrauma
Anguilla	American eel	Atlantic	400-1200 mm	
Petromyzontidae	Pacific lamprey, sea lamprey	Atlantic, Pacific	200 mm	
Acipenseriformes	Sturgeon, paddlefish	Mississippi river basin, Atlantic, Pacific	62-400 mm	

Table 1: fish species to study for downstream passage in the United States

Natel is using a scientific approach to understand the effectiveness of the RHT at passing all affected fish species downstream. This process is summarized as follows:

1. Conduct through-turbine passage characterization tests under the most relevant operating conditions that allow for direct observation and behavioral data collection across all relevant fish species and life stages. Publish the data in a peer-reviewed journal and share broadly with fish protection decision makers in the USFWS, NOAA NMFS, USGS, etc.
2. Justify the relevance of peer-reviewed laboratory studies to fishery regulators to meet goals for fish protection at the proposed hydropower site by showing that the conditions (fish size relative to turbine, head) at the site in question are less severe than what has been studied and peer-reviewed.
3. Gain regulatory approval and install turbines without fine exclusion screens.
4. Widespread adoption: regulators and consultants recommend fish-safe turbines to meet customer and legal requirements while simplifying hydropower plant design and operations.

At the time of this report, Natel is in the midst of disseminating turbine passage test results for a variety of fish species through peer-reviewed journal publications, conducted both within the scope of this project as well as without. The American eel tests conducted with PNNL in Fall 2021 have been published; additionally (outside of this grant project) a subset of these same eels were passed a second time through the turbine under the same conditions after a 6-day delay, and assessed for injuries or mortalities over an additional 7-day period. Any hydropower project with

the same or less extreme conditions would be expected to produce the same or better outcome for eel passage. Similar passage tests have been conducted with juvenile alosines, juvenile sturgeon, and salmonids using the same principles as the eel study.

2.2.2. Project Tasks

The project team entered the period of performance with desktop and small scale laboratory tests (Amaral et al, 2020) indicating that the RHT turbine runner geometry would enable high survival of proportionately large fish, generally more challenging due to the fish size being large relative to the thickness of the runner blades. Fish length to blade thickness ratio is a key metric in determining how severe a blade strike event will be; relatively thin blades in comparison to fish length lead to consistently high rates of spinal injury and other traumas leading to mortality. This is one of the primary reasons why conventionally designed turbine runners have low survival rates (Amaral et al, 2018).

Three major passage tests were planned and executed within this portion of the project scope, with each test event requiring months of preparatory planning and trials, approximately a week to conduct each test session, and subsequent data analysis and report writing. Two full scale field tests of rainbow trout (salmonid representative) were conducted in 2020 and 2022, and American eel were tested in a subscale turbine in 2021. Each of these tests resulted in no statistically significant differences in mortality between treatment and control groups, demonstrating the very high fish passage survival rates of the RHT turbine.

2.2.3 2020 Full Scale Rainbow Trout Passage Test

The initial project proposal included the opportunity to utilize a prototype field test facility in central Oregon that Natel was in the process of constructing at the time. This facility has a 1.9m diameter, 4.7m net head, 300kW axial flow unit incorporating the fish-safe RHT runner design. The project team noted the high value of obtaining test results using large adult fish in a full scale test early in the project timeline - this would allow for adjustments to design work and inform subsequent testing plans. For this reason a major test was frontloaded early in the project. Rainbow trout were utilized in this test for multiple reasons: they are generally accepted representatives of salmonid species which (along with eel, sturgeon, and shad) are at the critical intersection of resource conservation efforts and new + repowering hydropower. Additionally, they are considered a native species in the Deschutes, the watershed area where the testing was conducted. Rainbow trout are relatively easily acquired and transported from farming facilities.

Figure 42: the prototype RHT D190 turbine which was used to conduct the full scale passage tests.

Natel and PNNL team members collaborated to develop a detailed testing plan for full scale live and sensor fish testing at the Monroe Drop facility. Three test conditions (treatments) were planned: control and two operating conditions, with one corresponding to best efficiency and one corresponding to maximum power at full flow. Each treatment was planned to include 100 rainbow trout targeting 200 to 400 mm in length and 50 Sensor Fish releases. Control fish were planned to be used to evaluate the effects of handling, tagging, releasing, and recapturing, as well as to provide additional data on recapture probabilities. Assuming the control survival, passage survival, and recapture rates are ≥95%, a sample size of 100 fish per treatment was determined to be sufficient to attain passage survival (or malady-free rate) estimates with SE < 0.045, 95% of the time. The test plan was submitted to DOE for review and accepted; with the help of Corey Vezina of DOE, Roak Parker and Jonathan Hartman from the NEPA team, and additional input from Daniel Deng at PNNL, the required environmental reviews were completed in July in time for testing to proceed.

By early September, fish holding equipment was delivered to the site and set up; pumping systems for water circulation were assembled and tested; test and control injection hoses were installed along with necessary structural attachments within the turbine forebay; camera and lighting systems for attempted video capture of passage events were set up and tested.

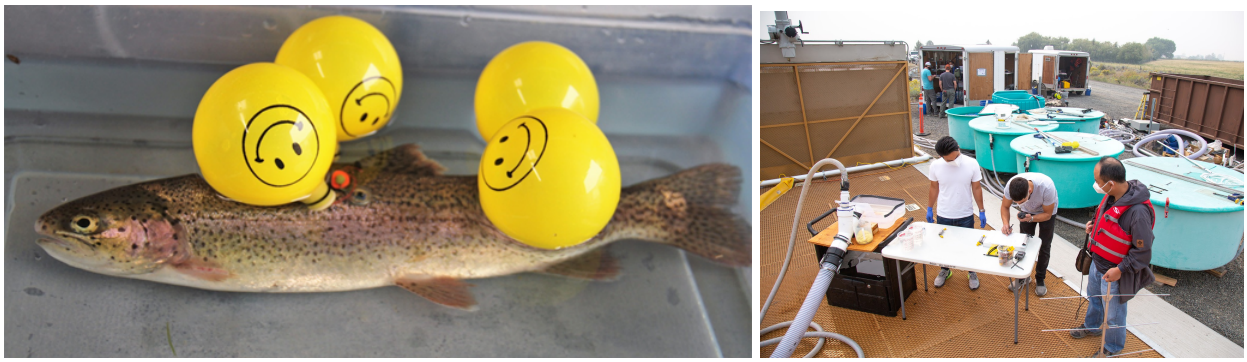

Figure 43: a tagged test trout (left) and onsite test execution (right) from summer 2020

Test execution went smoothly despite challenges from COVID and local wildfires. In summary: 60 test fish and 59 control trout averaging between 320 and 340 mm in length were tested, in addition to two different types of sensor fish. All turbine-passed fish were recovered successfully with zero immediate or delayed mortality. Further, it was observed that there were no indications that these large fish had passed through a hydro turbine at all (according to the onsite biologists from PNNL). Challenging circumstances (noted below, but in particular, hazardous smoke conditions) inhibited the full execution of the initially envisioned treatment design planned but fortunately the exceptionally high survival rates of the fish that were tested allowed for statistically significant samples sizes to be gathered in the windows of time when testing was able to occur.

Figure 44: a collection of images from testing work in central Oregon in early September.

The successful completion of this test happened thanks to numerous examples of dedication and effort from the project team. Not only were the substantial foreseen risks faced and overcome - including but not limited to a very tight test preparation timeline due to COVID-19 supply chain delays, the need for PNNL to develop their own recovery mechanisms after a sub-contractor fell through, and the rapid turnaround of required test planning and environmental approvals - but new last minute challenges were also managed. As the test dates approached the team faced a combination of a surprise shift in the irrigation district's flow schedule - shrinking the window of time to conduct tests - in conjunction with exceptionally poor air quality due to local wildfires (off-the-charts hazardous AQI). Though neither Natel nor PNNL could require team members to work those days, excitement around the groundbreaking nature of the work inspired the participants to pull together and make it happen regardless.

A preliminary report was shared internally within the project team and DOE for review. A coordinated press release was published between DOE, PNNL, and Natel in December 2020 to highlight the success of the testing program. Since then, a more thorough test report with results analysis has been completed and delivered to DOE. A journal publication is currently being authored for publication combining the test results of the 2020 and 2022 studies and will be forthcoming.

2.2.4 2021 American Eel Passage Test

The current state of knowledge of eel passage through turbines is minimal, and their distinct morphology from the highly studied salmonids warrants more research. Additionally, American eel (*Anguilla rostrata*) is increasingly a species of concern for the US FWS and NOAA NMFS as well as other stakeholders. To study the passage behavior and results of American eel through a fish safe turbine design, the project team developed a plan to study a range of eel sizes at Natel's Scale Hydraulic Test facility in Alameda, California. (Due to nonnative species restrictions, the team could not utilize the full scale field unit where rainbow trout testing was conducted).

The goal of the study is to gather quantitative and qualitative information on the behavior and survival of eels passing through an RHT axial flow turbine. Eels of different lengths were passed through the turbine and morbidity (for example, injuries) and mortality (and turbine passage survival) data as well as high-speed video footage of the eel passage and interaction with the blades was collected. The test turbine in this case was an RHT propeller unit with runner diameter D=55 cm. This is considered to be a scale model, with the full size RHT ranging from ~1 m and above. The leading edge of the 55 cm runner is approximately 60 mm thick, while an RHT with 1.9 m runner diameter has a leading edge approximately 210 mm thick.

In addition to working closely with experts from PNNL to develop the test plan, Natel cast a wide net for insight and guidance outside of the grant team. Collaborators and reviewers of the test plan ultimately included representatives from USFWS, NOAA-NMFS, USGS Conte Lab, and Kleinschmidt. One necessary precursor step to conduct this laboratory testing - a Restricted Species Permit from CA-DFW - was identified and the process was initiated early so Natel could hold and test this nonnative species. Prior work by Natel Energy had already established the key elements of a comprehensive passage test facility, including a fish holding system, treatment and control injection components, a clear runner housing for high speed videography, and a recovery setup utilizing a sloped wedge wire screen to separate the test fish from the bulk of the turbine flow. The facility had been tested using other species, but not yet for eel.

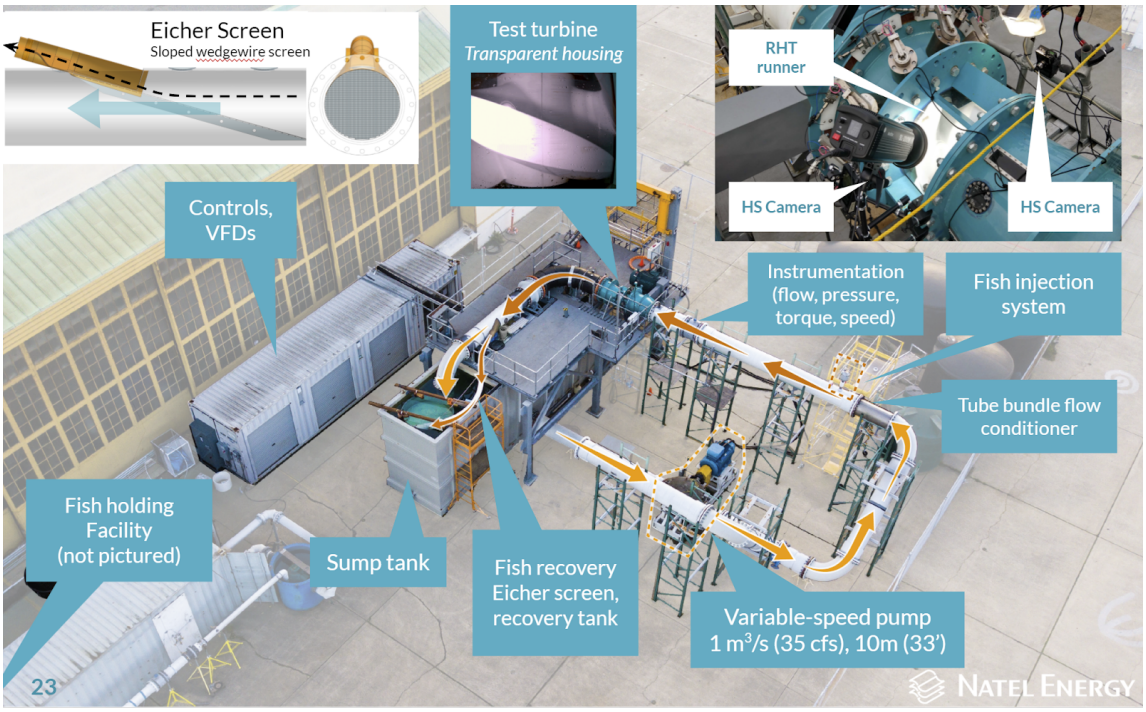

Figure 45: Diagram of the test facility layout

The Restricted Species Permit from CA-DFW was received in June 2021 and immediately following, Natel began to acquire small groups of eel to assess and de-risk both the live holding facilities and testing process. Injection, high speed videography, and recovery processes were evaluated. By the planned test date late August, over 200 eels of various sizes had been acquired and staged for testing.

During the week of August 30, 2021, Natel conducted the first portion of a novel fish passage test in collaboration with the Pacific Northwest National Laboratory (PNNL). In this phase of testing, 61 eels measuring 34-49 cm in length were tested, including 47 treatment fish which passed through the RHT, and 14 controls which were inserted into the system downstream of the turbine. The 55 cm diameter turbine operated at 670 rpm under 10m of hydraulic head.

Eels were tagged by PNNL prior to testing and data collected for each eel included girth, mass, and length measurements, photos documenting their condition before and after the test, and pre and post-test videos of the eels' swimming ability. Condition photos and swim videos were also collected at the approximate 48-hour point after testing. High-speed video of the eels passing through the RHT was collected for 90% of the treatment fish.

Figure 46: The test facility included a pre- and post-test evaluation area (foreground) and Natel's hydraulic test facility and RHT turbine with injection and recovery apparatus (background).

Figure 47: Pre- and post-test area showing photography and behavioral assessment areas.

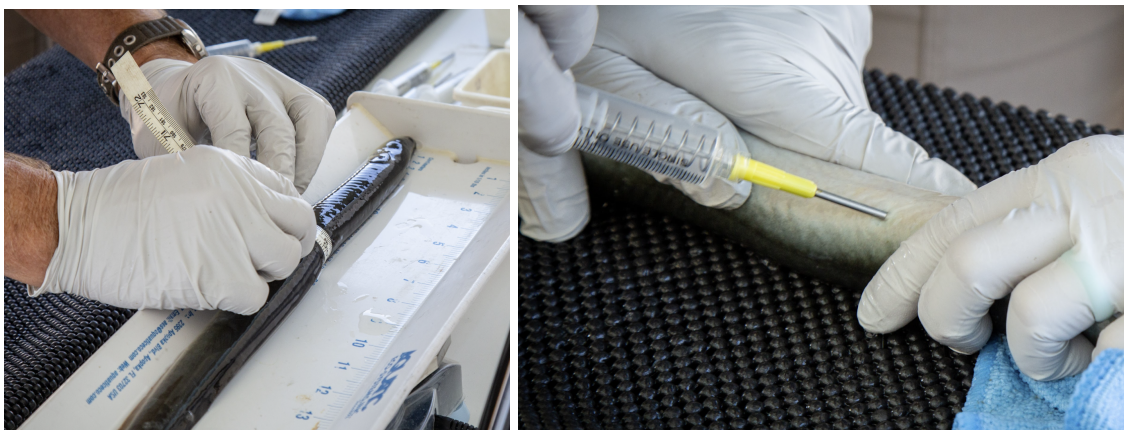

Figure 48: Measuring and tagging anesthetized eel.

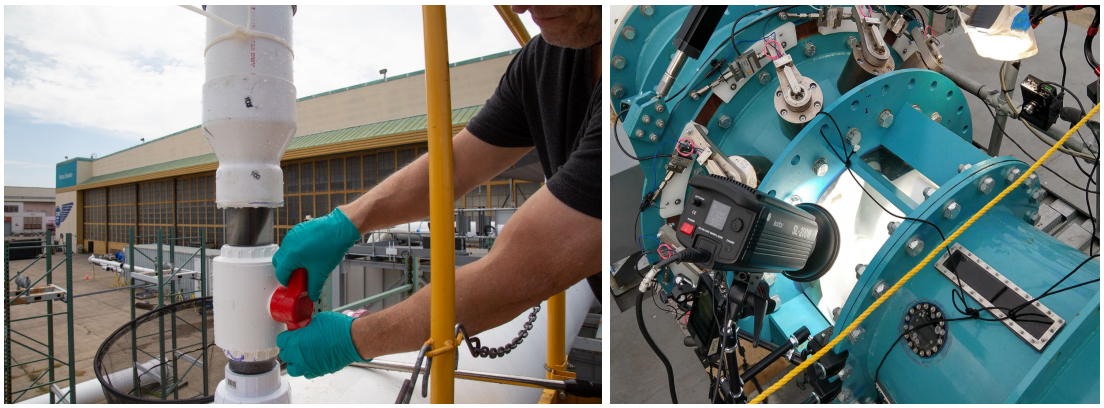

Figure 49: Tagged fish are loaded into an injection tank and inserted into the flow either upstream of the turbine, or downstream for control. High-speed cameras were arranged around an acrylic runner housing to capture passage in detail.

Figure 50: example frame capture from a high speed passage video.

Figure 51: example pre- and post-test photos.

Figure 52: post-test assessment included a behavioral test to assess for lethargy, loss of equilibrium, or other effects in addition to any observable injury.

In support of the original test plan, a group of approximately 200 eels were acquired, sorted by size, and held in two separate tank systems, each having its own biofilter and pump. Early in the week, very high ammonia levels were detected in the tank system which was holding the majority of the larger cohort of eels, despite attempts to mitigate via water swaps. By Wednesday September 1, it was clear that individuals in this tank system were in poor health, and the decision was made to not include these fish in the test. A decision was made to resume testing after making improvements in the fish holding infrastructure. After consulting with a number of aquatic bioscience experts including PNNL personnel and contacts at UC Davis, Natel implemented a major upgrade to the biofiltration and tank systems, resulting in a 2.6x increase in water volume per tank as well as a 2.4x increase in biofilter media volume per tank.

By late 2021 Natel had designed and constructed a fully upgraded recirculating aquatic system (RAS) to accommodate large quantities of fish. The RAS consisted of 4 300-gallon tanks connected to 2 upper and 2 lower IBC sump tanks apiece, each with its own barrel bioreactor.

Seeded biological media with established bacterial colonies for processing fish waste (ammonia and nitrite) was purchased from the eel supplier, American Unagi.

Figure 53: one half of the fully upgraded recirculating aquatic system for holding up to 45 kg of eels.

Following construction of the RAS, a second group of larger eels was tested the week of November 15, 2021. Group 2 consisted of 84 treatment and 29 control eels 46-66 cm in length. The turbine operating condition was identical to the previous round of tests, 670 rpm and 10m of hydraulic head.

High-speed videos of turbine passage; pre-test, post-test, and 48-hour swim assessment videos; and photos were collected throughout the test. The survival rate for all treatment and control eels across both Group 1 and Group 2 was 100%. 13 eels from Group 1 (9 treatment and 4 control) and 27 eels from Group 2 (21 treatment and 6 control) were X-rayed and evaluated for vertebral injuries and irregularities. No vertebral injuries were detected in any of the eels.

The project team authored a journal article describing the methods and results of this series of tests. This paper was accepted for publication in August 2022 in Transactions of the American Fisheries Society and subsequently published with open access. (Watson et al, 2022).

Figure 54: PNNL biologists inspect an eel for external injuries; high-speed video operators scrub through footage of eel passage through the turbine.

Figure 55: an eel is photographed for pre-test condition documentation.

Figure 56: turbulence in the recovery tub during turbine operation, just prior to eel recapture.

2.2.5 2022 Full-Scale Rainbow Trout Testing: Larger Fish

With the success of the 2020 field test of salmonids up to 400mm in length, a follow up test was planned to further push the boundaries of what a fish safe RHT turbine can accomplish by using even larger fish. Fish length to blade thickness ratio is a key metric in determining how severe a blade strike event will be; relatively thin blades in comparison to fish length lead to consistently high rates of spinal injury and other traumas leading to mortality (Amaral et al, 2020, and prior work cited in this reference). This follow up test still expected high survival rates based on scale laboratory testing, but the real world effects of adult fish at full scale required testing.

A test plan was drafted in Q2 2021 in collaboration between Natel Energy and PNNL, taking into account lessons learned from the Q3 2020 test. The availability of test fish of the required size was confirmed by PNNL, and laboratory tests were designed and planned to confirm the required configuration of balloon tags necessary to recover these larger fish. One test operating condition was designed to be evaluated along with a control group. Each treatment included 100 rainbow trout targeting 400 to 600 mm in length and 10 Sensor Fish releases. A total of 200 hatchery reared rainbow trout (400-600 mm) were to be used (100 test and 100 control). Control fish are used to evaluate the effects of handling, tagging, releasing, and recapturing, as well as to provide additional data on recapture probabilities. Assuming the control survival, passage survival, and recapture rates are ≥95%, a sample size of 100 fish were expected to be sufficient to attain passage survival (or malady-free rate) estimates with SE < 0.045, 95% of the time.

PNNL conducted the laboratory assessments of anesthesia and tagging methods in Q2 2021. Natel prepared and field tested a submersible high speed camera and light device to improve the ability to capture passage events. Field testing took place at the Monroe facility on May 23-28, 2022. Despite numerous scheduling challenges and the resolution of a last-minute equipment issue at the plant (a portion of the canal gate actuator broke a week before testing) the team, fish, and equipment made it to the site and testing ran rather smoothly.

Ultimately 105 treatment and 81 control fish between 330 and 530 mm in length were evaluated. Because these fish were larger than the trout used in the passage tests in 2020, the methods of tagging had to be adjusted. Fish were strapped into a restraint and tagged without anesthesia. While there were no immediate mortalities, external injuries were similar between treatment and control groups and attributable to tagging and handling, and no internal injuries were observed, there were substantial delayed mortality rates over the 48-hour holding period among both groups: 21.0% (17) Control, 21.9% (23) Treatment. The Fisher's Exact test statistic was 1, indicating no significant difference in mortality rates between control and treatment fish, Chi square ($p = 0.977$).

Five of the 105 fish passed through the turbine were captured on video by the cameras installed inside the turbine housing. Only a quarter of the runner area was visible because of failure of

some of the installed cameras and bubbles reducing visibility in part of the runner area. Despite a low video capture rate, the videos that were captured are illustrative of the experience of fish passing the leading edge of the RHT blades. Sensor fish data was also collected per the test plan, to corroborate with live fish findings.

A test report was authored by PNNL describing the methods and results of this field test. At the time of writing this report, a planned journal article submission is being jointly authored by PNNL and Natel and is expected to be submitted in 2023.

Figure 57: Preparation of a treatment fish at the forebay injection location.

Figure 58: a view from across the canal shows the turbine draft tube (left), control injection station and hose (center), and recovery team in place along the bank and on the water.

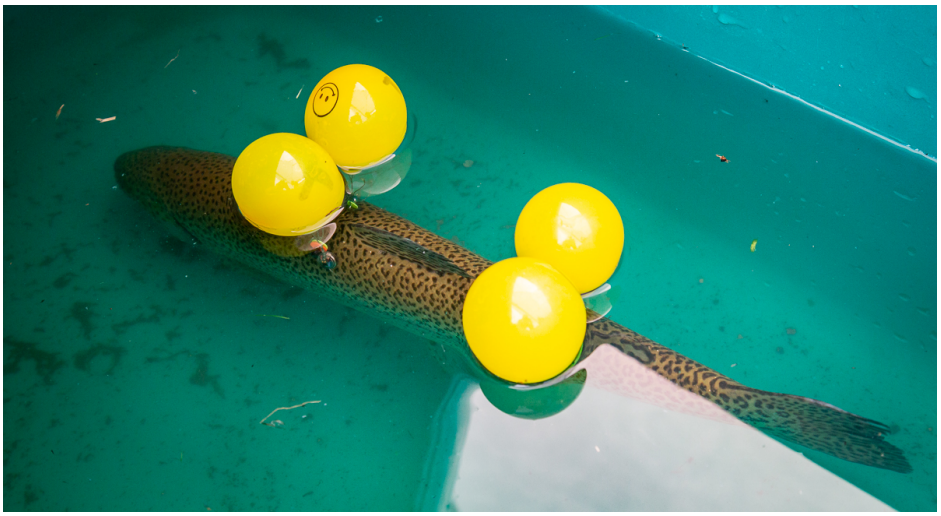

Figure 59: a recovered trout with inflated balloon tags awaits assessment.

Figure 60: After having its balloon and radio tags removed, a large rainbow trout from the Control group is weighed, measured, and assessed for injuries.

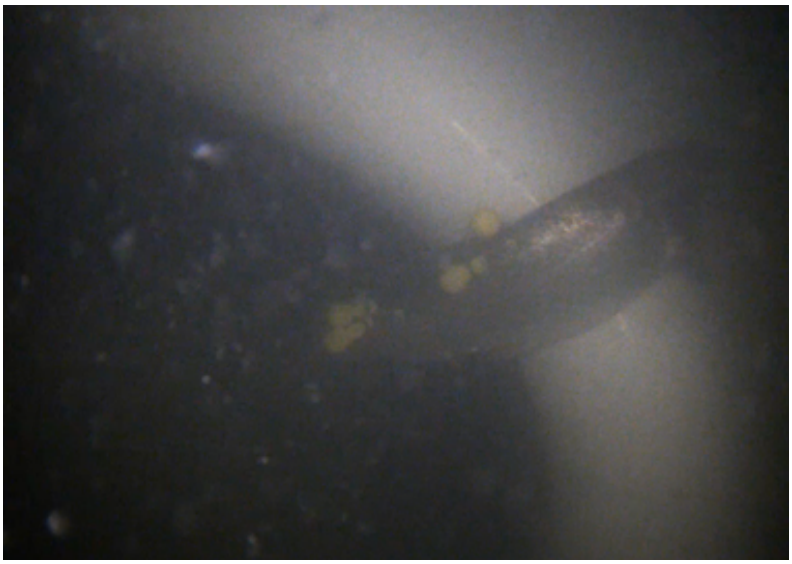

Figure 61: A rainbow trout is struck by the leading edge of an RHT blade. This frame is from video captured by the camera installed inside the turbine housing.

2.2.6 Summary of Findings

Three major passage tests were planned and executed within this portion of the project scope. Two full scale field tests of rainbow trout (salmonid representative) were conducted in 2020 and 2022, and American eel were tested in a subscale turbine in 2021. For each test, extensive stakeholder discussion was held to ensure maximum applicability and relevance of the work. Such engagement is strongly recommended for future turbine passage studies. Each of the tests conducted resulted in no statistically significant differences in mortality between treatment and control groups, demonstrating the very high (>99%) fish passage survival rates of the RHT turbine.

Recommended future work and considerations:

- Dialing in values for turbine design parameters that minimize turbine cost, while still achieving fish safety, through accurate modeling of passage survival. This requires tuning of the fish survival CFD simulation tools with experimental data, identifying the maximum fish size threshold for turbines of a particular size, and confirmation of barotrauma risk for turbine-passed fish.
- A solid understanding of barotrauma risk through the RHT will also assist in specification of turbine setting relative to tailwater, which affects plant construction costs.
- Expanding scope to the plant level. Safe downstream passage of all fish is fundamental to achieving full river connectivity. While up to 91% or more of all fish passing hydropower facilities are 15 cm in length or less (Mueller 2020), larger, older life stages of fish can still be very important to population survival. These fish need to be able to safely and

expediently pass around trash racks. Study of large fishes' ability to navigate conventional trash racks and utilize alternative downstream routes is critical for aiding plant design.

- A topic worthy of study at the plant level is the potential benefit of engineered refuge areas downstream of turbine outlets, to minimize predation risk for fish exiting turbine outlets.
- Any scaling nonlinearities from laboratory tests to full-scale field installations need to be identified and understood.
- A strong understanding of the injury mechanisms that are present in turbine passage and the physiological differences between fish of different life stages is needed to ensure that the RHT does not pose an unknown risk to fish in more vulnerable life stages.
- Understanding sublethal and cumulative effects of turbine passage, and any potential consequences on population survival, is critical.

2.3 Advanced Manufacturing Runner

The public version of this section has been edited to remove proprietary information prior to publication.

2.3.1 Motivation

Natel's new and novel Restoration Hydro Turbine (RHT) achieves both high efficiency and high fish survival rates at heads from 3 to 10 meters and above, enabled by uniquely shaped runner blades. Unlike the blades of traditional Kaplan and propeller turbines, the RHT runner blades are 10 - 15 times thicker; they also have a forward-sweeping leading edge, which directs fish inwards towards the hub of the runner where relative strike velocities are lower and more gentle.

While these features enable a more environmentally friendly turbine, they pose new structural challenges to typical runner design and manufacturing. A thicker blade is a heavier blade and a forward sweeping leading edge is a cantilevered mass. As a result, traditional solid metallic blades are no longer optimal because, for a 1 MW scale turbine, they are excessively heavy and expensive as solid blades and they are overly complicated to cast or machine as hollow or semi-hollow geometries. At the same time, the thicker geometry of the blades enables the consideration of alternative manufacturing methods and materials which would not provide sufficient stiffness in the footprint of a conventional solid steel design. Some of these alternative methods and materials permit net shape forming of hydraulic shapes, omitting costly 5-axis machining of large fluid surfaces.

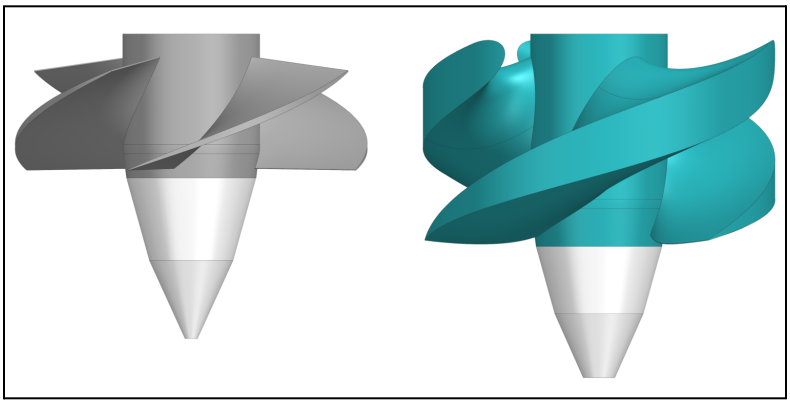

Figure 62: A traditional propeller-type blade for a 1.9 m diameter turbine would weigh about 130 kg in solid stainless steel (left). An RHT blade for a 1.9 m diameter turbine would weigh about 2200 kg in solid stainless steel (right).

A solid fish safe RHT blade would be significantly more massive than a traditional propeller blade. In the example of a 1.9m diameter runner at roughly 2200 kg, this blade would be about 17 times more expensive in material alone than the much thinner 130 kg conventional propeller

blade. The excessive weight of the solid RHT runner blades also puts added stress on the powertrain in horizontal machine configurations. In addition to increasing the stiffness requirements of the entire machine to avoid resonance issues in both horizontal and vertical configurations, this significantly drives up the cost of powertrain and structural components.

Entering into this project work, Natel had investigated the possibility of casting semi-hollow manganese bronze runner blades. While this cuts the weight of the runner by over 60%, manufacturing limitations still barred this path. Even with large investments in complex tooling and solidification analysis, a draftable, hollowed-out blade is not capable of withstanding 10 m head loading.

The solution identified as most compelling for solving these challenges is manufacturing runner blades using additive techniques, and specifically composite materials. Composite materials are advantageous because they have high stiffness-to-weight and strength-to-weight ratios. They can be molded into complex shapes that are very geometrically stable after forming, eliminating the need to precision-machine molded surfaces on expensive machines. Weighing in at a fraction of the mass of metallic blades, composite blades significantly reduce loads on the blade-to-hub joints when the runner experiences centrifugal loading, especially in runaway conditions. The lightweight design additionally relieves the supporting powertrain and eases the overall runner assembly process.

While concepts of RHT metallic blades were strength limited, composite blade designs are stiffness limited. The gap between the outer diameter of the runner and the inner diameter of the runner housing is very tightly controlled and the blade is only allotted a very small portion of that gap for radially deflecting in the tolerance stack up of the assembled machine. Essentially, the runner blades of a 1.9 m diameter machine cannot, under any loading condition, deflect radially outwards more than 0.33 mm. This design requirement focuses work on the stiffest, while cost effective, runner blades.

The first full scale meter diameter RHT runner was built during the summer of 2020: at 4.7 meters of net head, this unit produces 300 kW. Each of the blades consisted of continuous-fiber carbon-epoxy laminate components veiled in thin fiberglass with some internal shear web structures. The volume of the blade was filled with a 6 lb density expanding polyurethane foam to displace water.

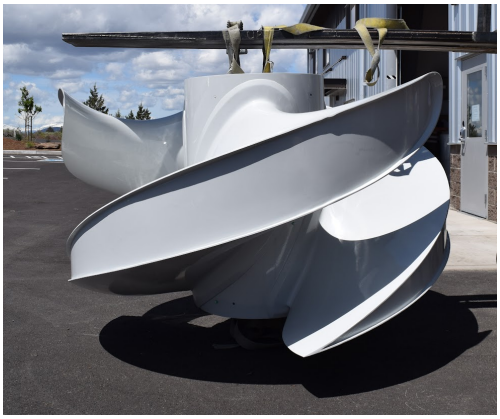

Figure 64: the finished prototype runner (right).

This design met target deflection, held our desired safety factors on both fatigue and ultimate strength of the laminate and the fasteners, and has proven extremely durable when operating at the site. This prototype has operated in debris-ridden and moderately sediment-laden water without any signs of abrasion or other wear. There were many instances in which branches, pebbles, and other debris were witnessed passing through the machine. These results drive great confidence that composite runners can continue to be developed and robustly implemented within the hydro industry.

Following this prototype development and entering the period of performance of this grant, the objectives were to take these initial findings and designs, step back to assess materials and the design space incorporating lessons learned, and focus back in on the optimal combination of material, process, and simplified design to minimize cost while meeting strength, stiffness, and durability requirements, thus maximizing the competitive potential of these fish safe runner geometries.

2.3.2 Activities and Methodology

Natel Energy's RHT turbine runner design has unique geometry that is well suited to take advantage of advanced manufacturing techniques to produce net shape parts with greatly reduced machining needs vs conventional cast blades. Project work began with assessments of requirements and prior work at Natel and elsewhere; literature review combined with industry collaboration and review with ORNL's Manufacturing Demonstration Facility (MDF) informed a downselection for combinations of substrate and coating(s) which could compete for durable, low cost runner production. Physical testing was conducted on a subset of options to evaluate durability. The resulting selected design elements were incorporated into a full scale (1.9m diameter) runner design. Individual full scale prototype blades were manufactured and underwent laboratory static and fatigue structural testing to evaluate both the manufacturing

approach as well as resulting component performance, while lab component tests of coupons assessed impact, immersion, and thermal effects on predicted runner blade life.

Design methodology greatly leveraged Finite Element Analysis (FEA), specifically NX Nastran's laminate composite modeling tools. Material manufacturers published specifications of material properties, confirmed through physical testing of coupons, were utilized in these models. Once designs met performance and cost criteria on paper, a series of coupon and subcomponent tests were performed to assess manufacturability, possible effects of defects from processing, and resulting performance against requirements.

2.3.3 Runner Design

Core to this portion of the project was first selecting the appropriate combination of material and manufacturing process. Composite materials are utilized in an extremely wide range of applications, from the low cost and highly scalable (marine, wind, construction etc) to very high cost, high strength, and precise (aerospace) and many flavors in between (automotive, consumer products, sports equipment, etc). Cost per kg for finished composite components can range from less than $10/kg to many hundreds or thousands of dollars per kilogram. Hydro is a highly competitive and cost motivated industry, and so the project team focused on materials and methods already utilized in adjacent industries where low manufacturing costs have been realized, but also where the materials could perform as needed to meet design requirements.

Fiberglass was selected for three primary reasons:

1. Of the various means to create a composite component by combining a reinforcement (typically fiberglass or carbon fiber) with a matrix (epoxy, vinyl ester, etc), different flavors of infusion / resin transfer molding are consistently the most scalable and economical. This method strikes a balance between the two extremes of using hand labor to wet out reinforcement plies, or pre-impregnating the reinforcement with a matrix, for the lowest cost at moderate to high production volumes. While it is difficult to reliably infuse carbon fiber laminates thicker than ~8 mm, infusions of fiberglass laminates have proven to be much more consistent. Heavyweight industrial applications of continuous fiberglass often utilize laminates in excess of 1-2 inches (25-50 mm) thick. Fiberglass is not as stiff nor as strong as carbon fiber, but the geometric stiffness benefit of utilizing a ~36 mm thick composite skin is enough to limit radial blade deflection at 10 m overspeed.
2. The coefficient of thermal expansion (CTE) of carbon steels is ~11×10^{-6}/°C. The CTE of carbon fiber is roughly 0/°C, and the CTE of fiberglass is between 5×10^{-6}/°C and 7×10^{-6}/°C. Turbine runner housings are carbon or stainless steel, as is the runner hub. Reducing the discrepancy in CTE between (a) the runner hub and blade and (b) the blade and runner housing reduces stresses induced at interfaces by the cyclic thermal loading of

exposure to temperatures varying between -30°C and +40°C and reduces the change in blade to housing gap as the ambient temperature of the machine changes.

3. Fiberglass composites have been heavily used throughout the marine and wind industries for decades. They are notable for both their impact and abrasion resistance in both of these environments. Fiberglass blades have been used on wind turbines since the 1990's and today exclusively dominate the market.

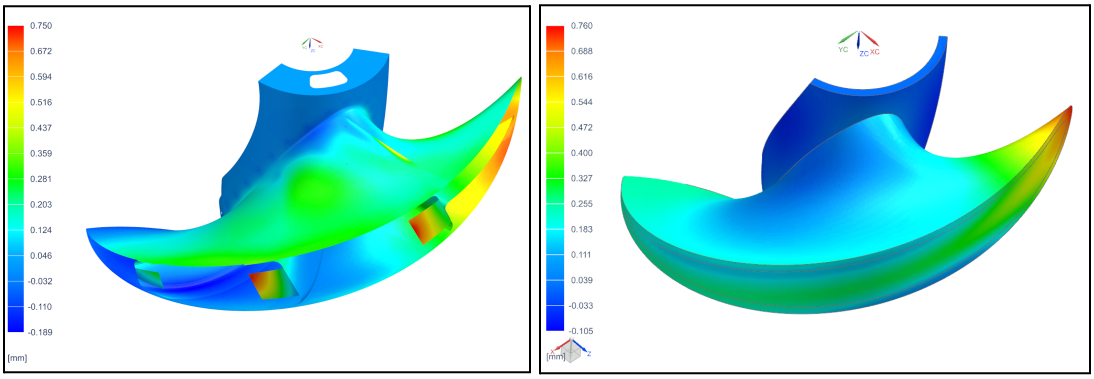

Figure 65: Radial deflection performance of the carbon fiber prototype runner blade in its 4.7 m head overspeed loading condition: 0.71 mm maximum radial deflection, 0.21 mm average radial deflection (left). Radial deflection performance of a monocoque fiberglass runner in a 10 m head overspeed loading condition: 0.76 mm maximum radial deflection, 0.26 mm average radial deflection (right).

In terms of both maximum and average radial deflection, the fiberglass blade achieves very similar displacement performance at 10 m head as does the carbon fiber blade design does at 4.7 m head, as shown above. Compared to the baseline design which had eight separate composite parts each, these blades are composed of only four composite components: leading edge, high pressure and low pressure skins, and outer diameter cap. Reducing the part count reduces the number of infusion tools and assembly jigs required to produce the blades and heavily decreases the amount of labor that goes into each blade. Though the glass blades require much thicker laminates, the glass goes down in heavyweight plies, laying up in fewer plies and with fewer labor hours for a 36 mm laminate than would be required for a 12 mm carbon fiber laminate.

The runner hub was another area of improvement that was targeted for both simplification and cost reduction. The resulting hub design is a simple, thick-walled forged steel hub. At a 1.5 - 2" wall thickness, the wall itself provides all of the stiffness and strength that is necessary to transmit all of the thrust and torque from the runner blades to the turbine shaft. These walls are thick enough that the runner can be mounted with a ring of axial fasteners at the upstream face of the hub. Face mounting the runner to the powertrain around the outer diameter of the hub frees up access to the entire interior of the hub from both the upstream and downstream sides, in addition to driving out all assembly and welding costs required to implement any internal structure.

Composites are not yet widely used in the hydro industry. As such, composite materials being considered for application need to be thoroughly tested to evaluate their expected performance and life expectancy in relevant conditions. A risk based assessment to runner performance and durability was conducted to focus project work.

Performance Risks

1. Stiffness / Deflection
   - If the blade deflects more than expected, it may contact the runner housing in operation, causing damage to the runner and/or runner housing
   - Mechanical properties could be affected by exposure to water
2. Hydraulic Profile
   - If the runner geometry does not match the intended hydraulic geometry, the machine may not perform as expected in terms of efficiency and power production
3. Cavitation due to surface roughness
   - If the surface of the blade is too rough, either due to manufacturing flaws or degradation of the fluid surface, cavitation may occur on the surface of the blade, decreasing the overall performance of the machine

Reliability Risks

1. Strength
   - Composite failure, joint failure, or hub failure
2. Material Creep
   - Blade shape changes after running under load for a period of time
3. Mechanical Fatigue
   - Composite, joint, and / or hub fail in fatigue due to the cyclic loading of starting and stopping the machine, changing load/speed, overspeeding occasionally during grid outages, or differences in hydraulic loads blade to blade
4. Thermal Fatigue
   - Interfaces consisting of different materials fail in fatigue due to cyclic exposure to temperature fluctuations in the water or due to cyclic exposure to freezing or excessively hot temperatures while the machine is stationary
5. Absorption Fatigue
   - Composite and/or composite interfaces fail in fatigue due to cyclic exposure to water and dry environments (flooded vs drained)
6. Corrosion
   - Exposure to water degrades materials over time
   - Galvanic corrosion due to incompatibility of adjacent materials degrades materials over time
7. Abrasion
   - Water and/or sediment/debris wear down the surfaces of the runner over time
8. Impact
   - Objects that make their way through the turbine impact and damage the blades

Figure 71: composite runner risk assessment summary

2.3.4 Mechanical Testing

Modulus (stiffness) testing of the selected materials was performed in-house on Natel's Shimadzu UTM with 36mm thick coupons (representative of the full laminate ply schedule). Material strength and modulus were also tested by Element Materials Technology in St Paul, MN. ASTM Standard D638 was used on Type III dogbone coupons. Both strength and modulus coupons were tested at room temperature, 0C and 40C.

	Expected	Measured (Natel)	Measured (Element)	Discrepancy
Modulus	19.6 GPa	21.5 GPa	24.1 GPa	+9% to +23%
Strength	340 MPa	N/A	253 MPa	-27%

Table 3: resulting stiffness and strength measurements

Results were consistent across all temperatures and once again we recorded modulus values higher than what was expected based on the material data sheet of the Vectorply material. Strength, on the other hand, was recorded ~27% lower than the expected 340 MPa UTS. We are

not yet sure where this discrepancy comes from, but considering that our max expected stress in the laminate is 17 MPa, we are not very concerned.

CTE was measured across qty 12 Type III dogbone coupons. Average CTE was measured at 11.65 X10-6 m/(m°C). The CTE of mild steels is 10.8-12.5 X10-6 m/(m °C) and the CTE of 304 SST is 17.3 X10-6 m/(m°C). This data tells us that the thermal stresses at joints between fiberglass and steels and the dimensional discrepancies between fiberglass and steel in fluctuating thermal environments will be minimal.

Water absorption was measured across qty 6 Type III dogbone coupons. The difference in mass between pre-soak and post-soak coupons indicates an absorption percentage of 0.41%. This falls within the normal range of most plastics.

Creep testing at Element Materials Technology resulted in negligible creep rates at both 8MPa loading (representative of max operating stress in the laminate) and 17 MPa loading (representative of max stress in the overspeeding condition) in both dry and submerged conditions.

Property	Test	Value	Meets/Exceeds Expectations	Comments
Modulus	ASTM D638	23.68 GPa	✓+	Measured across 0°C to 40°C temperature range
Ultimate Strength	ASTM D638	250.95 MPa	✓	Measured across 0°C to 40°C temperature range
Thermal Expansion	Type III dogbone coupon dimensions recorded across a 80°C temperature range	11.66 E-6 m/(m°C)	✓	CTE value falls between that of mild steels and stainless steels
Water Absorption	Type III dogbone mass recorded before and after room 1 week temp water soak	0.41%	✓	Will not affect structural properties or balancing
Creep	Type III dogbones loaded in tension to max expected stresses for 1 week's time. Change in extension recorded	negligible	✓	Loaded in room temperature/humidity and submerged in 10°C water

Table 4: summary of mechanically tested performance values for fiberglass coupons

2.3.5 Environmental Testing

The first round of abrasion testing concluded in Q1 2022. This was an extremely informative test which enabled the project team to downselect coatings and directly predict the abrasion performance of the composite blade over the lifetime of the turbine.

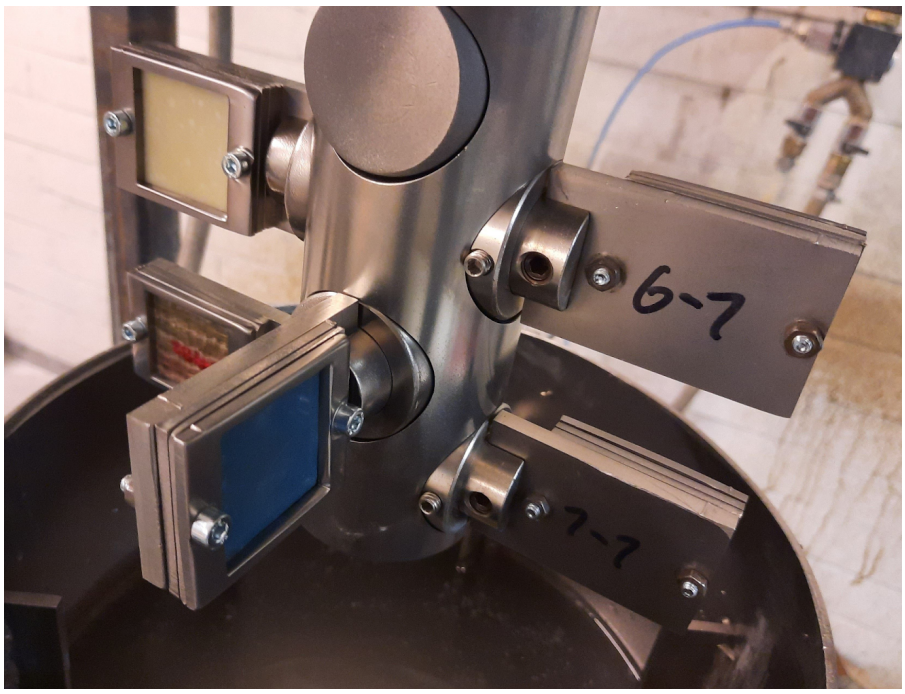

Figure 72: Slurry pot setup at Tampere University's Wear Center.

8 slurry pot abrasion tests were run at Tampere University's Wear Center in Tampere, Finland. Each test consisted of 6 small flat plate samples rotating at 1510rpm (15 m/s max contact velocity) through a slurry of 20% quartzite particles by weight mixed into water. Two ranges of particle sizes were tested: 50-200um and 100-600um. To ensure equitable flow exposure and consistent particle size, each 3 hour test was paused every hour to replace the slurry and to rearrange the coupons on the main shaft. Samples were dried, weighed and photographed before and after each test. The change in mass of each sample over the course of the test was used in conjunction with the known density of either the core material or the coating used to protect it to calculate the volume lost from each sample. Volume loss as opposed to mass loss is the best metric that can be used to evaluate the abrasion resistance of each material for this application as volume loss on the runner blade surfaces will directly affect hydraulic performance, and materials being tested have different densities.

	50-200um Quartzite			100-600um Quartzite		
Material/Coating	**Mass Loss [g]**	**Volume Loss [cm^3]**	**Volume Loss / Exposed Area [mm]**	**Mass Loss [g]**	**Volume Loss [cm^3]**	**Volume Loss / Exposed Area [mm]**
SST 410	0.178	0.023	0.021	0.547	0.071	0.065
GFRP uncoated	0.302	0.181	0.166	1.853	1.11	1.09
Polyurethane	0.466	0.364	0.334	1.954	1.526	1.40
Silicon Carbide	0.411	0.240	0.221	1.594	0.932	0.856
Epoxy Polyamide	0.749	0.554	0.509	1.685	1.249	1.146
Nickel	0.245	0.028	0.025	0.797	0.09	0.082
CTD 133 Coating	0.078	0.057	0.052	0.317	0.230	0.211
CTD K08 infused laminate	0.067	0.037	0.034	0.745	0.414	0.380

Table 5: Erosion data. Red highlighting indicates coatings that wore all the way through, thus some mass removal that is accounted for was actually lost vinyl ester composite as opposed to coating.

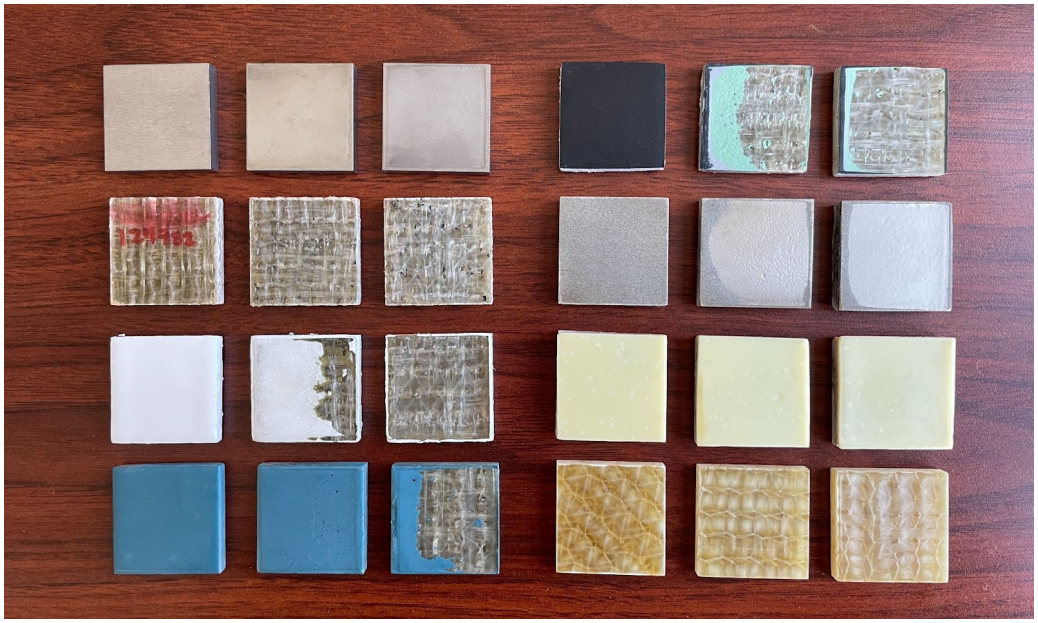

Figure 73: Eight sample types that were sent to Tampere University for slurry pot erosion testing. From top to bottom, left to right: 410 stainless steel (control), baseline fiberglass/vinyl ester composite, fiberglass composite coated in: polyurethane paint, silicone carbide reinforced epoxy, a marine grade epoxy polyamide paint, a 1mm thick nickel plate, CTD 133 toughened epoxy coating, and finally fiberglass infused with an cavitation resistant resin CTD K08.

The metric 'volume loss / exposed area' is essentially the average loss of material thickness across the sample. It is important to remember that these coupons are undergoing rotary motion, so the entire coupon does not experience the same contact speeds; therefore the actual material thickness loss will be greater than the calculated number above at the outer edge of the coupon and smaller at the inner edge of the coupon.

The polyurethane and epoxy polyamide paints wore all the way through in all tests. The silicon carbide reinforced epoxy coating only wore all the way through in the 100-600 um tests. It is relevant to note here that the silicon carbide coating was significantly thicker than these other two coatings to begin with (2.5-5X thicker).

Findings:

1. The volume of material that is removed from a given coating on a sample of a specific size while operating for a given amount of time (3 hours) in a given concentration of sediment (200g/L) with particles of a certain size (50-200um) and material (quartzite)
2. The same as above with 100-600um particles.

Combining this data with known information about the test samples and the testing conditions, data fits were developed specific to each type of coating that can predict the amount of material loss (measured in the erosion depth) as a function of time, particle size, sediment concentration, and contact velocity. These enable predictions of how long a coating will last at any site for which suspended sediment concentration and particle size is available.

While the equations are limited to predicting erosion on surfaces that are oriented perpendicular to the direction of flow, they are still expected to be conservative for the RHT blade as the highest velocity areas of the blade (the outer diameter tip of the leading edge) will erode the most, but the RHT leading edge has a forward sweeping angle by design which will reduce the impact energy of particles moving normal to the blade surface.

As a case study, water quality reports were found for the Susquehanna river at the Conowingo Dam in Maryland (Schubel, 1972). Taking into account surface speeds along the profile of the blade and the researched concentration and sizes of sediment in the waterway, the slurry pot results were translated into predictive results for this site on the Susquehanna. Conservatively it was assumed the suspended sediment concentration at that site is 30 mg/L. Of that 30 mg/L, 1 mg/L of those particles are 100-600um, 5 mg/L of those particles are 50-200um, and the rest of the particles are smaller than 50um. Based on the data collected from the initial slurry pot abrasion studies, computed results tell us that at the outer diameter of the RHT blade, where the blade has the highest contact velocity with the water and suspended sediment (reiterating here again that these methods assume normal contact as opposed to the ~33° angle of the RHT blade tip), a stainless steel RHT blade would see a 0.6mm erosion depth after 30 years of operation. An

uncoated fiberglass blade on the other hand, would see 5.41mm of erosion depth at the same point. If protected by the CTD 133 coating or layer of CTD K08 infused glass, the erosion depths would be 1.54mm and 1.36mm respectively at that same point.

In known clearwater sites a coating such as polyurethane, silicon carbide or epoxy polyamide may be effective at protecting the surfaces of the blades for an extended period of time, and with some less aggressive testing of shorter duration and smaller particle size, this lifetime could be more accurately calculated with the help of annual sediment load data. In a river with substantial sediment at the upper bound of our operating speed however, a tougher coating is needed to prevent erosion from reaching the composite substrate.

The CTD 133 coating is also a solid choice. While it doesn't match the performance of stainless, it can be sprayed on in as many layers as necessary to start with whatever initial coating thickness is desired. Additionally, it can be easily repaired by painting more coating back onto the blade locally. Data from CTD (Composite Technology Development) pending publication outlines that the cavitation erosion resistance of this particular coating is >10x better than baseline stainless 410.

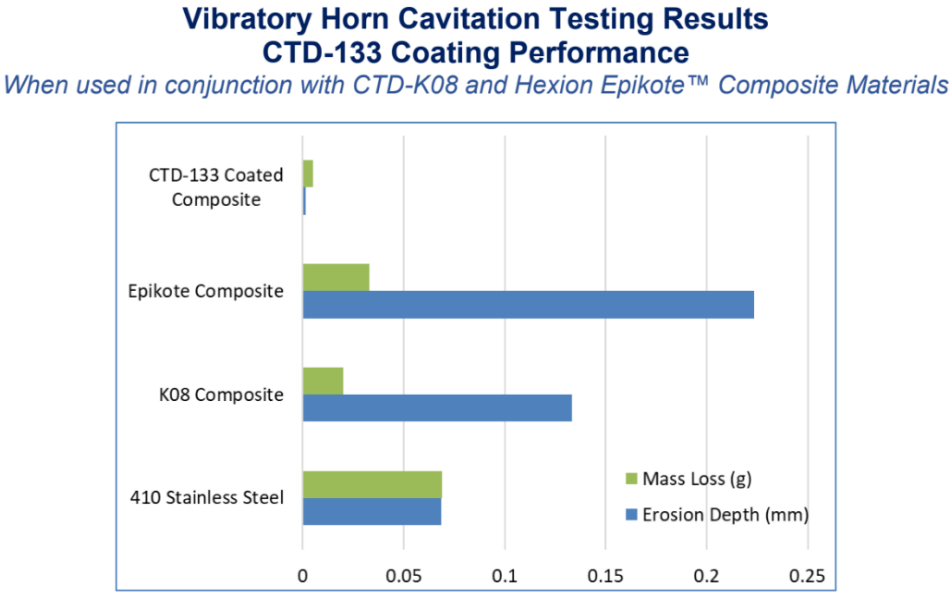

Figure 75: Cavitation erosion performance data of CTD 133 and CTD K08 compared to unprotected composites and 410 stainless steel. Data courtesy of Composite Technology Development.

Material cost for this coating would be ~$4,000 per D190 runner, though there would be some significant labor cost required to apply it as it would take many layer to build up the 2mm coating thickness in a controlled and uniform manner - nonetheless it would make our composite blades very tough and in most sites, the coating would never need to be maintained.

Further refining the abrasion tests to match realistic operating conditions, a study was run to observe the difference in erosion performance between samples of different shapes. Propeller/kaplan plate-style samples were run in the same set up as both straight, cylindrical and thick, swept samples. The cylindrical coupons directly test the effect of object thickness / radius of leading edge curvature on the erosion performance, and the swept samples further tests the effect of contact angle between the leading edge and the erosive particle on the erosion performance of thick geometries. The latter is a direct representation of a Natel RHT leading edge and the ratio of the leading edge thickness of both the cylindrical and swept coupons to the propeller-style plate coupon is representative of the difference in thickness between an RHT blade and traditional propeller blade produced at the same turbine scale.

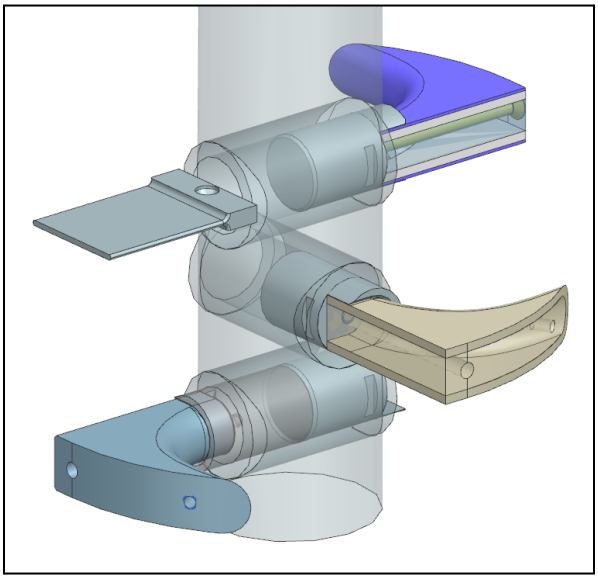

Figure 76: Slurry pot model for the next round of testing. A representative propeller style sample (top left) was directly compared to an RHT style stainless steel sample (bottom left) and RHT style composite samples both coated with CTD 133 (top right) and uncoated (middle right).

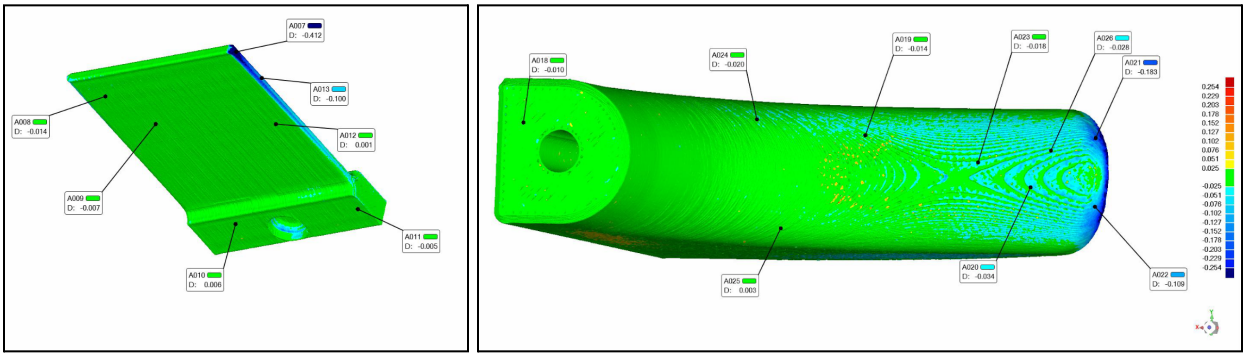

Figure 77: 3D scan comparison of slurry pot testing results using a straight, thin leading edge vs. the thicker swept RHT geometry. It is important to note that a typical tip condition of proximity to a cylindrical housing was not possible due to the design of the slurry pot; for this reason results at the very

tip of each blade should be disregarded. The straight leading edge shows a predictable linear increase in wear with radial position, while the RHT geometry shows very little material loss in the area of study.

Coupons used in this first form-focused test were simple 3D printed ASA parts. This was the fastest way to produce and test these coupons in the same material. Each coupon was 3D scanned before and after testing which was crucial considering that sediment actually embedded itself into the soft plastic during testing and in many cases led to a net mass increase, invalidating our method of using mass change to evaluate material loss.

The scans show that while the prop style coupon lost ~0.41 mm of material from the very tip where the contact velocities are highest, the cylindrical coupon lost ~0.2 mm and the swept coupon only lost ~0.18 mm. While this is clearly not a perfect test as the 3D printed coupons have clear imperfections, visible print layers and the contact surface varies in print orientation, these results are very encouraging. This preliminary data indicates that in equivalent operating conditions, it would take roughly twice as long for an RHT blade to wear away to the same degree as a propeller blade assuming they were built from the same material. Along that vein, an RHT blade made of a material with roughly half the abrasive erosion performance as stainless steel would wear away at roughly the same rate as a stainless steel propeller blade operating in equivalent conditions.

Additional studies are planned beyond the performance period to more closely study the form-dependent abrasive erosion behavior in stainless steel and fiberglass composite materials. These tests will allow us to directly compare expected RHT abrasion performance to the abrasion performance of traditional style machines that are currently operating in the field. Standard documents such as IEC 62364 outline abrasion lifetime prediction models for Kaplan, Francis, and propeller style runner blades, and this test will allow for direct comparison of the RHT blade design within the standardized context.

2.3.6 Impact Testing

Impact tests were carried out to the ASTM D7136 testing standard. This test involves striking a coupon normal to the surface of the coupon with a 5.5 kg hardened steel impactor with a spherical tip. Drop heights were calculated based on expected strike energies of two different objects contacting the blade at the very outer diameter at maximum operating speed. Those two objects are a 1 kg rock and a 1.5 kg piece of wooden debris. These objects were selected based on expectations of the largest objects that would make their way through a trash rack located upstream of the turbine. An RHT turbine will have an approximate maximum tip speed of 25 m/s. The saddle of the blade, which is a surface that sits normal to the direction of the flow through the turbine, will have a maximum speed of roughly 13 m/s. The tip of the blade, by comparison, sits at a 32° angle to the direction of flow, so the normal component of the flow velocity contacting the tip of the blade is also roughly 13 m/s. This normal component of the

contact velocity is uniform across the majority of the blade by design because it is a major factor that affects fish survival.

Figure 81: wooden (oak) impactor backed by steel mass set up to impact a carbon fiber coupon.

An original set of impact tests were run with the ASTM D7136 standard hardened steel impactor with the spherical tip. This set of testing was a good way to compare impact resistance from a relative standpoint between different materials; however, the severity of damage induced by this impactor was not representative of what would actually be seen if a piece of debris were to make its way through the turbine.

All impact testing was based around the cases of either a 1.5 kg piece of wooden debris or a 1 kg rock / piece of concrete passing through the turbine and striking the very tip of the runner blade at a contact speed of 25 m/s. In the first pass of testing, the standard steel impactor was used to strike the coupons with these representative energies but 1) the impactor was of a high material hardness and 2) the full impact energy was applied in a strike that is normal to the surface of the coupon even though the tip of the blade where the blade sees the highest linear speeds is actually angled at about 60° relative to the flow passing through the machine.

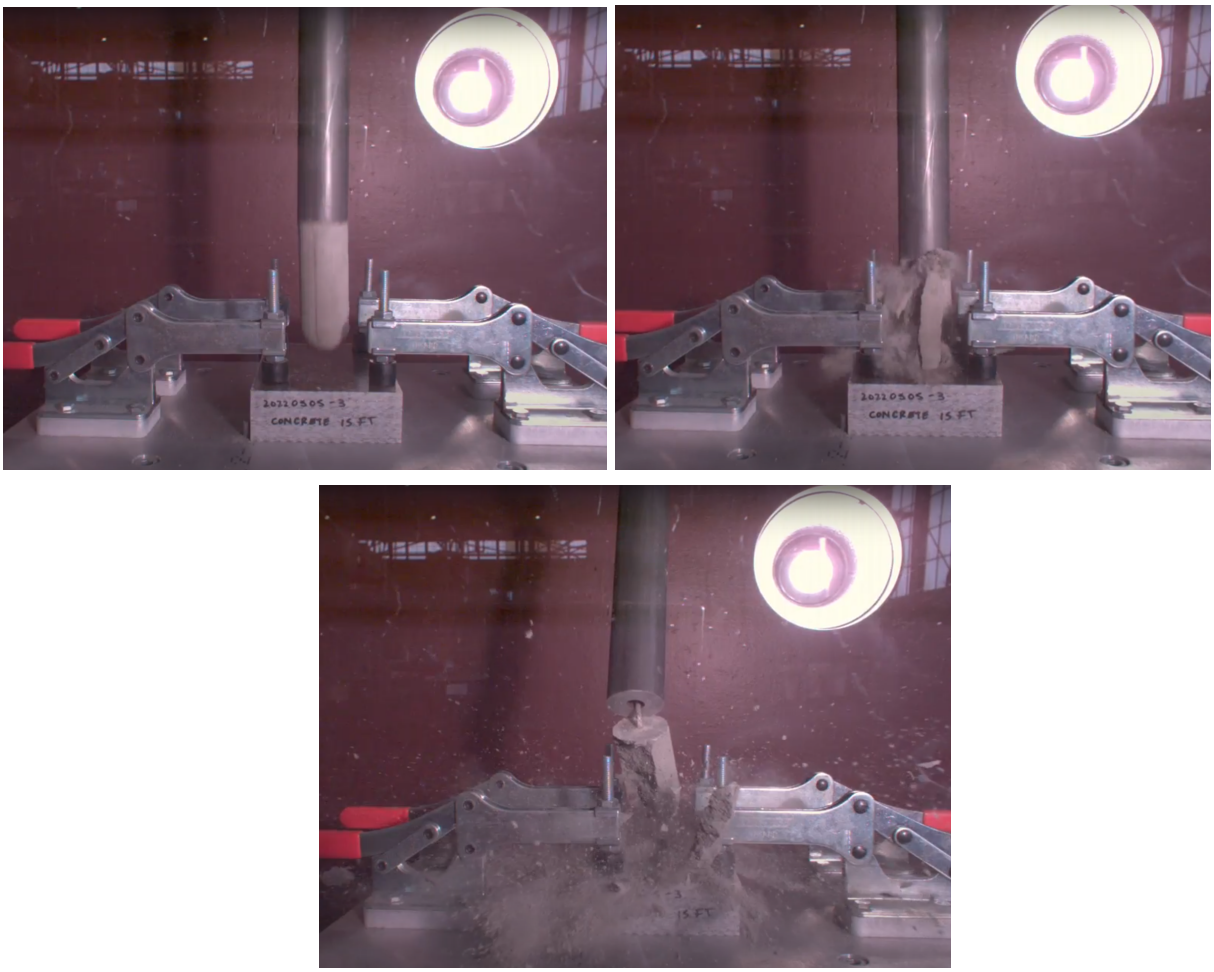

Figure 82: Screenshot sequence from the high speed video footage of a concrete impactor backed by a steel mass impacting a fiberglass coupon.

Accounting for more realistic conditions, impact tests were reconfigured for the second round of testing. Impactor tips were fashioned out of oak hardwood and concrete. Due to the fact that both wood and concrete are considerably less dense than steel, only the tip of the impactor was produced out of the material of interest and a steel bar was used to back the tip to achieve the impactor mass required to achieve the desired strike energies. The strike energies were also adjusted from the original set of tests to accommodate the fact that this impact setup only allows for normal strike. As a result, we ran impact tests with wood from a 22 ft drop height (representative of the normal strike of a 1.5 kg piece wooden debris contacting the tip of the blade at a 25 m/s linear strike speed) and with concrete from a 15 ft drop height (representative of the normal strike of a 1 kg piece of concrete contacting the tip of the blade at a 25 m/s linear strike speed).

Images of all of the coupons taken before and after impact testing are included below in this report. Scanning analysis was not completed on these coupons but it is very clear that no

significant damage was inflicted on any of them. There are no signs of delamination in any of the test coupons, and for the coupons that seem to have some scuffing on the impact surfaces, that type of damage is cosmetic only.

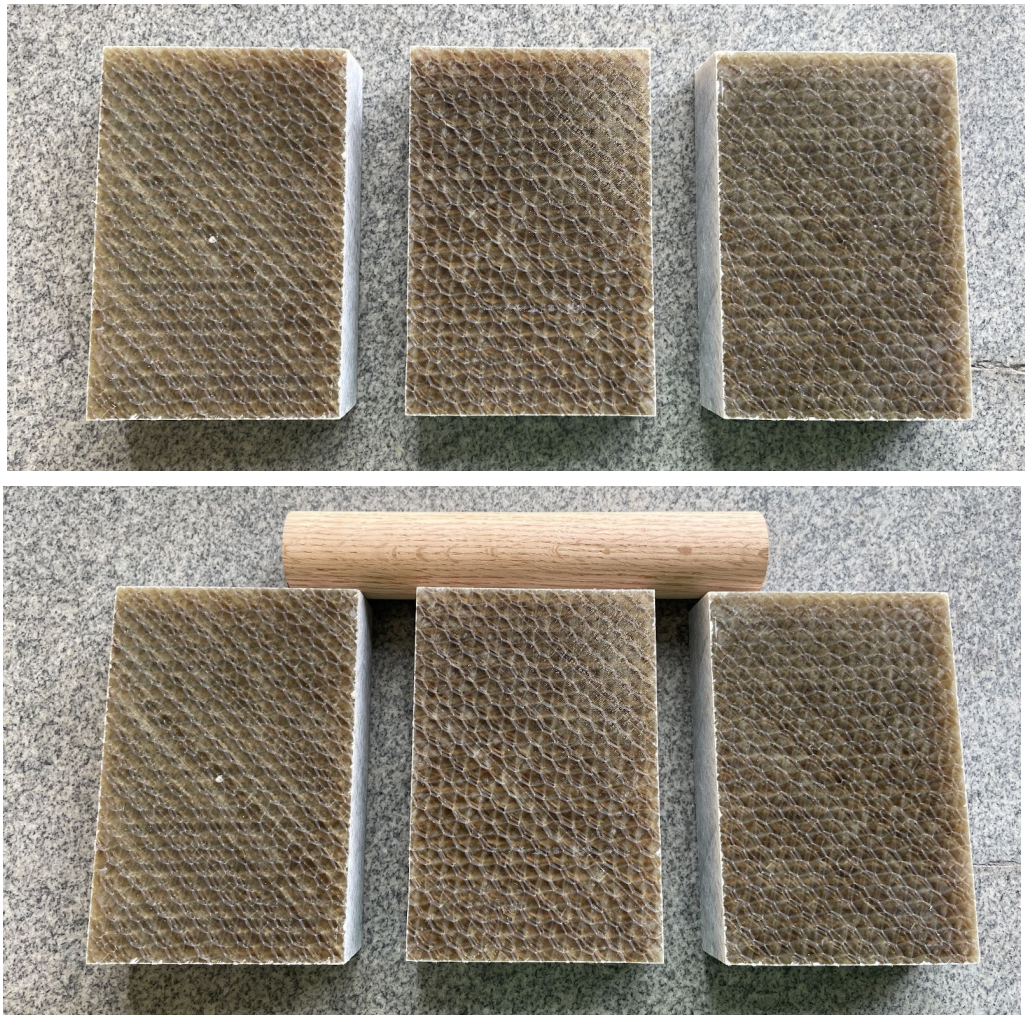

Figure 83: 36 mm thick fiberglass before (top) and after (bottom) impact with wooden impactors dropped from 22 ft.

Figure 84: 36 mm thick fiberglass before (top) and after (bottom) impact with concrete impactors dropped from 15 ft.

2.3.7 Mechanical Joint Testing

This section containing proprietary information has been removed from the public version of this report.

2.3.8 Full Scale Manufacturing and Component Testing

Figure 97: full scale leading edge load tester

After validating the joint design both analytically through modeling and simulation and experimentally through coupon level testing, a full scale blade test was planned. The goal of this test was to move beyond simple couple testing and incorporate two additional important factors into the experimental strength testing of the blade root joint:

1. Actual blade root geometry
2. Load distribution across the joint

The leading edge laminate of the RHT fiberglass blade is the most complex component of the entire composite structure and the joint at the root is the most highly loaded. A rocker style hydraulically actuated full scale leading edge tester was developed to carry out the testing of the leading edge root. The design stemmed from the concept of loading the leading edge from a single point with a specific load vector to distribute loads into the root in a representative manner. The loading vector was determined through an iterative process that positioned the loading point between the high pressure and low pressure sides of the leading edge and altered the load vector by tweaking multipliers of unit vector loads applied to that point for both BEP and OS cases.

The goal of loads development was to match the loads (tensile, moment, shear) at the root attachment. Additionally, it was important to try to have the overall distribution and direction of

loads match that of the operating cases. Once the loading vectors were established, the tester was designed to enable appropriate loading of the leading edge.

In this rocker-style tester, the placeholder hub mounts to a large, self-reacting steel weldment. The hub is positioned by a waterjet jig which positions the datum surfaces of the hub to the datum surfaces of the weldment. There is a jig to position the hub for BEP loading and a separate jig to position the hub for runaway loading. This ensures that the loading vector applied to the leading edge follows the intended design.

The weldment's rocker tower supports a set of rocker arms. The rocker arms have two sets of precision match drilled pin holes in the middle of their span. One of these sets of holes is used to load the blade in the BEP condition and the other set is used to load the blade in the runaway condition. The pin that passes through these sets of holes attaches to a pin passing through the leading edge via a linkage. The linkage consists of two spherical rod ends connected by a load cell. The load allows for live-time reading of the magnitude of load passing into the blade along the designed loading vector. On the other end of the tester weldment, there is a shorter tower which supports a 4" diameter hydraulic cylinder. The base of the cylinder is mounted to the short tower via another pin passing through a spherical bearing. The rod side of the cylinder directly couples to another spherical rod end which attaches to the right end of the rocker via another pin.

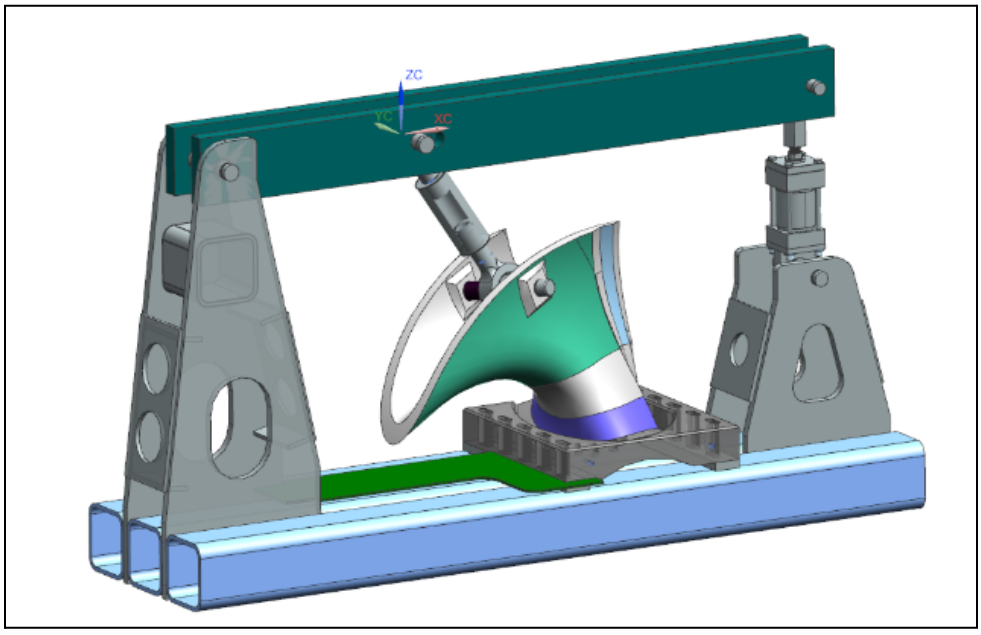

Figure 100: model of the test setup.

The rocker configuration allows us to use mechanical advantage to exert extremely large loads to the leading edge without requiring a very large hydraulic cylinder. The runway case requires the application of 131 kN to the leading edge, but only 46 kN of load is required on the actuator side.

The tester structure was designed to handle 3X the nominal overspeed load (so 393 kN) so that parts could be tested to failure. The self reacting design of the tester weldment allows the entire tester to be carted around and placed where it is most convenient for either testing, assembly, or maintenance.

In addition to the load cell, the tester was equipped with dial indicators and strain gauges. Dial indicators were mount directly to the based of the weldment with magnetic bases and measured the change in vertical distance between the base and the very tip of the leading edge. The strain gauges were placed in the areas expected to see the highest stresses in the BEP and OS conditions. The high stress location was not the same across these two cases, so two separate strain gauges were applied and the respective appropriate strain gauge was monitored for the BEP and overspeed cases during testing.

Once the completed fiberglass leading edge component was assembled into the tester, it was first configured in the BEP testing condition, following the specifications of the test plan. The hydraulic cylinder was slowly manually pumped up until the in line load cell registered 92 kN. For safety purposes, video footage was taken of the dial indicator that was set up to register displacement at the leading edge to prevent the need to have people within the vicinity of the tester. The tester was cycled between 0 kN and 92 kN a couple times to allow the tester to settle to a stable point and the dial indicator was re-zeroed. The cylinder was slowly pumped up again, and the pressure and load cell force were called out along the way to mark the dial indicator video recording for later review. After reaching the 92 kN, the tester was unloaded and the dial indicator returned to its original 0 point, indicating that no permanent deformation occurred. The tester was then cycled for 100 cycles. Throughout that entire time, the measured force vs. strain was linear and consistent. The displacement was also consistent across cycles in that the max displacement was consistent and the blade always returned back to the 0 point.

The one peculiar observation during BEP testing was that the displacement profile of the leading edge tip was not linear. The tip actually dropped 0.001-0.002” towards the test frame prior to pulling away from the tester 0.005” as expected. Even more peculiar was the fact that as the pressure was released from the cylinder, the dial indicator seemed to retrace the deflection profile but actually dipped even close to the tester upon unloading that it did during loading but it always returned back to 0 in its fully unloaded state.

This strange behavior was ultimately attributed to the fact that the rod end attached to the pin that passes through the blade was not completely constrained. There was about 1.5 mm of clearance between the faces of the spherical joint and the spacers that located it. It is suspected that the rod end was slipping down the pin until it butted up against the spacer firmly and then we the part was unloaded more rapidly, it faced less friction load due to the application of kinetic friction

instead of static friction and actually slid back farther than it did during the loading process before returning to its neutral zeroed state.

The tester was reconfigured into its runaway loading configuration once BEP testing was complete. The same process was repeated with the runaway condition as was completed with the BEP cycling and 100 OS cycles were also complete but at an in-line linkage load of 131 kN. Again, force vs. strain was linear and the dial indicator returned to its zero point after each cycle. In contrast to the BEP displacement profile, the runaway displacement profile was extremely linear. It is likely that the same rod end slippage was not an issue here as the vector used to apply load to the blade pin in the OS condition was oriented much closer to the normal direction of the pin, reducing the shear load on the rod end.

After low cycle fatigue was complete in both BEP and runaway cases, the load cell was swapped out of the tester and replaced with a coupling nut as the load cell being used was only rated for 50,000 lb-f or 222 kN. Since the strain was very linear throughout runaway testing and the hydraulic pressure required to achieve the 131 kN along that load vector was known, it was determined to be acceptable to load the leading edge component to failure without a load cell in place as there were alternative indicators of the force.

Failure loading was conducted twice (as the part itself did not fully fail). During the first run, typical fiber pops were heard almost as soon as the blade was loaded above the 1X multiplier of runaway load. These signatures are typical of composite structures in an initial load cycle. Deflection and strain remained linear and a loud fiber failure was heard between 250 and 270 kN or 1.9-2.0x design load. Conservatively, the test was halted and the blade was unloaded. The dial indicator, however, did not return to its zero position. It moved beyond its zero position by about 0.020” indicating that the tip of the leading edge returned to a position closer to the base of the tester than where it had started. Upon further review of the test footage, it was determined that the sounds heard were likely not an indication of the failure of the root attachment and so a second test was executed.

During the second test, the fiberglass did not make any sounds as the part was loaded back up to the 250 kN point where the last test had halted. This confirms that the sounds heard during the first run were just fiber settling as opposed to the start of failure. The leading edge made it up to 367 kN or 2.8x the OS load when significant fiber failures were audibly detected and the part was again unloaded. Again the tip of the leading edge returned to a point about 0.020” below where it had started. Upon later inspection, it turned out that the 2” steel pin that passes through into the leading edge laminate has actually yielded under these extremely high loads and was altering the blade displacement read outs when the part was unloaded.

While the load applied to the leading edge was not directly recorded throughout the failure testing of the leading edge component due to the insufficient rating of the available load cell,

hydraulic pressure was manually read out and documented throughout the process to map it against the dial indicator displacement and strain gauge data. After post processing, it is clear that both map very linearly to the load / pressure, however, some sort of failure around 2.7x the OS load broke the linearity and beyond that point the strain value did not recover.

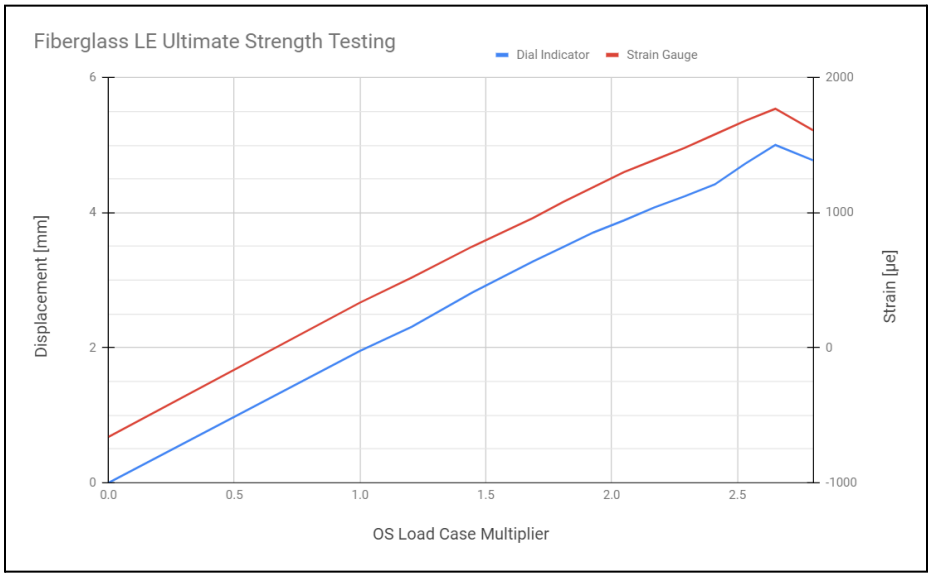

Figure 102: load vs displacement in the runaway loading case

Both the tip displacement and strain values are very closely aligned with the expected displacement and strain predicted by the analytical model. This is a positive confirmation that our modeling techniques and material properties align with reality and that we can expect the full runner to behave as anticipated.

Upon disassembly of the blade from the tester, it was very obvious that the pin passing through the leading edge had yielded as it could not be budged in either direction. It was also clear that the fiberglass pad up that had been infused and bonded to the inside surfaces of the leading edge laminate has started to fail. There was clear separation in the adhesive used to bond the pad ups to the main laminate; there were signs of the delamination in the bag side plies of the leading edge component; and the pad ups themselves were starting to see delamination.

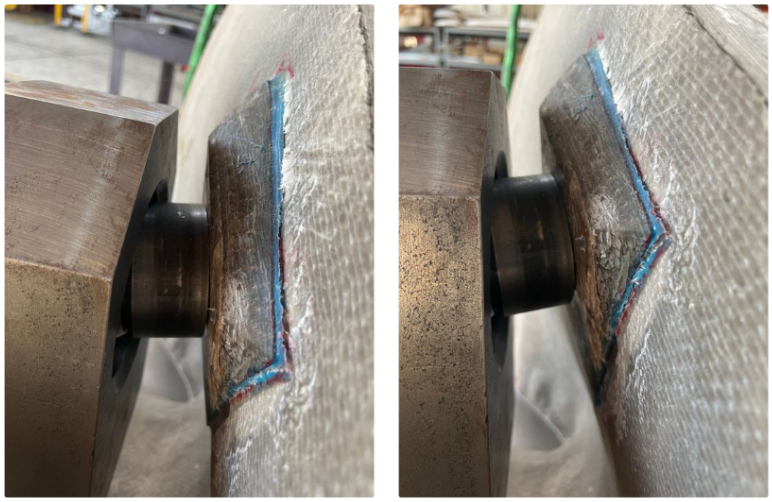

Figure 103: failure, not of the test article but of the buildup area for test point loading.

2.3.9 Summary of Findings

Extensive materials testing has led to the full characterization of the fiberglass / vinylester composite layup under all operating conditions of the RHT. Stiffness, strength, absorption, thermal expansion and creep have all been verified across the relevant temperature and submergence conditions and have been found to be satisfactory for constructing a runner that will meet all of the necessary design requirements. Abrasion and impact behavior of the composite material has been thoroughly studied and results indicate that the combination of the composite RHT blade and a selection of protective coatings and materials can lead to a robust runner which can last just as long as a metallic kaplan or propeller if not longer without the need of service for repair. The blade shape which is designed to be gentle on fish, is also inherently more gentle on debris and sediment as well, meaning that the thick, swept geometry does not see impact events or abrasive erosion as extreme as one would see in a kaplan or propeller style turbine operating under the same conditions. So while the composite material used to construct these blades may not be apples to apples as hardy as traditional cast stainless steel, when combined with the favorable shape of the RHT, these blades can be designed to withstand equally rigorous conditions. Further investigation is still being pursued in this area, but coupon level testing has shown very positive results.

With durability addressed, the composite manufacturing techniques enable Natel's RHT runner to be brought to market within a reasonable cost. As an alternative to costly and complex castings, the composite runner blades can be produced on a much shorter timeline for significantly lower cost while also eliminating the need for expensive machining operations by producing net shape components.

3. Project Conclusions

This project successfully evaluated the proposed module design space and assessed the performance of optimized configurations. Through analysis, it has been shown that compact overflowed fish-safe generation modules can be designed to perform efficiently and effectively, with inflow / outflow ("plant level") head losses of around 5% (typical for hydro facilities) and turbine hydraulic efficiencies greater than 90%. A range of module configurations, using both vertical-axis and horizontal-axis machines, were studied and costed. For the studied design net head range of 2 to 10m, higher head designs at 9 to 10m (very much still "low head" in the hydro industry) have an estimated installed cost of ~$1600/kW, mapping comfortably within the SMH EDES target of <$6000/kW for a full plant. At lower heads the number of economic sites will depend on overall plant costs, and at very low heads below 5m such projects will increasingly require advantages of existing infrastructure (access, interconnection, non-powered dam structures etc) to be viable.

Through laboratory and field testing, the team quantitatively demonstrated the ability to include downstream passage into generation module functionality, opening up broad opportunities to eliminate design, capital, testing, and maintenance costs of bespoke exclusion systems. RHT turbines with high tip speeds (~20m/s) offer excellent survival (no significant difference between control and treatment groups of tested salmonid and anguillid species) for proportionately large fish (length of up to 30% of turbine diameter for salmonids, and up to 120% of turbine diameter for eels). (Watson et al, 2022)

The technology readiness level of a full scale composite fish-safe runner design was advanced through design and testing to meet all the strength, fatigue, stiffness, and environmental durability criteria studied, at lower cost than conventional manufacturing methods. Functional prototypes passed all critical tests and this design is ready for initial production, field implementation, and lifecycle evaluation.

Natel Energy is very grateful for the support of the project team and the Water Power Technologies Office during the execution of this project. Field testing with live fish, in particular, offered a wide range of challenges which demanded a high degree of collaboration and proactivity to be successfully completed. The team at Pacific Northwest National Laboratory proved up to the task. Additionally, the numerous review sessions conducted by Kleinschmidt, WPTO, ORNL MDF, and a number of agency and industry experts were highly valuable for the planning and design elements of the project. The project team is proud of the extent and quality of work accomplished during this project and look forward to seeing increased application of fish safe turbine designs and advanced, low-cost manufacturing methods!

4. References

Amaral, S., Coleman, B., Rackovan, J., Withers, K., Mater, B. (2018). Survival of fish passing downstream at a small hydropower facility. Marine and Freshwater Research 69, 1870-1881.

Amaral, S., Watson, S., Schneider, A., Rackovan, J., Baumgartner, A. (2020). Improving survival: injury and mortality of fish struck by blades with slanted, blunt leading edges. Journal of Ecohydraulics 5.2, 175-183, DOI: 10.1080/24705357.2020.1768166. https://www.tandfonline.com/doi/full/10.1080/24705357.2020.1768166

Beauson, J. & B., Povl. (2016). Wind Turbine Blades: An End of Life Perspective. 10.1007/978-3-319-39095-6_23.

Calles, O., Olsson, I.C., Comoglio, C., Kemp, P.S., Blunden, L., Schmitz, M., & Greenberg, L.A. Size-dependent mortality of migratory silver eels at a hydropower plant, and implications for escapement to the sea. Freshwater Biology, 55, 2167–2180. doi:10.1111/j.1365-2427.2010.02459.

Coutant, C., Mann, R., & Sale, M. (2006). Reduced spill at hydropower dams: Opportunities for more generation and increased fish protection. ORNL/TM-2005/179 https://info.ornl.gov/sites/publications/Files/Pub3857.pdf

Hanson, C.H., White, J.R., & Li, H.W. (1977). Entrapment and Impingement of Fishes by Power Plant Cooling Water Intakes: An Overview. Marine Fisheries Review.

Jansen, H.M, Winter, H.V., Bruijs, M.C.M, & Polman, H.J.G. Just go with the flow? Route selection and mortality during downstream migration of silver eels in relation to river discharge. ICES Journal of Marine Science, 64, 1437–1443.

Mueller, M., Knott, J., Pander, J. & Geist, J. (2020) Fischökologisches Monitoring an innovativen Wasserkraftanlagen Zusammenfassung zum Abschlussbericht 2020 Band 11: Standortübergreifende Verbesserungsmöglichkeiten für den Fischschutz und die Gewässerökologie (ohne Schachtkraftwerk). Prepared for Bayerisches Landesamt für Umwelt.

O'Connor, P., DeNeale, S., Chalise, D., Centurion, E., Maloof, A. (2015). Hydropower baseline cost modeling, version 2. ORNL (Oak Ridge National Laboratory) ORNL/TM-2015/471.

ORNL ((Oak Ridge National Laboratory). (2018; 2021). 2017 and 2020 Hydropower Market Reports.

Ovidio, M., Dierckx, A., Bunel, S., Grandry, L., Spronck, C., & Benitez, J. P. (2016). Poor Performance of a Retrofitted Downstream Bypass Revealed by the Analysis of Approaching Behaviour in Combination with a Trapping System. River Research and Applications, 33(1), 27–36. doi:10.1002/rra.3062

Sandia National Laboratories. (2003). Blade Manufacturing Improvements Remote Blade Manufacturing Demonstration, prod-ng.sandia.gov/techlib-noauth/access-control.cgi/2003/030719.pdf.

Schubel, J. R. (1972). Suspended Sediment Discharge of the Susquehanna River at Conowingo, Maryland, during 1969. Chesapeake Science, 13(1), 53. doi:10.2307/1350551

USBR (U.S. Bureau of Reclamation). 2016. Intake Vortex Formation and Suppression at Hydropower Facilities. USBR Research and Development Office Science and Technology Program, Final Report ST-2016-6359-1. https://www.usbr.gov/research/projects/detail.cfm?id=6359

USFWS (U.S. Fish and Wildlife Service). 2019. Fish Passage Engineering Design Criteria. USFWS, Northeast Region R5, Hadley, Massachusetts.

Watson, S., Schneider, A., Santen, L., Deters, K., Mueller, R., Pflugrath, B., Stephenson, J., Deng, Z. (2022). Transactions of the American Fisheries Society 151:711-724. DOI: 10.1002/tafs.10385. https://afspubs.onlinelibrary.wiley.com/doi/epdf/10.1002/tafs.10385

Witt, A., Smith, B., Tsakiris, A., Papanicolaou, T., Lee, K., Stewart, M. (2017). Exemplary Design Envelope Specification for Standard Modular Hydropower Technology. ORNL (Oak Ridge National Laboratory) ORNL/TM-2016/298/R1.